
TRACKING CHANGING PROBABILITIES VIA DYNAMIC LEARNERS

Omid Madani*
omidmadani@yahoo.com

ABSTRACT

Consider a predictor, a learner, whose input is a stream of discrete items. The predictor’s task, at every time point, is *probabilistic multiclass prediction*, *i.e.* to predict which item may occur next by outputting zero or more candidate items, each with a probability, after which the actual item is revealed and the predictor learns from this observation. To output probabilities, the predictor keeps track of the proportions of the items it has seen. The stream is unbounded (lifelong), and the predictor has finite limited space. The task is *open-ended*: the set of items is unknown to the predictor and their totality can also grow unbounded. Moreover, there is *non-stationarity*: the underlying frequencies of items may change, substantially, from time to time. For instance, new items may start appearing and a few recently frequent items may cease to occur again. The predictor, being space-bounded, need only provide probabilities for those items which, at the time of prediction, have *sufficiently high* frequency, *i.e.* the *salient* items. This problem is motivated in the setting of *Prediction Games*, a self-supervised learning regime where concepts serve as *both the predictors and the predictands*, and the set of concepts grows over time, resulting in non-stationarities as new concepts are generated and used. We design and study a number of predictors, *sparse moving averages (SMAs)*, for the task. One SMA adapts the sparse exponentiated moving average (EMA) and another is based on queuing a few count snapshots, keeping dynamic per-item histories. Evaluating the predicted probabilities, under noise and non-stationarity, presents challenges, and we discuss and develop evaluation methods, one based on bounding log-loss. We show that a combination of ideas, supporting *dynamic predictand-specific* learning rates, offers advantages in terms of faster adaption to change (plasticity), while also supporting low variance (stability). Code is made available.

*“Occasionally, a new knot of significations is formed.. and our natural powers suddenly merge with a richer signification.”*² Maurice Merleau-Ponty [52]

Keywords Learning and Development, Developmental Non-Stationarity, Sparse Moving Averages, Online Learning, Lifelong Open-Ended Learning, Multiclass Prediction, Probabilistic Prediction, Probability Reliability, Categorical (Semi)Distributions, Change Detection, Dynamic Learning Rates, Stability vs Plasticity

1 Introduction

The external world is ever changing, and change is everywhere. This non-stationarity takes different forms and occurs at different time scales, including periodic changes, with different periodicities, and abrupt changes due to unforeseen events. In a human’s life, daylight changes to night, and back, and so is with changes in seasons taking place over weeks and months [34]. Appearances of friends change, daily and over years. Language use and culture evolve over

^{*}Much of this work was conducted while at Cisco Secure Workload.

²When a new concept, *i.e.* a recurring pattern represented in the system, is well predicted by the context predictors that it tends to co-occur with (other concepts in an interpretation of an episode, such as a visual scene), we take that to mean the concept has been incorporated or integrated (into a learning and developing system), and we are taking “skill”, in the quote, to mean a pattern too (a sensorimotor pattern). We found the quote first in [57], and a more complete version is: “*Occasionally, a new knot of significations is formed: our previous movements are integrated into a new motor entity, the first visual givens are integrated into a new sensorial entity, and our natural powers suddenly merge with a richer signification*” (“*knot of significations*” has also been translated as “*cluster of meanings*”) [52].

years and decades: words take on new meanings, and new words, phrases, and concepts are introduced. Change can be attributed to physical processes, or agents’ actions (oneself, or others). A learning system that continually predicts its sensory streams, originating from the external world, to build and maintain models of its external world, needs to respond and adapt to such **external non-stationarity** in a timely fashion. As designers of such systems, we do not have control over the external world, but hope that such changes are not too rapid and drastic that render learning futile [18, 62, 35, 30, 75, 31].

We posit that complex adaptive learning systems need to cope with another source of change too: that of their own **internal**, in particular **developmental, non-stationarity**. Complex learning systems have multiple adapting subsystems, homogeneous and heterogeneous, and these parts evolve and develop over time, and thus their behavior changes over time. As designers of such systems, we have some control over this internal change. For instance, we may define and set parameters that influence how fast a part can change. To an extent, modeling the change could be possible too. Of course, there are tradeoffs involved, for example when setting change parameters that affect internal change, favoring adaptability to the external world over stability of internal workings.

A concrete example of internal vs. external non-stationarity occurs within the *Prediction Games* approach [43, 40, 41], where we are investigating systems and algorithms to help shed light on 1) how a learning system could develop high-level (perceptual, structured) *concepts* from low-level sensory information, over time and many learning episodes, primarily in an unsupervised (self-supervised) continual learning fashion, and 2) how such concept (structure) learning, and imposing one’s structures onto the input episodes, could be beneficial for subsequent efficient learning, prediction, and reasoning applications. In the course of exploring such systems, we have found that making a conceptual distinction between internal (developmental or endogenous) and external (exogenous) nonstationarity is fruitful. In Prediction Games, the system repeatedly inputs an episode, such as a line of text, and determines *which of its higher level concepts*, such as words (n-grams of characters), are applicable. This process of mapping stretches of input characters into higher level concepts is called *interpretation*. The system begins its learning with a low level initial (hard-wired) concept vocabulary, for example the characters, and over many thousands and millions of episodes of interpretation (of practice), grows its vocabulary of represented concepts, which in turn enable it to better interpret and predict its world. In Prediction Games, each concept, or an explicitly represented pattern (imagine ngrams of characters for simplicity), is *both a predictor and a predictand*, and a concept can both be composed of parts as well as take part in the creation of new (higher-level) concepts (a *part hierarchy*). After a new concept is generated, it is used in subsequent interpretations, and existing concepts co-occurring with it need to learn to predict it, as part of the process of integrating a new concept within the system. Prediction is probabilistic: each predictor provides a probability with each predictand (item that it predicts). Supporting probabilistic predictions allows for making appropriate decisions based on information utility [43], such as answering the question of which higher-level concepts should be used in the interpretation of the current episode. Thus, the generation and usage of new concepts leads to internal non-stationarity from the vantage point of the existing concepts, *i.e.* the existing predictors.³ From time to time, each concept, as a predictor, will see a change in its input stream due to the creation and usage of new concepts (see also Sect. 8.1.3). This change is due to the collective workings of the different system parts. We envision such systems to contain different parts (of learning, inference, and so on) working and developing together, a growing collective intelligence. In this paper, we focus on advancing solutions for the prediction task.

Previously, we addressed the non-stationarity faced by the predictors (due to the discovery and use of new concepts) via, periodically, cloning existing concepts and learning from scratch for all, new and cloned, concepts [41]. However, this retraining from scratch can be slow and inefficient, and leads to undesired non-smoothness or abrupt behavior change in the output of the system. It also requires extra complexity in implementation (cloning, support for multiple levels), and ultimately is inflexible if the external world also exhibits similar non-stationary patterns. In this paper, we develop **sparse moving average (SMA)** techniques that handle such transitions more gracefully. We note that the structure of concepts learned can be probabilistic too, and non-stationarity can be present there as well, *i.e. both intra-concept as well as inter-concept relations can be non-stationary*. The algorithms developed may find applications in other non-stationary multiclass domains, such as in recommenders and personal assistants (continual personalization), and we conduct experiments on several data sources: Unix command sequences entered by users, reflecting their changing daily tasks and projects, and natural language text (in addition to experiments on synthesized sequences).

Thus our task is online multiclass probabilistic prediction under non-stationarity, and we use the term “item” in place of “concept” or “class” for much of the paper. We develop techniques for a *finite-space predictor*, one that has limited space (memory), a constant independent of stream length, which translates to a limit on how low a probability the predictor can support and predict well. In this paper, we focus on learning probabilities above a minimum probability (support) threshold of a given p_{min} parameter (set to 0.01 or 0.001 in our experiments). Supporting lower probabilities

³Internal vs. external are of course relative to a point of reference.

requires larger space in general, and the utility of learning lower probabilities also depends on the input (how stationary the world is).⁴

The input stream to a predictor is unbounded (or indefinite), and the set of items the predictor will see is unknown to it, and this set can also grow without limit. In other words, the task is *life-long* and *open-ended*. From time to time the proportion of an item, a predictand, changes. For instance, a new item appears with some frequency, *i.e.* an item that had hitherto 0 probability (non-existent), starts appearing with some significant frequency above p_{min} . Possibly, a few other items' probabilities may need to be reduced at around the same time. The predictand probabilities that a single predictor needs to support simultaneously can span several orders of magnitude (*e.g.* supporting both 0.5 and 0.02). As a predictor adapts to changes, we want it, to the extent feasible, to change only the probabilities of items that are affected. As we explain, this is a form of (statistical) stability *vs.* plasticity dilemma [1, 53, 50]. While fast convergence or adaptation is a major goal and evaluation criterion, specially because we require probabilities, which take some time to learn, we allow for a *grace period*, or an allowance for *delayed response* when evaluating different techniques: a predictor need not provide a (positive) probability as soon as it has observed an item. Only after a few sufficiently recent observations of the item, do we require prediction.⁵ We show how each predictor keeping its own **predictand-specific learning-rates** and supporting **dynamic rate changes**, *i.e.* both rate increases and decreases (rather than keeping them fixed, or only allowing change in one direction, such as monotone decreasing), improves convergence (after a change) and prediction accuracy, compared to the simpler moving average techniques. These extensions entail extra space and update-time overhead, but we show that the flexibility that such extensions afford can be worth the costs.

We list our assumptions and goals, *practical probabilistic prediction*, for non-stationary multiclass lifelong streams, as follows:

- (Assumption 1: Saliency) Aiming at learning probabilities that are sufficiently high, *e.g.* $p \geq 0.001$. Such a range will be useful and adequate in real domains and applications (and a consequence of the space constraints of a predictor).
- (Assumption 2: Approximation) Approximately learning the probabilities is adequate, for instance, to within a deviation ratio of 2 (the relative error can also depend on the magnitude of the target probability, Sect. 3.4).
- (Performance Goal: Practical Convergence) Strive for efficient learners striking a good balance between speed of convergence and eventual accuracy, *e.g.* a method taking 10 item observations to converge to within vicinity of a target probability is preferred over one requiring 100, even if the latter is eventually more stable or precise.

Our focus is therefore neither convergence in the limit nor highly precise estimation. We also note that in practical applications, there may not be 'real' or true probabilities,⁶ but probabilities are useful foundational *means* to achieve system functionalities beyond non-probabilistic prediction (*e.g.* a plain ranking) of the future possibilities. If a new target event of interest occurs every few seconds, then a system that converges to sufficiently accurate probabilities withing a few 10s of seconds is preferred to a system requiring several minutes or hours. Similarly, if the event occurs once a day, then convergence in days is strongly preferred over many weeks or months.⁷ To the best of our knowledge, both the task and problem formulation as well as much of the SMA and evaluation techniques developed are novel (building on much previous work, see Sect. 9).

This paper is organized as follows. We next present the formal problem setting and introduce notation. This includes the idealized non-stationary generation setting (Sect. 2.1.1). We have this setting in mind when developing the algorithms. Sect. 3 explains the ways we evaluate and compare the prediction techniques. We review proper scoring, motivate log-loss (logarithmic loss) over quadratic loss, and adapt log-loss to the challenges of non-stationarity, noise, and incomplete distributions, where we also define drawing from (sampling) and taking expectations with respect to incomplete distributions. To handle infrequent ("noise") and new items, we develop a bounded variant of log-loss and show when it remains useful, *i.e.* approximately proper, for evaluation (Sect. 3.8 and Appendix A.3). We next present and develop several SMAs: The Sparse EMA SMA uses a learning rate (Sect. 4), while the Qs SMA is based on counting and averaging (Sect. 5), followed by a hybrid (Sect. 6) which combines the benefits that each offers: the stability of EMA and the plasticity of Qs. We begin with sparse EMA and present a convergence property under the

⁴We note that the problem can also be formulated as each predictor having a fixed space budget, and subject to that space, predict the top k (recently) highest proportions items. With this, the successfully predicted probabilities, depending on the input stream, can be lower than a fixed p_{min} threshold.

⁵For internal non-stationarity, we have some control over the rate of change (*e.g.* see Sect. F.2).

⁶In Prediction Games, higher-level concepts and their co-occurrence probabilities are the constructs of the system itself.

⁷Higher level concepts in Prediction Games are less frequent than the lower-level ones, and the useful conditional probabilities (co-occurrences) often can span below 0.1 down to 0.001, and perhaps lower.

$[o], [o]_1^N$, etc. : infinite & finite item sequences, $[o]_1^N := [o^{(1)}, \dots, o^{(N)}]$, $o^{(t)}$ is the item observed at time t .
PRs, DIs, SDs : prob abilities (PRs), prob. d istributions (DIs), and semi-d istributions (SDs).
SMA : a Sparse Moving Average predictor, such as the sparse EMA and Qs predictors (Sect. 4, 5, 6).
$\mathcal{P}, \mathcal{W}, \mathcal{W}_1, \mathcal{W}_2$, etc. : \mathcal{P} is used for a true underlying SD, and $\mathcal{W}, \mathcal{W}_1, \mathcal{W}_2$ are estimates (<i>e.g.</i> output of an SMA).
$[\mathcal{W}]_1^N$: first N outputs of an SMA (predictor). Each prediction, $\mathcal{W}^{(t)}$, is a SD (or converted to one).
$\text{sup}(\mathcal{W})$: the support set of SD \mathcal{W} . Every SD has finite support (subset of all items \mathcal{I}).
$\text{a}(\mathcal{W}), \text{u}(\mathcal{W})$: $\text{a}(\mathcal{W})$ the allocated PR mass, $\sum_{i \in \text{sup}(\mathcal{W})} \mathcal{W}(i)$, $\text{u}(\mathcal{W}) := 1 - \text{a}(\mathcal{W})$ (unallocated)
p^* : For a binary event, observation $o \in \{0, 1\}$, the true probability of the positive, 1, outcome.
positive outcome, 1 : whenever the target item of interest is observed (0 otherwise).
NS item : a Noise item, <i>i.e.</i> not seen recently in the input stream sufficiently often (currently).
p_{\min} and p_{NS} : used for filtering and scaling, and bounding log-loss on NS items (Sect. 3.5).
p_{\min} can be interpreted as the minimum PR supported by an SMA.
c_{NS} : when evaluating, count-threshold used by a practical NS-marker algorithm (3.5).
O_{\min} : in synthetic experiments, observation count threshold on salient items (Sect. 7.2, 7.3).
EMA : The Exponentiated Moving Average (EMA). We develop sparse multiclass variants of it (Sect. 4).
$\beta, \beta_{\min}, \beta_{\max}, \dots$: learning rates (for EMA variants), $\beta \in [0, 1]$, β_{\min} is minimum allowed, etc.

Table 1: A summary of the main notations, abbreviations and terminology, parameters, etc. See Sect. 2.

stationary scenario, quantifying the worst-case expected number of time steps to convergence in terms of a (fixed) learning rate. Here, we motivate why we seek to enhance EMA, to have a variable rate, even though it could handle some, small, drifts. This change alone is not sufficient. We then present the Qs method, based on queuing of count-based snapshots, which is more responsive to (large) change than EMA, but has more variance (Sect. 5). We present analyses (unbiased estimation), and two variants of queuing. This is followed by the hybrid approach we call DYAL (Sect. 6), which keeps predictand-specific learning rates for EMA and uses queuing to adapt to changes in a timely manner. We conduct both synthetic experiments, in Sect. 7, where the input sequences are generated by known and controlled changing distributions, and on real-world data, in Sect. 8. These sequences can exhibit a variety of phenomena (inter-dependencies), including external non-stationarity. We find that the hybrid DYAL does well in a range of situations, providing evidence that the flexibility it offers is worth the added cost of keeping per-predictand learning rates and queues. Appendices contain further material, in particular, the proofs of technical results, and additional properties and experiments. Python code for SMAs and experimentation is available on GitHub [44].

2 Preliminaries: Problem Setting, Notation, and Evaluation

Our setting is online discrete open-ended probabilistic prediction under non-stationarity. Time is discrete and is denoted by the variable t , $t = 1, 2, 3, \dots$. A predictor *processes* a stream of items (observations): at each time, it predicts then observes and updates. Exactly one (discrete) item occurs and is observed at each time t in the stream. We use the parenthesized superscript notation for the variable corresponding to the item observed at time t , *i.e.* $o^{(t)}$, and similarly for other sequenced objects as well, for instance an estimated probability \hat{p} at time t is denoted $\hat{p}^{(t)}$, though we may drop the superscript whenever the context is sufficiently clear (that it is at a particular time point is implicit). Each item is represented and identified by an integer (or string) id in the various data structures (sequences, maps, ...), and can be viewed as belonging to an infinite unordered (categorical and nominal⁸) set (*e.g.* the set of finite strings). We use letters A, B, C, \dots and also integers $0, 1, 2, 3, \dots$ (but no ordering implied) for referring to specific items in examples. We use the words “sequence” and “stream” interchangeably, but ‘stream’ is used often to imply the infinite or indefinite aspect of the task, while ‘sequence’ is used for the finite cases, *e.g.* for evaluations and comparisons of prediction techniques. A sequence is denoted by the brackets, or array, notation $[]$, thus $[o]_1^N$ denotes a sequence of N observations: $[o^{(1)}, o^{(2)}, \dots, o^{(N)}]$ (also shown without commas $[o^{(1)}o^{(2)} \dots o^{(N)}]$). Fig. 1(a) shows an example sequence. Online processing, of an (infinite) stream or a (finite) sequence, means repeating the *predict-observe-update* cycle, Fig. 2(a): at each time point, predicting (a semi-distribution, see next Sect. 2.1) and then observing. The predictor is an online learner that updates its data structures after each observation. This mode of operation (and evaluation) has been named *prequential* in probabilistic sequence forecasting [14] (see also [7]). Our problem setting is similar to another recent work on predicting (infinite-support) changing distributions in computational learning theory [50]. In that work, the authors do not focus on space-bounded predictors (*e.g.* the history can grow with the stream) and

⁸In this work, we assume no ordering on the items. However, a future direction is when the items have known associated costs or rewards. The term “categorical” may have finiteness connotations, but not here.

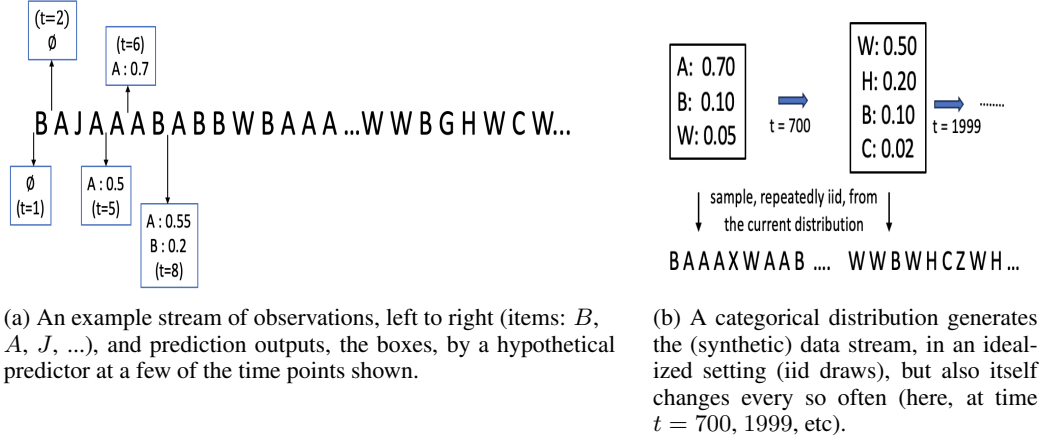


Figure 1: (a) An example sequence of items (the capital letters) together with several prediction outputs of a hypothetical predictor, in rectangular boxes, shown for a few time points (not all outputs are shown to avoid clutter). The sequence is observed from left to right, thus at time $t = 1$, item B is observed ($o^{(1)} = B$), and respectively at times 2, 3, and 4, items A , J , and again A are observed ($o^{(3)} = J$, $o^{(4)} = A$, etc). A prediction output is a map of item to probability (PR), and can be empty. Mathematically, it is a semi-distribution SD (Sect. 2.1). At each time point, before the observation, the predictor predicts, *i.e.* provides a SD (zero or more items, each with a PR). In this example, at times $t \leq 4$, nothing is predicted (empty maps, or $\mathcal{W}^{(1)} = \mathcal{W}^{(4)} = \{\}$, and only two empty outputs, at $t = 1$ and $t = 2$, are shown). At $t = 8$, $\mathcal{W}^{(8)}$ is predicted, where $\mathcal{W}^{(8)} = \{A:0.55, B:0.2\}$ (*i.e.* A is predicted with PR 0.55, and B with PR 0.2). (b) The input sequence can be imagined as being generated by a SD \mathcal{P} : at each time point, for the next entry of the sequence, an item is drawn, iid (Sect. 2.1.1). However, the SD \mathcal{P} changes from time to time, such as certain item(s) being removed and new item(s) inserted in \mathcal{P} . In the above example, in changing from the left (initial) $\mathcal{P}^{(1)}$ to the right distribution, $\mathcal{P}^{(2)}$ (at $t = 700$), A is dropped (becomes 0 PR), while H and C are inserted, and W increases in PR while B is unchanged.

the proposed algorithm, with a dynamic history size, is not empirically assessed (see Sections 5.8 and 9 for further details). Table 1 provides a summary of the main notations and terminology used in this paper. Sect. 3.6 describes the format we use for pseudocode, when we have presented pseudocode for a few functions.

2.1 Probabilities (PRs), Distributions (DIs), and Semi-distributions (SDs)

We use the abbreviation PR to refer to a probability, *i.e.* a real number in $[0, 1]$. Prediction is probabilistic, and in particular in terms of *semi-distributions*.⁹ A (categorical) semi-distribution (SD) \mathcal{W} , in this paper, is a real-valued (or PR-valued) function defined over a finite or infinite set of items $\mathcal{I} = \{0, 1, 2, \dots\}$, such that $\forall i, \mathcal{W}(i) \in [0, 1]$, and $\sum_{i \in \mathcal{I}} \mathcal{W}(i) \leq 1.0$. Whether or not \mathcal{I} is infinite, the *support*, denoted $\text{sup}(\mathcal{W})$, *i.e.* the set of items i with $\mathcal{W}(i) > 0$, is finite in the SDs that we work with in our experiments: In particular, $|\text{sup}(\mathcal{W})|$, at any time t , does not exceed 100s to 1000s depending on space limits on the predictor (or algorithmic parameters, Sect. 2.1.2). Let $a(\mathcal{W}) := \sum_{i \in \mathcal{I}} \mathcal{W}(i)$, *i.e.* the allocated probability mass of \mathcal{W} , and let $u(\mathcal{W}) := 1 - a(\mathcal{W})$, *i.e.* the unallocated or free mass of \mathcal{W} .¹⁰ When $a(\mathcal{W}) > 0$ we say \mathcal{W} is non-empty, and when $0 < a(\mathcal{W}) < 1$, we call \mathcal{W} a *strict* SD. Let $\min(\mathcal{W}) := \min_{i \in \text{sup}(\mathcal{W}(i))} \mathcal{W}(i)$, and defined as 0 when \mathcal{W} is empty. A useful view (when evaluating, see Sect. 3.10, and in proofs, see *augmenting* in Sect. A.3) is to imagine that the free mass $u(\mathcal{W})$ is given to a special item (not seen in the input stream), yielding a *distribution*: A probability distribution (DI) \mathcal{W} is a special case of a SD, where $a(\mathcal{W}) = 1$. From a geometric viewpoint, DIs are points on the surface of a unit-simplex, while SDs can reside in the interior of the simplex too: a typical predictor’s predictions SD \mathcal{W} starts at 0, the empty SD, and, with many updates to it, moves towards the surface of the simplex. The prediction output¹¹ at a certain time t is denoted $\mathcal{W}^{(t)}$,

⁹We are borrowing the naming used in [21]. Other names include sub-distribution and partial distribution.

¹⁰To help clarity, we often use the symbol ‘:=’ to stand for “defined as” when defining and introducing notation. We will use the plain equal sign, ‘=’, for making claims or stating properties, for instance $u(\mathcal{W}) + a(\mathcal{W}) = 1$.

¹¹Following literature on partially observed Markov decision processes, we could also say that each predictor maintains a *belief state*, a SD here, which it reveals or outputs whenever requested.

and we can imagine that a prediction method is any online technique for converting a sequence of observations, $[o]_1^N$, one observation at a time, into a sequence of predictions $[\mathcal{W}]_1^N$ (of equal length N), as shown in Fig. 2(b). But note that $\mathcal{W}^{(t)}$ is output before observing $o^{(t)}$ (prediction occurs before observing and updating). We use \mathcal{P} to refer to an underlying or actual SD generating the observations, in the ideal setting (see next), and \mathcal{W} to refer to estimates and prediction outputs (often strict SDs), and $\mathcal{W}^{(t)}$ form *moving* (changing) SDs.

A SD is implemented via a map data structure:¹² item \rightarrow PR (or $\mathcal{I} \rightarrow [0, 1]$), where the keys are item ids and the values are PRs (usually positive). The map can be empty, *i.e.* no predictions (for instance, initially at $t = 1$). $\mathcal{W}(i)$ is 0 if item i is not in the map. Periodically, the maps are pruned, items with smallest PRs dropped, for space and time efficiency.

We use braces and colons for presenting example SDs (as in the Python programming language). For instance, with $\mathcal{P} = \{0:0.5, 1:0.2\}$, \mathcal{P} has support size of 2, corresponding to a binary event, and item 0 has PR 0.5, and 1 has probability 0.2, $\min(\mathcal{P}) = 0.2$, $\mathbf{a}(\mathcal{P}) = 0.7$, and $\mathbf{u}(\mathcal{P}) = 0.3$, so \mathcal{P} is a strict SD in this example.

2.1.1 Generating Sequences: an Idealized Stream

We develop prediction algorithms with an idealized non-stationary setting in mind, which we describe next. Under the *stationary iid assumption* or generation setting, an idealized setting, we imagine the sequence of observations being generated via independently and identically drawing (iid) items, at each time point, from a true (actual or underlying categorical) SD \mathcal{P} . Because $\mathbf{a}(\mathcal{P})$ can be less than 1, not exhaustively covering the probability space, we explain what it means to generate from a SD below. Under an **idealized but non-stationary** setting, we assume the sequence of observations is the concatenation of subsequences, of possibly different lengths, where each subsequence follows the stationarity setting, and is long enough for (approximately) learning its PRs. Thus one can imagine a sequence of SDs $[\mathcal{P}] = \mathcal{P}^{(1)}, \mathcal{P}^{(2)}, \dots$ (moving SDs, Fig. 1(b)), and the j th *stable subsequence* of observations, $[o]_{t_j}^{t_{j+1}}$, is generated by $\mathcal{P}^{(j)}$, for the duration $[t_j, t_{j+1}]$ (and $\mathcal{P}^{(j+1)}$ generates for $[t_{j+1} + 1, \dots]$). Each (stable) subsequence corresponds to a *stable* period or phase, stationary iid setting, where the underlying SD \mathcal{P} is not changing. This assumption of periods of stability are also similarly described in [58], who study keeping track of a changing multinomial distribution with fixed known number of items k (see Sect. 9 for further discussion). We assume that each stable subsequence is long enough for learning the new PRs: any item with a new PR should remain stable for some time, *i.e.* *be observed sufficiently many times*, before its PR changes in a subsequent SD \mathcal{P} . In synthetic experiments (Sect. 7.2 and 7.3), we use an observation-count threshold O_{\min} as a way of controlling the degree of non-stationarity, and we report the prediction performance of various predictors under different O_{\min} settings. See also Sect. F.2 on how the concept generation speed (the rate of generation of new items) can be controlled within Prediction Games, which influences the extent of (internal) non-stationarity.

2.1.2 Salient and Noise (NS) Items, and Generating with Noise

In this paper, we are interested in predicting and evaluating PRs p that are sufficiently large, $p \geq p_{\min}$, where the support threshold $p_{\min} = 0.01$ in most experiments. With respect to a SD \mathcal{W} , an item i is said to be *salient* iff $\mathcal{W}(i) \geq p_{\min}$, and otherwise it is *NS* (non-salient, or noise, or not seen recently sufficiently often). If \mathcal{W} is the output of a predictor, we say the predictor (currently) regards i as salient or NS as appropriate. In synthetic experiments, when the underlying SD \mathcal{P} is known, an item is either truly salient or NS, and as \mathcal{P} is changed, the same item i may be NS at one point ($\mathcal{P}^{(t)}(i) < p_{\min}$), and become salient at another ($\mathcal{P}^{(t+1)}(i) \geq p_{\min}$), and change status several times.¹³ In practice, in evaluations, when we do not have access to a true \mathcal{P} , we use a simple NS marker based on whether an item has occurred sufficiently often recently (see 3.5). A challenge for any predictor is to quickly learn to predict new salient items while ignoring the noise.¹⁴

For sequence generation, when drawing from a SD \mathcal{P} , with probability $\mathbf{u}(\mathcal{P}) = 1 - \mathbf{a}(\mathcal{P})$ we generate a noise (NS) item. A simple option that we use in most experiments is to generate a unique noise id: the item will appear only once in the sequence. Sect. 7.3 explains how we generate sequences with NS items in the synthetic experiments,

¹²Although a list or array of key-value pairs may suffice when the list is not large or efficient random-access to an arbitrary item is not required. In this paper, prediction provides the PRs for all items represented, thus all items are visited, and updating takes similar time. See also Sect. D.1.

¹³The concept of out-of-vocabulary (OOV) in language modeling is similar. Here, the idea of NS items is more dynamic.

¹⁴Noise, as we have defined, is relative and practical, and arises from the finiteness of the memory of a predictor along with other computational constraints (applicable to any practical predictor, and similar to randomness defined relative to computational constraints). Given a finite-space predictor with k bits of space, an item can have positive but sufficiently low frequency, below 2^{-k} , therefore not be technically noise, but that would foil the finite-space predictor. Identifying true noise would require access to the infinite stream.

and discusses alternative methods (see also 3.8 on drawing items from SDs). For evaluation too, NS items need to be handled carefully, specially when using log-loss. See Sect. 3.5.

2.1.3 Binary Sequences, and the Stationary Binary Setting

The *stationary binary setting*, and binary sequences generated in such settings, will be useful in the empirical and theoretical analyses of the prediction techniques we develop. A stationary binary sequence can be generated via iid drawing from a DI $\mathcal{P} = \{1: p^*, 0: 1 - p^*\}$, where $p^* > 0$ is the *true or target* PR to estimate well via a predictor that processes the binary sequence. A binary sequence also arises whenever we focus on a single item, say item A , in a given original sequence containing many (unique) items. The original sequence $[o]$ is converted to a binary $[o_b]$, $[o] \rightarrow [o_b]$, in the following manner: if $o^{(t)} = A$ then $o_b^{(t)} = 1$, and $o_b^{(t)} = 0$ otherwise (or $o_b^{(t)} = [[o^{(t)} = A]]$, where $[[x]]$ denotes the Iverson bracket on the Boolean condition x).

2.1.4 Examples and Possibilities

The ideal generation model described encompasses a variety of challenging possibilities: a salient item’s PR may change suddenly and by small (drifts) or large amounts, an extreme case being its PR changing to zero or below the support threshold p_{min} (disappearance). One salient item, with say probability 0.03 may remain stable for a long time, while other items, possibly with higher PRs, may keep changing (shifting or oscillating or disappearing and reappearing). Sect. 7.2 explores a setting involving oscillations between two values. A good predictor makes (substantial) changes to its PR estimates only when appropriate (keeping PR estimates of stable items stable). The proportion of the noise items in the stream can change too, *e.g.* from 0.01 to 0.05 (proportion of the stream), to 0.1 and back. An online predictor needs to cope with and track such changes effectively. A good evaluation technique should also appropriately reward robust tracking, for detecting changes not only in the PR estimations of the salient items but also the mass allocated to the NS (noise) portion of the stream (Sect. 3.5).

Of course, real-world sequences can be even more complex and deviate from the above idealization in multiple (non-iid sampling) ways, motivating empirical comparisons of the SMAs that we develop on real-world datasets.

2.2 Prediction Techniques: Sparse Moving Averages (SMAs)

We refer to the predictors we develop as *sparse (multiclass) moving averages* (SMAs), such as the sparse EMA predictor (Sect. 4) and the Qs predictor (Sect. 5). A moving average in its most basic form tracks the changes of a scalar value by keeping a running (recency-biased) average. Here, instead of a scalar, the observation at time t can be viewed as a sparse (possibly infinite) vector of 0s with a single 1 at the dimension equal to the id of the observed item [47, 74],¹⁵ and the techniques developed and studied here are different ways of keeping *several* running averages, *i.e.* estimated proportions of the items deemed salient, to predict the future probabilistically. The number of proportions that are tracked is also kept under a limit, *i.e.* kept sparse, for space and time efficiency.

Note that there are two major motivations for having a limited (sparse) memory: one stemming from resource boundedness or the need for space and time efficiency, and another for adapting to non-stationarities. The two goals or considerations can be consistent or can trade off.

Note also that with an all-knowing adversary generating the input sequence, in particular knowing the workings of the predictor, as soon as positive PRs are output by the predictor for an item, the adversary can change the subsequent proportion of that item in the remainder of the stream, for instance to 0, rendering the PR predictions of the predictor, as soon as they become available, useless. Our basic assumption is that realistic streams have structure and are not generated by such adversaries.

3 Evaluating Probabilistic Predictors

In this section we develop and discuss techniques for evaluating open-ended probabilistic multiclass sequential prediction in the face of non-stationarity, in particular so that we can compare different prediction techniques. As Fig. 2(b) shows, a prediction technique is any method that converts a sequence of observations, $[o]_1^N$, into a same-length sequence, $[\mathcal{W}]_1^N$, of predictions, each sequence member $\mathcal{W}^{(t)}$ is an SD, where $\mathcal{W}^{(t)}$ is output before $o^{(t)}$ is observed. We develop methods for evaluating the predictions $[\mathcal{W}]_1^N$, given $[o]_1^N$, and possibly other extra information. A minimal desirable would be that in the stationary iid setting, when there is a true non-changing model (a distribution) that is

¹⁵Variations of the task are plausible and useful too, that is zero or more than a single 1, but relatively few, in the input vector. We focus on the multiclass case (exactly one 1) in this paper.

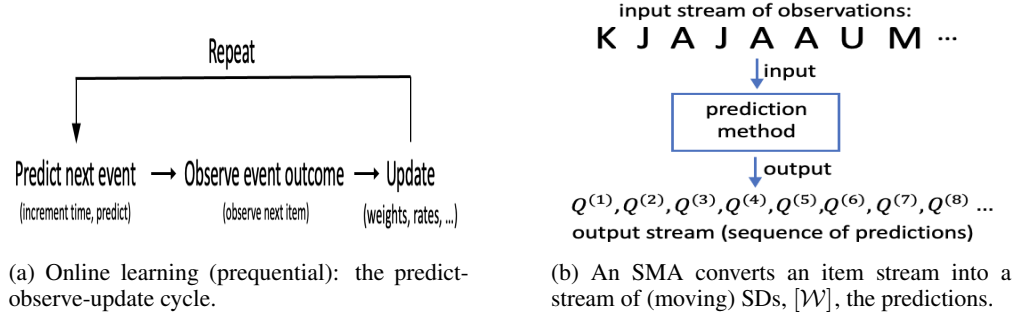


Figure 2: (a) Online processing a stream or sequence means repeating the prequential *predict-observe-update* cycle
(b) An SMA converts a stream of item observations, $[o]$, to a stream of predictions, $[\mathcal{W}]$, or $[o]_1^N \rightarrow [\mathcal{W}]_1^N$.

generating the data, that a predictor quickly converges in its predictions to a good approximation of the true model. We develop this further next. We then describe and motivate proper scoring (under unknown true probabilities) and explain why we prefer log-loss (logarithmic loss) over quadratic loss, and adapt log-loss to SDs, and the challenges of noise and non-stationarity.

3.1 Deviation Rates: when True PRs are Known

For the purposes of evaluating the estimated PRs, we first assume we know the true PRs, which is the case in our synthetic experiments (Sect. 7). In particular, we begin with the binary iid setting of Sect. 2.1.3 where we have a generated binary sequence with p^* being the PR of 1. We take a prediction method and feed it this sequence: it processes this sequence and generates a sequence of probability estimates. Let $[\hat{p}]_1^N$ denote its sequence of estimates for the positive, 1, outcome. Thus $\hat{p}^{(t)}$ is the estimated PR at time t , $\hat{p}^{(t)} \geq 0$. Here, we motivate performance or error measures (quality of output probabilities) that are based on relative error or ratio, a function of $\frac{\hat{p}^{(t)}}{p^*}$, vs. based on the difference in magnitude $p^* - \hat{p}^{(t)}$ (such as the quadratic $(p^* - \hat{p}^{(t)})^2$).

In many applications, including the Prediction Games setting, different items carry different rewards, and the system needs to select a subset of items to optimize an expected utility measure (expected reward). Sufficient accuracy of the PRs that the different items receive is important. While we do not specify the rewards in this paper, nor the particular way the expected reward is computed, in general, we seek to limit the *relative* error in estimating probabilities. For instance, as we are computing expectations, confusing a one-in-twenty event (true PR or target probability $p^* = 0.05$) with a one-in-one-hundred event ($p^* = 0.01$), could be considered a worse error, compared to predicting an event with $p^* = 0.55$ with an estimated PR of 0.5 (even though the absolute difference of the latter two is higher).

In particular, with the true probability p^* , $p^* > 0$, and the estimates $\hat{p}^{(t)}$ forming a sequence $[\hat{p}]_1^N$, for a choice of a deviation bound d , eg $d = 2$, we define the *deviation-rate* $dev([\hat{p}]_1^N, p^*, d)$ as the following sequence average:

$$dev([\hat{p}]_1^N, p^*, d) = \frac{1}{N} \sum_{t=1}^N deviates(\hat{p}^{(t)}, p^*, d) \quad (\text{the deviation rate, with } p^* > 0) \quad (1)$$

$$deviates(\hat{p}, p^*, d) = \left[\left[\hat{p} = 0, \text{ or (otherwise), } \max\left(\frac{p^*}{\hat{p}}, \frac{\hat{p}}{p^*}\right) > d \right] \right] \quad (\text{it is 0 or 1}) \quad (2)$$

where $[[x]]$ is the Iverson bracket, yielding value 1 when condition x is true, and 0 otherwise. Note that when \hat{p} is 0, the condition is true and $deviates(0, p^*, d)$ is 1 for any d . We seek a small *deviation-rate*, i.e. a large deviation, when $\max(\frac{p^*}{\hat{p}^{(t)}}, \frac{\hat{p}^{(t)}}{p^*}) > d$, occurs on a sufficiently small fraction of times t only, e.g. say 10% of the time or less. While initially, the first few times a predictor observes an item, we may get large deviations, we seek methods that reach lowest possible deviation-rates as fast as possible. We do not specify what d should be, nor what an acceptable deviation rate would be (which depends on the sequence, i.e. what is feasible, in addition to the prediction method), but, in our synthetic experiments (Sect. 7), where we know the true PRs, we report deviation rates for a few choices

of d . More generally, we track multiple item PRs, and we will report two variations: at any time t , when the observed item’s estimated PR deviates, and when *any* (salient) item in \mathcal{P} suffers too large of a deviation (Sect. 7.3).

Deviation rates are easy to understand (interpretable), but often in real-world settings, we do not have access to true PRs. Therefore, we also report on *logarithmic loss* (*log-loss*), and this approach is discussed and developed next, in particular for the case of SDs and NS items.

3.2 Unknown True PRs: Proper Scoring

Data streams from a real world application are often the result of the confluence of multiple interacting and changing (external) complex processes. But even if we assume there is a (stationary) DI \mathcal{P} that is sampled iid, and thus true PRs exist, remaining valid for some period of time, see Sect. 2.1.1), most often, we do not have access to \mathcal{P} . This is a major challenge to evaluating probabilistic predictions. There exist much work and considerable published research literature, in diverse domains such as meteorology and finance, addressing the issues of unknown underlying PRs, when predicting with (estimated) PRs. In particular, the concept of *proper scoring rules* has been developed to encourage *reliable* probability forecasts¹⁶ [9, 28, 70, 77, 27, 22, 71]. A proper scoring rule would lead to the best possible score (lowest if defined as costs, as we do here) if the technique’s PR outputs matched the true PRs. Not all scoring rules are proper, for instance, plain absolute loss (and linear scoring) is not proper [9]. And some are *strictly* proper, *i.e.* the true DI is the unique minimizer of the score [27]. Two major families of proper scoring rules are either based on (simple functions of) the predicted PRs raised to a power, a quadratic variant is named after Brier [9], or based on the logarithm (log probability ratios) [28, 70]: log-loss and variants. Propriety may not be sufficient, and a scoring rule also implicitly imposes measures of closeness or (statistical) distance on the space of candidate SDs, and we may prefer one score over another based on their differences in sensitivity.

We review proper scoring and the two major proper scorers below, log-loss and quadratic loss, specializing their distance property for our more general setting of SDs in particular, and we argue below, that in our utility-based or reward-based application, we strongly favor log-loss over quadratic scoring, for its better support for PRs with different scales and decision theoretic use of the estimations. This is despite several very desirable properties of the quadratic (such as boundedness and symmetry) in contrast to log-loss, and that we have to do extra work to adapt log-loss for handling 0 PRs (NS items). See also [19, 56] for other considerations in favor of log-loss. We note that our proposal for evaluating the noise portion of the stream is useful under either loss (see Sect. 3.10), and our code reports either loss [44].

3.3 Scoring Semi-Distributions (SDs)

For scoring (evaluating) a candidate distribution, we assume there exists the actual or true, but unknown, distribution (DI) \mathcal{P} . We are given a candidate SD \mathcal{W} (*e.g.*, the output of a predictor), as well as N data points, or a sequence of N observations $[o]_1^N$, $t = 1, \dots, N$, to (empirically) score the candidate. Recall that we always assume that the support set of a SD is finite, and here we can assume the set \mathcal{I} over which \mathcal{P} and \mathcal{W} are defined is finite too, *e.g.* the union of the supports of both. It is possible that the supports are different, *i.e.* there is some item j that $\mathcal{W}(j) > 0$, but $\mathcal{P}(j) = 0$, and vice versa.

A major point of scoring is to assess which of several SD candidates is best, *i.e.* closest to the true \mathcal{P} in some (acceptable) sense, even though we do not have access to the DI \mathcal{P} . It is assumed that for the time period of interest, the true generating DI \mathcal{P} is not changing, and the data points are drawn iid from it. The score of a SD \mathcal{W} is an expectation, and different scorers define the real-valued function $\text{ScoringRule}(\mathcal{W}, o)$ (*i.e.* the “scoring rule”) differently:

$$\mathcal{L}(\mathcal{W}|\mathcal{P}) = \mathbb{E}_{o \sim \mathcal{P}}(\text{ScoringRule}(\mathcal{W}, o)) \quad (\text{loss of a SD } \mathcal{W}, \text{ given true DI } \mathcal{P}) \quad (3)$$

Thus the $\mathcal{L}()$ (score) of a SD \mathcal{W} is the expected value of the function $\text{ScoringRule}()$, where the expectation is taken with respect to (wrt) the true DI \mathcal{P} .¹⁷ In practice, we compute the average $\tilde{\mathcal{L}}()$ as an empirical estimate of \mathcal{L} :

$$\tilde{\mathcal{L}}(\mathcal{W}, [o]_1^N) = \frac{1}{N} \sum_{t=1}^N \text{ScoringRule}(\mathcal{W}, o^{(t)}) \quad (\text{an empirical estimate of loss}) \quad (4)$$

¹⁶Other terms, or related concepts, used in the literature include calibrated, honest, trust-worthy, and incentive-compatible probabilities.

¹⁷Following [65], we have used the conditional probability notation (the vertical bar), but with the related meaning here that the loss (or score) is wrt an assumed underlying DI \mathcal{P} generating the observations (instead of being wrt an event).

computed on the N data points $[o]_1^N$ (assumed drawn iid from \mathcal{P}). Thus, for scoring a candidate SD \mathcal{W} , *i.e.* computing its (average) score, we do not need to know the true DI \mathcal{P} , but only need a sufficiently large sample of N points drawn iid from it. However, for understanding the properties of a scoring rule, the actual SD \mathcal{P} is important. In particular, as further touched on below, the score is really a function of an (implicit) statistical distance between the true and candidate distributions. The details of the scoring rule definition, `ScoringRule()`, determines this distance. Different scoring functions differ on the scoring rule `ScoringRule(\mathcal{W}, o)`, *i.e.* how the PR outputs of SD, given the observed item was o , is scored. We also note that the minimum possible score, when $\mathcal{W} = \mathcal{P}$ (for strictly proper losses), can be nonzero. We next develop a bounded version of log-loss. Appendix A.1 explains why the \mathcal{L}_2 (Brier) loss is not sufficiently sensitive and does not suit our task, despite several attractive properties.

3.4 On the Sensitivity of log-loss

The LogLoss and the log rule are based on simply taking the $\ln()$ (the natural log) of the probability estimated for the observation o [28, 70], and thus should be sensitive to relative changes in the PRs (PR ratios):

$$\text{LogLoss}(\mathcal{W}|\mathcal{P}) := \mathbb{E}_{o \sim \mathcal{P}}(\text{LogRule}(\mathcal{W}, o)), \text{ where } \text{LogRule}(\mathcal{W}, o) = -\ln(\mathcal{W}(o)). \quad (5)$$

The scoring rule can be viewed as the well-known KL (Kulback-Leibler) divergence of \mathcal{W} from the Kronecker vector, *i.e.* the distribution vector with all 0s and a 1 on the dimension corresponding to the observed item o . This boils down to $-\ln(\mathcal{W}(o))$. Similar to the development for \mathcal{L}_2 , where QRule is shown in terms of the Euclidean distance (Appendix A.1, Lemma 4), here LogLoss can be shown to correspond to the KL divergence [36, 12] on SDs:

Definition 1. *The entropy of a non-empty SD \mathcal{P} is defined as:*

$$H(\mathcal{P}) = -\sum_{i \in \mathcal{I}} \mathcal{P}(i) \ln(\mathcal{P}(i)) \quad (6)$$

The KL divergence of \mathcal{W} from \mathcal{P} (asymmetric), also known as the relative entropy, denoted $KL(\mathcal{P}||\mathcal{W})$, is a functional, defined here for non-empty SD \mathcal{P} and SD \mathcal{W} :

$$KL(\mathcal{P}||\mathcal{W}) := \sum_{i \in \mathcal{I}} \mathcal{P}(i) \ln \frac{\mathcal{P}(i)}{\mathcal{W}(i)}. \quad (7)$$

Note that in both definitions, by convention (similar to the case for DIs in [12]), when $\mathcal{P}(i) = 0$, we take the product $\mathcal{P}(i) \ln(x)$ to be 0 (or i need only go over $\text{sup}(\mathcal{P})$, in the above definitions). The divergence $KL(\mathcal{P}||\mathcal{W})$ can also be infinite (denoted $+\infty$) when $\mathcal{P}(i) > 0$ and $\mathcal{W}(i) = 0$.

Lemma 1. *Given DI \mathcal{P} and SD \mathcal{W} , defined over the same finite set \mathcal{I} ,*

$$\text{LogLoss}(\mathcal{W}|\mathcal{P}) = H(\mathcal{P}) + KL(\mathcal{P}||\mathcal{W}).$$

This is established when both are DIs, for example by [65], and the derivation does not change when \mathcal{W} is a SD: $\text{LogLoss}(\mathcal{W}|\mathcal{P}) = -\sum_{i \in \text{sup}(\mathcal{P})} \mathcal{P}(i) \ln(\mathcal{W}(i)) = -\sum_{i \in \text{sup}(\mathcal{P})} \mathcal{P}(i) \ln(\mathcal{W}(i)) - H(\mathcal{P}) + H(\mathcal{P})$ (*i.e.* add and subtract $H(\mathcal{P})$), and noting that the first two terms is a rewriting of the $KL()$, establishes the lemma.

Note that the entropy term in log-loss is a fixed positive offset: only $KL()$ changes when we try different candidate SDs with the same underlying \mathcal{P} . As in Sect. A.1 (for \mathcal{L}_2 and Euclidean), this connection to distance helps us see several properties of LogLoss. From the properties of KL [12], it follows that LogLoss is strictly proper (and asymmetric, unlike \mathcal{L}_2). Furthermore, the expression for KL divergence helps us see that log-loss is indeed sensitive to the ratios (of true to candidate probabilities). In particular, log-loss can grow without limit or simply **explode** (*i.e.* become infinite) when $\mathcal{P}(i) > 0$ and $\mathcal{W}(i) = 0$, for instance, in our sequential prediction task, when an item has not been seen before. We discuss handling such cases in the next section. On the other hand, we note that the dependence on the ratio is dampened with a $\ln()$ and weighted by the magnitude of the true PRs, as we take an expectation. In particular, we have the following property, a corollary of the connection to $KL()$, which quantifies and highlights the extent of this ratio dependence:

Corollary 1. *(LogLoss is much more sensitive to relative changes in larger PRs) Let \mathcal{P} be a DI over two or more items (dimensions), with $\mathcal{P}(1) > \mathcal{P}(2) > 0$, and let $m = \frac{\mathcal{P}(1)}{\mathcal{P}(2)}$ (thus $m > 1$). Consider two SDs \mathcal{W}_1 and \mathcal{W}_2 , with \mathcal{W}_1 differing with \mathcal{P} on item 1 only, in particular $\mathcal{P}(1) > \mathcal{W}_1(1) > 0$, and let $m_1 = \frac{\mathcal{P}(1)}{\mathcal{W}_1(1)}$ (thus, $m_1 > 1$). Similarly, assume \mathcal{W}_2 differs with \mathcal{P} on item 2 only, and that $\mathcal{P}(2) > \mathcal{W}_2(2) > 0$, and let $m_2 = \frac{\mathcal{P}(2)}{\mathcal{W}_2(2)}$. We have $\text{LogLoss}(\mathcal{W}_2|\mathcal{P}) < \text{LogLoss}(\mathcal{W}_1|\mathcal{P})$ for any $m_2 < m_1^m$.*

<pre> FC(\mathcal{W}) // Filter & cap \mathcal{W}. // \mathcal{W} is an item to PR map. // Parameters: p_{NS}, p_{min}, both in $[0, 1]$ $\mathcal{W}' \leftarrow \text{ScaleDrop}(\mathcal{W}, 1.0, p_{min})$ // Filter If $a(\mathcal{W}') \leq 1.0 - p_{NS}$: // Already capped? Return \mathcal{W}' // Nothing left to do. <math>\alpha \leftarrow \frac{1-p_{NS}}{a(\mathcal{W}')} // Scale down by α. Return $\text{ScaleDrop}(\mathcal{W}', \alpha, p_{min})$ ScaleDrop($\mathcal{W}, \alpha, p_{min}$) // Filter and scale. $scaled \leftarrow \{\}$ For item i, PR $prob$ in \mathcal{W}: $prob \leftarrow \alpha * prob$ If $prob \geq p_{min}$: // Keep the salient. $scaled[i] \leftarrow prob$ Return $scaled$ </math></pre> <p>(a) Filtering & capping a map \mathcal{W}, yielding a constrained SD: no small PRs and the sum is capped.</p>	<pre> loglossRuleNS($o, \mathcal{W}, markedNS$) // Parameters: p_{NS}, p_{min}. The current // observation is o, and \mathcal{W} is the // predictions (an item to PR map). $\mathcal{W}' \leftarrow \text{FC}(\mathcal{W})$ // filter and cap \mathcal{W}. $prob \leftarrow \mathcal{W}'.get(o, 0.0)$ If $prob \geq p_{min}$: // $o \in \text{sup } \mathcal{W}'$? Return $-\ln(prob)$ // plain log-loss. // $o \notin \text{sup } \mathcal{W}'$: the predictor thinks o is // a new/noise item. The NS-marker If not $markedNS$: // disagrees. Return $-\ln(p_{NS})$ // highest loss. // They both agree o is NS // Use the unallocated PR mass, $u(\mathcal{W}')$. $p_{noise} \leftarrow u(\mathcal{W}')$ // note: $p_{noise} \geq p_{NS}$ Return $-\log(p_{noise})$ </pre> <p>(b) When computing log-loss, handling new or noise items (bounded loss when $p_{NS} > 0$).</p>
--	--

Figure 3: Functions used in evaluating the probabilities. (a) CapAndFilter() is applied to the output of any predictor, at every time t , before evaluation, performing filtering (dropping small PRs below p_{min}) and, if necessary, explicit capping, *i.e.* normalizing or scaling down, meaning that the final output will be a SD \mathcal{W}' , where $a(\mathcal{W}') \leq 1 - p_{NS}$ (or $u(\mathcal{W}') \geq p_{NS}$). $p_{NS} = p_{min} = 0.01$ in experiments. (b) Scoring via log-loss, handling NS items (bounded log-loss).

The proof is simple and goes by subtracting the losses, $\text{LogLoss}(\mathcal{W}_1|\mathcal{P}) - \text{LogLoss}(\mathcal{W}_2|\mathcal{P})$, and using the KL() expressions for the log-loss terms and simplifying (Appendix A). Thus, with a reasonably large multiple m, m_2 needs to be very large for $\text{LogLoss}(\mathcal{W}_2|\mathcal{P})$ to surpass $\text{LogLoss}(\mathcal{W}_1|\mathcal{P})$. As an example, let $\mathcal{P} = \{1:0.5, 2:0.05, 3:0.45\}$, then $m = 10$, and reduction by $m_1 \geq 1$, only in PR of item 1, yields $\text{LogLoss } l_1$ that is $\frac{m_1^{10}}{m_2}$ higher than $\text{LogLoss } l_2$ that would result from reducing PR of item 2 only, by m_2 . For example, with $\mathcal{W}_1 = \{1:0.25, 2:0.05, 3:0.45\}$, and with $\mathcal{W}_2 = \{1:0.5, 2:p, 3:0.45\}$, as long as $p > \frac{0.05}{2^{10}} \approx 10^{-4}$, $\text{LogLoss}(\mathcal{W}_1|\mathcal{P}) > \text{LogLoss}(\mathcal{W}_2|\mathcal{P})$ (or we have to reduce 0.05 a thousand times, 2^{10} , to match the impact of just halving 0.5 to 0.25).

When we report deviation-rates in synthetic experiments (Eq. 1), we ignore the magnitude of the PRs involved (as long as greater than p_{min}), but log-loss incorporates and is substantially sensitive to such. Because items with larger PRs are seen in the stream more often, such a dependence is warranted, specially when we use the PRs to optimize expected rewards (different predictands having different rewards). However, when a predictor has to support predictands with highly different PRs (*e.g.* at 0.5 and 0.05), we should anticipate that LogLoss scores will be substantially more sensitive to better estimating the higher PRs.

3.5 Developing log-loss for NS (Noise) Items

In our application, every so often a predictor observes new items that it should learn to predict well. For such an item o , $\mathcal{P}(o)$ was 0 before some time t , and $\mathcal{P}(o) \geq p_{min}$ after. Some proportion of the input stream will also consist of infrequent items, *i.e.* truly NS (noise) items, those whose frequency, within a reasonable recent time window, falls below p_{min} . A challenge for any predictor is to quickly learn to predict new salient items while ignoring the noise. Plain log-loss is infinite when the predictor assigns a zero PR to an observation o ($\mathcal{W}(o) = 0$), and more generally, large losses on infrequent items can dominate overall log-loss rendering comparing predictors using log-loss uninformative and useless. We need more care in handling such cases, if log-loss is to be useful for evaluation.

Our evaluation solution has 3 components:

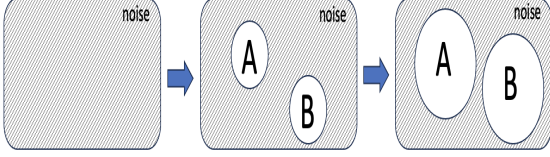
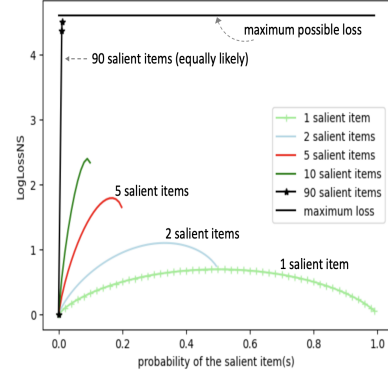
1. Ensuring that the output map of any predictor, whenever used for evaluation, is a SD \mathcal{W} such that $a(\mathcal{W}) \leq 1 - p_{NS}$, with $p_{NS} > 0$, thus some mass, $u(\mathcal{W}) \geq p_{NS}$, is left for possibly observing an NS item (the function $\text{FC}()$ in Fig. 3(a)).
2. Using a *simple NS-marker* algorithm, a (“third party”) “referee”, for determining NS status, as in Fig. 4(a).
3. A scoring rule (a policy) specifying how to score in various cases, *e.g.* based on whether or not an item is marked NS by the referee (the function $\text{loglossRuleNS}()$ in Fig. 3(b), a bounded version of log-loss).

```

isNS(o) // whether observation o is NS or not.
// Parameters: cNS (NS count threshold).
flaggedNS  $\leftarrow$  recentFrqMap.get(o, 0)  $\leq$  cNS
// Increment count of o.
Increment(o, recentFrqMap)
Return flaggedNS // Return the 0 or 1 decision.

```

(a) Pseudo code for a simple NS-marker.

(b) Venn diagram examples, depicting underlying SD \mathcal{P} with a background of noise, two salient items *A* and *B* growing in PRs as we go from left to right (middle $\mathcal{P}^{(2)}$ could be $\{A:0.1, B:0.1\}$), when plotting the lowest achievable loss in Fig. 4(c).

(c) Lowest achievable log-loss, via the LogLossNS() function, under a few generation regimes where salient items are equally likely.

Figure 4: (a) A simple NS-marker, a referee to mark an item NS or not, via a count map. In particular we used the Box technique of Sect. 5.8 (often with no limit on history size). (b) Venn diagrams, with background noise, are useful in picturing how sequences are generated, *e.g.* in synthetic experiments. Here, as we go from left to right in generating a lowest achievable loss plot of Fig. 4(c), three Venn digrams of the underlying SDs are shown for the case of two salient items (left $\mathcal{P}^{(1)} = \{\}$ while right $\mathcal{P}^{(3)}$ could be $\{A:0.25, B:0.25\}$). (c) Optimal (lowest achievable) log-loss using the LogLossNS() function of Fig. 3, as the PR of *k* salient items, all equally likely, is increased to maximum possible ($1/k$), from left to right. The lowest loss is (near) 0 when any observed item is noise (on the left) or, on the right, when there is a single salient item with PR 1.0. Maximum loss, of any predictor (not just the optimum), never exceeds $-\ln(p_{\min})$ (≈ 4.6 in this paper, when $p_{\min} = 0.01$), and for the optimum here, it is reached when there are $k \approx \frac{1}{p_{\min}}$ salient items, each with max PR $\approx p_{\min}$.

Fig. 3(a) shows the pseudocode for filtering and capping, FC(), applied to the output of any prediction method, before we evaluate its output. The only requirement on the input map \mathcal{W} passed to FC() is that the map values be non-negative. In this paper, all prediction methods output PR maps, *i.e.* with values in $[0, 1]$, though their sum can exceed 1.0. The function removes small values and ensures that the sum of the entries is no more than $1.0 - p_{NS}$, where $p_{NS} = 0.01$ in our experiments. Thus the output of FC(), a map, corresponds to a SD \mathcal{W}' such that $a(\mathcal{W}') \leq 1 - p_{NS}$ and $\min(\mathcal{W}') \geq p_{\min}$.

3.6 Notes on Pseudocode

We briefly describe how we present pseudocode, such as the examples of Fig. 3 and 4(b). The format is very similar to Python, *e.g.* using indentation to delimit a block such as function or loop body, and how we show iteration over the key and value pairs of a map. Function names are boldfaced. Importantly, not all parameters, such as flags, or state variables of a function, is given in its declaration to avoid clutter, but in the comments below its declaration, we explain the various variables used. In some cases, it is useful to think of a function as a method for an object, in object-oriented programming, with its state variables (or fields), some represented by data structures such as array or maps. For a map \mathcal{W} , $\mathcal{W}[i]$ is its value for key (item) *i*, but we also use $\mathcal{W}.get(i, 0)$ if we want to specify returning 0 when key *i* does not exist in the map. $\{\}$ denotes an empty map and $a(\mathcal{W})$ is the sum of its values (0 if empty map). We use \leftarrow for assignment, and $//$ to begin the comment lines (like C++). We favored simplicity and brevity at the cost of some loss in efficiency (*e.g.* some loops may be partially redundant). Not all the functions or the details are given (*e.g.* for the NS-marker of Fig. 4), but hopefully enough of such is presented to clarify how each function can work. The code, including several SMAs and a few sequences and evaluation utilities, in Python, is available on GitHub [44].

3.7 Empirical log-loss for NS (Noise) Items

Once we have an NS-marker and the $\text{FC}()$ function, given any observation $o^{(t)}$, and the predictions $\mathcal{W}^{(t)}$ (where we have applied $\text{FC}()$ to get the SD $\mathcal{W}^{(t)}$) and given the NS status of $o^{(t)}$ (via the NS-marker), we evaluate $\mathcal{W}^{(t)}$ using $\text{loglossRuleNS}()$, and take the average over the sequence:

$$\text{AvgLogLossNS}([\mathcal{W}]_1^N, [o]_1^N) = \frac{1}{N} \sum_{t=1}^N \text{loglossRuleNS}(o^{(t)}, \mathcal{W}^{(t)}, \text{isNS}(o^{(t)})) \quad (8)$$

The scoring rule $\text{loglossRuleNS}(o, \mathcal{W}, \text{isNS}(o))$ checks if there is a PR $p, p > 0$ assigned to o , $p = \mathcal{W}(o)$. If so, we must have $p \geq p_{\min}$ (from the definition of $\text{FC}()$), and the loss is $-\ln(p)$. Otherwise, if o is also marked NS (there is agreement), the loss is $\ln(1 - a(\mathcal{W}))$. From the definition of $\text{FC}()$, $1 - a(\mathcal{W}) \geq p_{\text{NS}}$. Finally, if o is not marked NS, the loss is $-\ln(p_{\text{NS}})$. In all cases, the maximum loss is $-\ln(p_{\text{NS}})$. Therefore, if we are interested in obtaining bounded losses then p_{NS} should be set to a positive value. On the other hand, if we are interested in learning a PR in a range down to a smallest value $p > 0$, then we should set p_{\min} to a value not higher than $p(1 - p_{\text{NS}})$ so items with PR as low as p are not possibly filtered in $\text{FC}()$ (see also Appendix A.3.3 on the threshold for distortion). p_{NS} should be set equal to p_{\min} in general: setting it lower unnecessarily punishes predictors for not predicting below $p_{\min} > p_{\text{NS}}$ (in $\text{loglossRuleNS}()$), and if set above p_{\min} , then a predictor need not bother learning to estimate around $p_{\min} < p_{\text{NS}}$ (the cost incurred for predicting noise or NS, $-\ln(p_{\text{NS}})$ would be better/lower). In our experiments, $p_{\min} = p_{\text{NS}} = 0.01$.

There are two parameters for the NS-marker, the size of the history (or window size) kept and the count threshold c_{NS} . For simplicity, no bound on length of the history is imposed in most evaluations (with an exception in Sect. 8.3.3). By default, we set $c_{\text{NS}} = 2$ for the NS-marker. This means an item is marked NS iff it has been seen $k \leq 2$ so far in the test sequence. Thus, to have low loss, a predictor should provide a (positive) PR after the 2nd observation of the item (for the 3rd and subsequent observations). We also report comparisons for other values in a few experiments to assess sensitivity of our comparisons to c_{NS} , and Sect. 8.3.3 reports on comparisons where the history is limited to the last 200. When comparing different predictors, computing and comparing $\text{AvgLogLossNS}()$ scores, we will often compare on the same exact sequences (with an identical NS-marker). We discuss a few alternative options to bounding log-loss and using a referee in the appendix, Sect. A.4.

3.8 The Near Propriety of loglossRuleNS

We first formalize drawing items using a SD \mathcal{P} , which enables us to define taking expectations wrt a SD \mathcal{P} . For this, it is helpful to define the operation of multiplying a scalar with a SD, or scaling a SD, which is also extensively used in the analysis of approximate propriety, Appendix A.3.

Definition 2. *Definitions related to generating sequences using a SD, and perfect filtering and NS-marker wrt to a SD:*

- (scaling a SD) Let SD \mathcal{P} be non-empty, i.e. $a(\mathcal{P}) \in (0, 1]$. Then, for $\alpha > 0, \alpha \leq \frac{1}{a(\mathcal{P})}$, $\mathcal{P}' := \alpha\mathcal{P}$ means the SD where $\sup(\mathcal{P}') := \sup(\mathcal{P})$ and $\forall i \in \sup(\mathcal{P}), \mathcal{P}'(i) := \alpha\mathcal{P}(i)$. When $\alpha = \frac{1}{a(\mathcal{P})}$, $\alpha\mathcal{P}$ is a DI and one can repeatedly draw iid from it.
- Drawing an item from a non-empty SD \mathcal{P} , denoted $o \sim \mathcal{P}$, means $a(\mathcal{P})$ of the time, drawing from $\alpha\mathcal{P}$, where $\alpha = \frac{1}{a(\mathcal{P})}$ (SD \mathcal{P} scaled up to a DI), and $1 - a(\mathcal{P})$ of the time generating a unique noise item. Repeatedly drawing items in this manner N times generates a sequence $[o]_1^N$ using \mathcal{P} ("iid drawing" from \mathcal{P}), and is denoted $[o]_1^N \sim \mathcal{P}$.
- (perfect marker) Given a non-empty SD \mathcal{P} , a perfect NS-marker wrt to \mathcal{P} , denoted $\text{isNS}_{\mathcal{P}}()$, marks an item i as NS iff $i \notin \sup(\mathcal{P})$.

Therefore, for a DI \mathcal{P} , the perfect NS-marker $\text{isNS}_{\mathcal{P}}()$ generates no NS markings on any sequence $[o]_1^N \sim \mathcal{P}$. More generally, for a SD \mathcal{P} , the perfect marker generates NS markings at about $u(\mathcal{P})$ fraction of the time on the stream $[o] \sim \mathcal{P}$. Appendix A.3.6 also defines a closer to practical threshold-marker.

Given a non-empty SD \mathcal{P} , $\text{FC}()$ and a perfect NS-marker $\text{isNS}_{\mathcal{P}}()$, $\text{LogLossNS}(\mathcal{W}|\mathcal{P})$ is defined as:

$$\text{LogLossNS}(\mathcal{W}|\mathcal{P}) := \mathbb{E}_{o \sim \mathcal{P}}(\text{loglossRuleNS}(o, \mathcal{W}, \text{isNS}_{\mathcal{P}}(o))) \quad (\text{log-loss for NS}) \quad (9)$$

Thus AvgLogLossNS() is the empirical average version of LogLossNS(), where we use a practical NS-marker instead of the perfect one.

3.9 Understanding the Behavior of LogLossNS

Fig. 4(c) shows the lowest achievable loss, the optimal loss, when using LogLossNS() in a few synthetic scenarios: as the PR of $k \geq 1$ equally likely salient items is raised from 0 to near k^{-1} each, and where we assume an item is marked seen only when its true PR is above p_{min} (and $p_{min} = p_{NS} = 0.01$). On the left extreme, there are no salient items (all PRs at 0 or below p_{min}), and a predictor achieves 0 loss by predicting an empty map, *i.e.* no salient items ($a(\mathcal{W}) = 0$). Here, both the NS-marker and the predictor agree that every observed item is noise. Next, consider the case of one (salient) item as its PR is raised from p_{min} . At the right extreme, where its probability nears 1.0, the minimum achievable loss approaches 0 as well. Note that due to the capping, we never get 0 loss (with $p_{NS} = 0.01$, we get $-\ln(0.99) \approx 0$). Midway, when p^* is around 0.5, we get the maximum of the optimum curve, yielding LogLossNS around $-\ln(0.5)$ (the salient item is observed half the time, and half the time both the NS-marker and predictor agree that the item observed is noise, with $p_{noise} = 0.5$). Similarly, for the scenarios with $k > 1$ items, the maximum optimal loss is reached when the items are assigned their maximum allowed probability, *i.e.* $\frac{1}{k}$.

Appendix A.3 gives other concrete examples of LogLossNS($\mathcal{W}|\mathcal{P}$) evaluation and develops some of its properties. For example, the minimizer of LogLossNS($\mathcal{W}|\mathcal{P}$) may not be \mathcal{P} (and may not be unique). We show that any minimizer \mathcal{W}^* cannot deviate from \mathcal{P} much, and has a certain form: certain low PR items of \mathcal{P} can be zeroed in \mathcal{W}^* , and their mass *proportionately* spread onto other (higher PR) items. This proportional spread implies low deviation when the total probability mass p of the low PR items of \mathcal{P} (near or below $p_{min} = p_{NS}$) is small. For instance, if the total such mass p is 0.1 in \mathcal{P} , then for any minimizer \mathcal{W}^* , the PR of any (salient) item i in \mathcal{W}^* , including the unassigned $u(\mathcal{W}^*)$, cannot deviate from its corresponding PR in \mathcal{P} by more than about 10% in a ratio sense: $\frac{\mathcal{W}^*(i)}{\mathcal{P}(i)} \leq 1.1$ (in general $\frac{1}{1-p}$, see A.3.5 and A.3.6). Note that comparators using LogLossNS($\mathcal{W}|\mathcal{P}$) would prefer a minimizer \mathcal{W}^* over other \mathcal{W} with high likelihood (would score it better, given a sufficiently large evaluation sample), motivating our focus on characterizing \mathcal{W}^* .

3.9.1 Visualizing Underlying SDs with Venn Diagrams

Fig. 4(b) shows a useful way to pictorially imagine a SD \mathcal{P} that is generating the observation sequence as a Venn diagram. Salient items (of \mathcal{P}) are against a background of noise, and when we change \mathcal{P} , for instance increase the PR of a salient item A , the area of its corresponding blob increases, and this increase can be obtained from reducing the area assigned to the background noise (as in Fig. 4(b) and the experiments of Fig. 4(c)), or one or more other salient item can shrink in area (while total area remaining constant at 1.0). When drawing, each item, including a noise item, is picked with probability proportional to its area.

3.10 Evaluating a Space-Bounded Predictor under Nonstationarity

We can use the same empirical evaluation log-loss formula of AvgLogLossNS() (Eq. 8) in the idealized non-stationary case, and as long as each subsequence is sufficiently long, a convergent prediction method should do well. In synthetic experiments, we try different minimum frequency requirements, O_{min} : an item needs to occur O_{min} times in a sequence before its probability can be changed. The lower the underlying p^* the more time points required before p^* is changed, as we expect one positive observation every $\frac{1}{p^*}$ time points. Note that if O_{min} is set too low, *e.g.* below 2 or 3, this would not allow sufficient time for learning a PR well, and the underlying p^* loses its meaning. We want a predictor that tracks changes in salient PRs well: a high PR item or items (*e.g.* above 0.1) may change in PR (*e.g.* disappear), while a low PR item (*e.g.* 0.03) may remain stable for a long time, or vice versa. The proportion of the mass that should be allotted to the noise portion of the stream can change too (*e.g.* from 0.1 to 0.5, then to 0.01, etc.) and good predictors should track such too (and, for example, not allocate all their mass onto the salient items). A good evaluation technique should score such honest and adaptive predictors well (see Appendix A.3.6). We note that evaluating proper PR assignment to the noise portion of the stream is applicable whether we use log-loss or \mathcal{L}_2 loss.

With real-world sequences, a variety of phenomena such as periodicity and other dependencies can violate the iid assumptions, and it is an empirical question whether, on real sequences, the predictors compare as anticipated based on their various, presumed or expected, strengths and weaknesses stemming from consideration of the ideal setting of Sect. 2.1.1. This underscores the importance of empirical experiments on different real-world sequences.

EmaUpdate(o) // latest observation o .

// $EmaMap$ is item to PR, learning rate $\beta \in (0, 1]$.

// Other param: $doHarmonicDecay$ flag.

For each item i in $EmaMap$:

$EmaMap[i] \leftarrow (1 - \beta) * EmaMap[i]$ // Weaken.

// Strengthen edge to o (insert edge if not there).

$EmaMap[o] \leftarrow EmaMap[o] + \beta$ // Boost.

If $doHarmonicDecay$: // reduce rate?

$\beta \leftarrow DecayRate(\beta)$ // see (b) and Sect. 4.3

(a) Plain EMA updating.

DecayRate(β)

// Other parameters: $\beta_{min} \in (0, 1)$, is the
// minimum allowed learning rate.

// $\beta_{max} \in (0, 1]$, is the maximum and
// the initial learning rate for EMA with
// harmonic decay.

$\beta \leftarrow \frac{1}{\frac{1}{\beta} + 1.0}$ // harmonic decay.

Return $\max(\beta, \beta_{min})$

(b) Harmonic decay of rate.

Figure 5: Pseudo code of (a) sparse EMA with a single learning rate β , either fixed (“static” EMA), or (b) decayed with a harmonic schedule down to a minimum β_{min} (“harmonic” EMA, Sect. 4.3). The working of an EMA update can be split in two steps (Fig. 6): 1) weaken, *i.e.* weaken all existing edge weights (entries of the map $EmaMap$), and 2) strengthen, *i.e.* boost (the weight of) the edge to the observed item (target). The map entry is created if it doesn’t already exist (edge insertion). Initially (at $t = 1$), there are no edges. EMA enjoys a number of desirable properties, such as the probabilities in $EmaMap$ forming a SD, and approximate convergence (Sect. 4).

deviation threshold \rightarrow	$d = 1.5$		$d = 2.0$	
learning rate \rightarrow	$\beta = p^*/5$	$\beta = p^*/20$	$\beta = p^*/5$	$\beta = p^*/20$
$p^* = 0.1$	47, 0.19 \pm 0.02	213, 0.01 \pm 0.01	35, 0.04 \pm 0.01	140, 0.001 \pm 0.002
$p^* = 0.01$	520, 0.20 \pm 0.08	2200, 0.04 \pm 0.05	350, 0.05 \pm 0.04	1400, 0.02 \pm 0.03

Table 2: 10k-long sequences, 500 trials, for two target probabilities p^* , $p^* = 0.1$ and $p^* = 0.01$, and for two β settings for EMA, $\frac{p^*}{5}$ and $\frac{p^*}{20}$, the first time EMA’s estimate $\hat{p}^{(t)}$ reaches to within deviation threshold d (averaged over the trials), and the deviation-rate thereafter (and the std over the 500 trials) are reported. The initial estimate is 0 ($\hat{p}^{(1)} = 0$). For instance, when $p^* = 0.1$, EMA with $\beta = \frac{p^*}{5} = 0.02$ takes 47 time points on average to reach within $d = 1.5$ of $p^* = 0.1$ and thereafter it has deviation-rate of 19% (while with $\beta = \frac{p^*}{20}$, it has only 1% deviation-rate). A higher rate leads to faster convergence for EMA, but also higher variance.

4 The (Sparse) EMA Predictor

Our first SMA is the sparse exponentiated moving average (EMA), which gets its name from exponentially decreasing multipliers over the past values (as a function of time, see part (a) of the comparison picture Fig. 12). In past work we developed a variant specially designed for multiclass ranking and classification, where we observed its advantages for non-stationary tasks [47, 45]. Here we develop and analyze sparse EMA, focusing on probability prediction. Fig. 5 presents pseudo code. The SMA keeps a map, of item to PR, and it can be shown that the map is always a SD [47]. Initially, at $t = 1$, the map is empty. Each map-entry can be viewed as a connection, or a prediction relation, a weighted directed edge, from the predictor to a predictand, where the weight is the current PR estimate for the predictand. Prediction is straightforward: output the map’s key-value (or key-PR) pairs. An EMA update is a convex combination of the present observation with the past (running) average.¹⁸ When learning proportions as in this paper, the observation is either 0 or 1, and the update can be broken into two phases, first a weakening of the weights, of edges to existing predictands, which can be seen as PRs flowing from existing edges into an implicit (available) PR reserve, and then a strengthening of the edge to the observed item, PR flowing from the reserve to the target edge, as pictured in Fig. 6. This picture is useful when we extend EMA (Sect. 6). We next describe PR and SD estimation and their challenges, in particular speed of convergence *vs.* variance, and handling non-stationarity (versions of plasticity *vs.* stability trade-offs [1, 53])¹⁹, motivating extensions of plain static (fixed-rate) EMA (Sect. 4.3), further developing techniques used later in Sect. 6.

¹⁸EMA (also, EWMA) and other moving averages can also be viewed as a type of filter in signal theory and a (time) convolution [11], and find a variety of applications, such as in time-series analysis and forecasting (*e.g.* [73, 48]), and in reinforcement learning for value function updates (in temporal difference learning, [68, 11]).

¹⁹A similar trade-off has been termed drift error *vs.* statistical (variance) error in computational learning theory (*e.g.* [50, 54]).

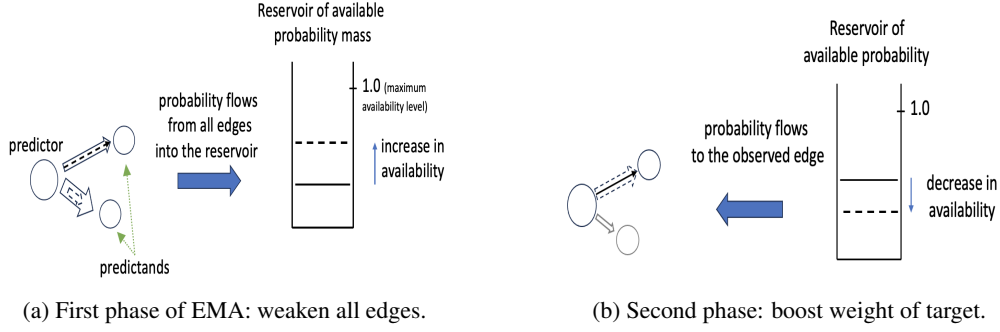


Figure 6: An EMA update can be seen as having two phases: *weaken-and-boost*. In the first phase, all existing edges from the predictor to the predictands (entries in the map) are weakened, which can be viewed as probability flowing from the edges to the reservoir of (unused or available) PR mass (the edges, after the weakening, reduced in weight, are shown smaller and dotted). In the 2nd phase, the edge to the observed item is strengthened. The reservoir is implicit: with SD \mathcal{W} corresponding to the map, the reservoir has PR mass $1 - a(\mathcal{W})$. Initially (at $t = 1$), with an empty map (no edges), the reservoir is full at 1.0.

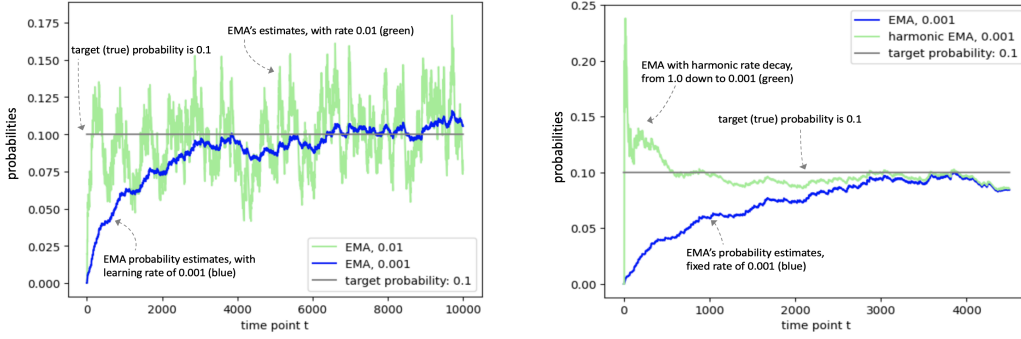


Figure 7: Given a single binary sequence, 10k long, with target $p^* = 0.1$ (the true PR of observing 1), convergence of the PR estimates, $\hat{p}^{(t)}$, by EMA variants: (a) for the static or fixed-rate version of EMA, under two different learning rates, $\beta = 0.01$ and $\beta = 0.001$. A higher rate, $\beta = 0.01$, can lead to faster convergence, but also causes high variance. (b) With harmonic decay, the estimates converge faster (possibly with a high-variance initial period).

4.1 Convergence

It can be shown that the EMA update, with $\beta \in [0, 1]$, preserves the SD property: when the PR map before the update corresponds to a SD $\mathcal{W}^{(t)}$, $\mathcal{W}^{(t+1)}$ (the map after the update) is a SD too. Furthermore, EMA enjoys several convergence properties under appropriate conditions, *e.g.* the sum of the edge weights (map entries) increases, converging to 1.0 (*i.e.* to a DI), and an EMA update can be seen to be following the gradient of quadratic loss [47]. Here, we are interested in convergence of the map weights as individual PR estimates.

In the stationary iid setting (Sect. 2.1.1), we show that the PR estimates of EMA converge, probabilistically, to the vicinity of the true PRs. We focus on the EMA estimates for one item or predictand, call it A : at each time point t , a positive update occurs when A is observed, and otherwise it is a negative update (a weakening), which leads to the stationary binary setting (Sect. 2.1.3), where the target PR is denoted p^* . The estimates of EMA for item A , denoted $\hat{p}^{(t)}$, form a random walk. While often, *i.e.* at many time points, it can be more likely that $\hat{p}^{(t)}$ moves away from p^* , such as when $\hat{p} \leq p^* < 0.5$, when \hat{p} does move closer to p^* (upon a positive observation), the gap reduces by a

relatively large amount. The following property, in particular, helps us show that the expected gap, $|p^* - \hat{p}|$, shrinks with an EMA update, under an appropriate condition. It also connects EMA's random walk, the evolution of the gaps for instance, to discrete-time martingales, fundamental to the analysis of probability and stochastic processes (*e.g.* the gap is a supermartingale when $\hat{p}^{(t)} < p^*$) [76, 66].

Lemma 2. *EMA's movements, i.e. changes in the estimate $\hat{p}^{(t)}$, satisfy the following properties, where $\beta \in [0, 1]$:*

1. *Maximum movement, or step size, no more than β : $\forall t, |\hat{p}^{(t+1)} - \hat{p}^{(t)}| \leq \beta$.*
2. *Expected movement is toward p^* : Let $\Delta^{(t)} := p^* - \hat{p}^{(t)}$. Then, $\mathbb{E}(\Delta^{(t+1)} | \hat{p}^{(t)} = p) = (1 - \beta)(p^* - p) = (1 - \beta)\Delta^{(t)}$.*
3. *Minimum expected progress size: With $\delta^{(t)} := |\Delta^{(t)}| - |\Delta^{(t+1)}|$, $\mathbb{E}(\delta^{(t)}) \geq \beta^2$ whenever $|\Delta^{(t)}| \geq \beta$ (i.e. whenever \hat{p} is sufficiently far from p^*).*

The lemma is established by writing down the expressions, for an EMA update and the gap expectation, and simplifying (see Appendix B). It follows that $\mathbb{E}(\hat{p}^{(t+1)} | \hat{p}^{(t)} = p^*) = p^*$ (or $\mathbb{E}(\Delta^{(t+1)} | \Delta^{(t)} = 0) = 0$), and the *expected direction* of movement is always toward p^* . The above property would imply that a positive gap should always shrink in expectation, *i.e.* $\mathbb{E}(|\Delta^{(t+1)}|) < |\Delta^{(t)}|$ when $|\Delta^{(t)}| > 0$, but there is an exception when \hat{p} is close to p^* , *e.g.* when $\hat{p} = p^*$. This also occurs with a high $\beta = 1.0$ rate: the expectation of distance $|\Delta^{(t+1)}|$ often expands when $\beta = 1.0$. However, it follows from the maximum movement property, that when \hat{p} is sufficiently far, at least β away from p^* , the sign of $\Delta^{(t)}$ does not change, and property 2 implies that the gap is indeed reduced in expectation (property 3), which we can use to show probabilistic convergence:

Theorem 1. *EMA, with a fixed rate of $\beta \in (0, 1]$, has an expected first-visit time bounded by $O(\beta^{-2})$ to within the band $p^* \pm \beta$. The required number of updates, for first-visit time, is lower bounded below by $\Omega(\beta^{-1})$.*

The proof, presented in Appendix B, works by using property 3 that expected progress toward p^* is at least β^2 while our random walker $\hat{p}^{(t)}$ is outside the band ($|p^* - \hat{p}^{(t)}| > \beta$). It would be good to tighten the gap between the lower and upper bounds. Table 2 suggests that the upper bound may be subquadratic, perhaps linear $\Theta(\beta^{-1})$. We expect that one can use techniques such as Chernoff bounds to show that the number of steps to a first time visit of the bound is also bounded by β^{-2} with very high probability, and that there exists a stationary distribution for the walk concentrated around p^* . We leave further characterizing the random walk to future work.

4.2 Convergence Speed vs. Accuracy Tradeoff

It follows from the lower bound, $\Omega(\frac{1}{\beta})$, that the smaller the rate β the longer it takes for \hat{p} to get close to p^* . A higher rate β , *e.g.* 0.01, require 10 times fewer observations than 0.001, or leads to faster convergence, for higher target PRs (with $p^* \gg \beta$). On the other hand, once sufficiently near the target PR p^* , we desire a low rate for EMA, to keep estimating the probability well (Fig. 7). Alternatively, a high rate would cause unwanted jitter or variance. Consider when $\beta \gtrsim p^*$, *i.e.* the β is itself near or exceeds the target p^* in magnitude. Then when the estimate is also near, $\hat{p} \approx p^*$, after an EMA positive update, we get $\hat{p} \gtrsim 2p^*$, or the relative error shoots from near 0 to near 100% (an error with the same magnitude as the target being estimated).²⁰

Once \hat{p} is sufficiently near, we can say we desire stability, better achieved with lower rates. At an extreme, if we knew that p^* would not change, and we were happy with our estimate \hat{p} , one could even set β to 0. In situations when we expect some non-stationarity, *e.g.* drifts in target PRs, this is not wise. A rule of thumb that reduces high deviation rates while being sensitive to target PR drifts, is to set β to, say, $\frac{p^*}{10}$, so that the deviation rate at $d = 1.5$ is no more 10% (some acceptable percentage of the time). As we don't know p^* , if we are interested in learning PRs in a range, *e.g.* $[0.01, 1.0]$, and we are using plain EMA, then we should consider setting β to $\frac{0.01}{10}$ (a function of the minimum of the target PR range).

4.3 From $\Omega(\beta^{-1})$ to $O(\frac{1}{p^*})$, via Rate Decay

The above analysis tells us that when we want to learn target PRs in a diverse range, such as $[0.01, 1.0]$, and when using plain fixed-rate (static) EMA, we need to use a low rate to make sure smaller PRs are learned well, which sacrifices

²⁰When the estimate is at target, $\hat{p}^{(t)} = p^*$, the only situation when there is no possible movement away from p^* is at the two extremes when $p^* = 1$ or $p^* = 0$ ($\hat{p}^{(t+1)} = p^*$ for any β , if $p^* \in \{0, 1\}$ and $\hat{p}^{(t)} = p^*$).

speed of convergence for larger p^* for accuracy on smaller ones: a relatively large target, say $p^* > 0.1$, requires 100s or 1000s of time points to converge to an acceptable deviation-rate with a low $\beta \approx 0.001$, instead of 10s, with $\beta \approx 0.01$. This motivates considering alternatives, such as EMA with a changing rate. A variant of EMA, which we will refer to as *harmonic EMA*, has a rate decaying over time with each update, in a *harmonic* manner. the rate $\beta^{(t)}$ starts at a high value $\beta^{(1)} = \beta_{max}$ (e.g. $\beta_{max} = 1.0$), and is reduced gradually with each (positive or negative) update, via:

$$\beta^{(t+1)} \leftarrow \left(\frac{1}{\beta^{(t)}} + 1 \right)^{-1} \quad (\text{the harmonic decay of the learning rate: a double reciprocal})$$

For instance, with $\beta^{(1)} = 1$, then $\beta^{(2)} = (1+1)^{-1} = \frac{1}{2}$, $\beta^{(3)} = ((\frac{1}{2})^{-1} + 1)^{-1} = \frac{1}{3}$, $\beta^{(4)} = \frac{1}{4}$, and so on, yielding the fractions in the harmonic series. We let the β go down to no lower than the floor $\beta_{min} \in (0, 1)$ as shown in Fig. 5(b), though making the minimum a fraction of the PR estimates may work better. Fig. 12(a) shows how past observations are down-weighted by this variant (and compared to plain static EMA and other SMAs). We have observed in prior work that such a decay regime is beneficial for faster learning of the higher PRs (e.g. $p^* \gtrsim 0.1$), as it is equivalent to simple counting and averaging to compute proportions.²¹ This does not negatively impact convergence or the error-rate on the lower PRs (such as $p^* \lesssim 0.05$). In particular, with harmonic-decay, one requires $O(\frac{1}{p^*})$ time points instead of $\Omega(\frac{1}{\beta})$ for convergence to within a positive (constant) multiplicative deviation d (Appendix A in [41]). Note that the changing rate β also indicates the predictor's confidence in its current estimate, assuming the target PR does not change: the lower the β compared to an estimate \hat{p} , the less likely \hat{p} will change substantially in subsequent updates.

This manner of changing the rate also establishes a connection between the learning-rate based EMA, and the counting-based methods of Sect. 5.

4.4 Non-Stationarity Motivates Per-Edge Learning Rates

The harmonic decay technique is, however, beneficial only initially for a predictor: once the learning rate is lowered, it is not raised again in plain EMA of Fig. 5. If one could increase the rate, the predictor could learn to predict a new item's PR faster. However, that disrupts the PR estimates for existing currently stable items. Different items should not, in general, interfere with one another: imagine a predictor already predicting an item A with a certain PR sufficiently well. Ideally learning to predict a new item B should not impact the PR of an existing item A , unless A and B are related, or correlated, such as when B is replacing A . This consideration motivates keeping a separate learning rate for each predictand, or per prediction edge (supporting edge-specific rates). Such extensions would be valuable if one could achieve them without adding substantial overhead, while keeping the desired convergence and SD preservation properties of EMA (Sect. 4.1). Section 6 describes a way of achieving this goal. To support the extension, we also need to detect changes, for when to increase a learning rate, and we next develop an SMA that can be used both for change detection, as well as for giving us the initial estimate for a (new) predictand's PR together with an initial learning rate. We expect that this type of predictor would have other uses as well (e.g. see Sect. D.1).

5 The Queues Predictor

We begin with the stationary setting for a binary event, continually estimating the PR of outcome 1 from observing a sequence of 0s and 1s. We then adapt the counting technique to the non-stationary case and present the queuing technique for efficiently tracking the PRs of multiple items. We conclude in Sect. 5.8 with a counting variant we call the Box predictor, that could also naturally be implemented via a queue for efficiency, and discuss a dynamic (adaptive windowing) variant of it. Appendices C and D contain further analyses as well as a more efficient variant of queuing.

5.1 The Stationary Binary Case

To keep track of the proportion of positive occurrences, two counters can be kept, one for the count of total observations, simply time t , and another for the count of positive observations, $N_p^{(t)}$. The probability of the target item, or the proportion of positives, at any point, could then be the ratio $\hat{p}^{(t)} = \frac{N_p^{(t)}}{t}$, which we just write as $\hat{p} = \frac{N_p}{t}$, when it is

²¹This manner of reducing the rate is equivalent to reduction based on the update count of EMA, and we referred to it as a count-based (or frequency-based) decay and it was shown equivalent to averaging [41]. To see the equivalence, one can expand and note the telescoping product, or use induction: The estimate after the update at $t, t \geq 2$ is $\hat{p}^{(t)} = \beta^{(t)} o^{(t)} + (1 - \beta^{(t)}) \hat{p}^{(t-1)}$, where $\beta^{(1)} = 1, \dots, \beta^{(t)} = \frac{1}{t}$, or $1 - \beta^{(t)} = \frac{t-1}{t}$, and we have $\hat{p}^{(t-1)} = \frac{\sum_{i=1}^{t-1} o^{(i)}}{t-1}$ (induction hypothesis), and combining, we obtain the simple average: $\hat{p}^{(t)} = \frac{\sum_{i=1}^t o^{(i)}}{t}$.

(positives observed) \rightarrow	$N_p=10$			$N_p=50$			$N_p=200$	
(deviation thresh.) $d \rightarrow$	1.1	1.5	2.0	1.1	1.5	2.0	1.1	1.5
$p^* = 0.30$	0.735 ± 0.002	0.13	0.009 ± 0.001	0.42	0.001	0.00	0.11	0.00
$p^* = 0.10$	0.742 ± 0.004	0.18	0.024 ± 0.001	0.48	0.002	0.00	0.15	0.00
$p^* = 0.05$	0.75 ± 0.004	0.20	0.030 ± 0.001	0.49	0.003	0.00	0.17	0.00
$p^* = 0.01$	0.76 ± 0.004	0.20	0.036 ± 0.001	0.50	0.004	0.00	0.18	0.00

Table 3: Deviations in the plain stationary setting. In this simplified setting, a binary sequence is generated iid using a fixed but unknown target probability p^* , or $\mathcal{P} = \{1:p^*, 0:1-p^*\}$, and we use the plain count-based proportion $\hat{p} = \frac{N_p}{N}$ to estimate p^* (Sect. 5). 20k sequences are generated, each long enough so that there are 200 positive, 1, outcomes. Fractions of sequences in which the deviation of the estimation \hat{p} from the target probability p^* exceeded a desired threshold d , i.e. when $\max(\frac{p^*}{\hat{p}}, \frac{\hat{p}}{p^*}) > d$ (see Eq. 2), is reported at a few time snapshots. Thus, with $p^* = 0.1$ (2nd row), in about 74% of the 20k sequences, immediately after $N_p = 10$ positive outcomes has been observed in the sequence so far, we have either $\frac{p^*}{\hat{p}} > 1.1$ or $\frac{\hat{p}}{p^*} > 1.1$ (thus, either the estimate $\hat{p} < \frac{0.1}{1.1}$ or $\hat{p} > 0.11$). This deviation ratio goes down (improves) to 48% after $N_p = 50$ positive observations, and further down to 15% when $N_p = 200$. In summary, we observe that as more time is allowed, the deviations go down, and for smaller p^* the problem becomes somewhat harder (larger deviation rates).

clear that an estimate \hat{p} is at a time snapshot. This proportion estimator is unbiased with minimum variance (MVUE), and is also the maximum likelihood estimator (MLE) [32, 16] (see also Appendix C). Table 3 presents deviation ratios defined here as fraction of the 20k generated binary sequences, each generated via iid drawing from $\mathcal{P} = \{1: p^*, 0: 1 - p^*\}$, for a few $p^* \in \{0.3, 0.1, 0.05, 0.01\}$. The value of $deviates(p^*, \hat{p}, d)$ is either 0 or 1 (Eq. 2), and is snapshotted at the times t when N_p first hits 10, 50, or 200 along the sequence. We get a deviation fraction (ratio) once we divide the violation count, the number of sequences with $deviates$ value of 1, by the total number of sequences (20k). As the number of positive observations increases (the higher the N_p), from 10 to 50 to 200, the estimates $\hat{p}^{(t)}$ improve, and there will be fewer violations, and the deviation ratios go down. These ratios are also particularly helpful in understanding the deviation rates of the queuing technique that we describe next.

The above counting approach is not sensitive to changes in the proportion of the target.²² We need a way to keep track of only recent history or limiting the window over which we do the averaging. Thus, we are seeking a *moving average* of the proportions. A challenge is that we are interested in a fairly wide range of PRs, such as tracking both 0.1 or higher (a positive in every ten occurrences) as well as lower proportions such as 0.01 (one in a hundred), and a fixed history window of size k , a “box” predictor (Sect. 5.8 and Fig. 12), of all observations for the last k time points, is not feasible in general unless k is very small, i.e. the space and update-time requirements can be prohibitive computationally.²³

5.2 Queuing Counts

Motivated by the goal of keeping track of only recent proportions, we present a technique based on queuing a few simple count bins, which we refer to as the **Qs** method. Here, the predictor keeps, for each item it tracks, a small number of count snapshots (instead of just one counter), arranged as cells of a queue. Each positive observation triggers allocation of a new counter, or queue cell. Each queue cell yields an estimate of the proportion of the target item, and the counts over multiple cells can be combined to obtain a single PR for that item. Old queue cells are discarded as new cells are allocated, keeping the queue size within a capacity limit, and to adapt to non-stationarities. We next explain the queuing in more detail. Figure 8 presents pseudocode, and Sect. 5.4 discusses techniques for extracting PRs and their properties such as convergence.

5.3 The Qs Method: Keep a Map of Item \rightarrow Queue

The Qs method keeps a one-to-one map, $qMap$, of items to (small) queues. At each time point t , $t \geq 1$, after outputting predictions using the existing queues in the map, it updates all the queues in the map.²⁴ If the item observed at t , $o^{(t)}$, does not have a queue, a queue is allocated for it and inserted in the map first, before the updating of all queues. For

²²In addition, with a fixed memory, there is the potential of counting overflow problems. See Sect. D.1.

²³Many predictors, thousands or millions and beyond, could execute the same updating algorithm, e.g. in Prediction Games.

²⁴And other functions can be supported, such as querying for a single item and obtaining its probability and/or the counts. We are describing the main functions of updating and prediction.

```

PredictUpdateViaQs([o])
// Input is sequence [o] = [o(1), o(2), ...].
qMap ← {} // An empty map, item → queue.
t ← 0 // Discrete time.
Repeat // Increment time, predict, observe.
  t ← t + 1 // Increment time.
  GetPredictions(qMap) // Get the predictions.
  // Use observation at time t, o(t), to
  UpdateQueues(qMap, o(t)) update qMap.
  If t % 1000 == 0: // Periodically prune qMap.
    PruneQs(qMap) // (a heart-beat method).

GetPredictions(qMap)
// Returns a map: item → PR.
W ← {} // allocate an empty map.
For each item i and its queue q in qMap:
  // One could remove 0 PRs here.
  W[i] ← GetPR(q)
Return W // The final predictions.

UpdateQueues(qMap, o) // latest observation o.
If item o ∉ qMap: // when o ∉ qMap, insert.
  // Allocate & insert q for o.
  qMap[o] ← Queue()
For each item i and its queue q in qMap:
  If i ≠ o:
    // All but one will be negative updates.
    NegativeUpdate(q) // Increments a count.
  Else: // Exactly one positive update.
    // Add a new cell, with count 1.
    PositiveUpdate(q)

Queue(cap = 3) // Allocates a queue object.
// Allocate q with various fields (capacity, cells, etc.)
q.qcap ← cap // max size cap, cap > 1.
// Array (or linked list) of counts.
q.cells ← [0, ..., 0]
// Current size or number of cells (≤ cap).
q.nc ← 0
Return q

GetPR(q) // Extract a probability, from the number
// of cells in q, q.nc, and their total count.
If q.nc ≤ 1: // Too few cells (grace period).
  Return 0
Return  $\frac{q.nc-1}{\text{GetCount}(q)-1}$ 

GetCount(q) // Get total count of all cells in q.
Return  $\sum_{0 \leq j < q.nc} q.cells[j]$  // sum over all the cells.

NegativeUpdate(q) // Increments cell0 count.
// The back (latest) cell of q is incremented.
If q.nc ≥ 1: // Do nothing, if no cells.
  q.cell[0] ← q.cells[0] + 1

PositiveUpdate(q) // Adds a new (back) cell.
// Existing cells shift one position. Oldest cell is
// discarded, in effect, when q is at capacity.
If q.nc < q.qcap:
  q.nc ← q.nc + 1 // Grow the queue q.
For i in [1, ..., q.nc - 1]: // Inclusive.
  q.cells[i] ← q.cells[i - 1] // shift (counts).
q.cells[0] ← 1 // set newest, cell0, to count 1.

```

Figure 8: Pseudo code of the main functions of the Qs method (left), and individual queue operations (right). Each predictor keeps a one-to-one map of items to queues, $qMap$, where each queue is a small list of counts, yielding a probability for a single item. For methods of extracting probabilities from the counts and their properties (variations of $GetPR()$), see Sect. 5.4, and for pruning, see Sect. 5.6 and Fig. 10.

any queue corresponding to an item $i \neq o^{(t)}$, a **negative update** is performed, while a **positive update** is performed for the observed item $o^{(t)}$. Thus at every time point, exactly one positive update and zero or more negative updates occur. Every so often, the map is pruned (Sect. 5.6). Operations on a single queue are presented in Fig. 8(b) and described next, and Fig. 9 illustrates these queue operations with examples.

A new cell, **cell0**, at the back of the queue, is allocated each time a positive outcome is observed, and its counter is initialized to 1. With every subsequent (negative) observation, *i.e.* until the next positive outcome, cell0 increments its counter. The other, **completed**, cells are in effect frozen (their counts are not changed). Before a new back cell cell0 is allocated, the existing cell0, if any, is now regarded as completed and all completed cells shift to the “right” one position, in the queue (Figure 9(b)), and the oldest cell, **cellk**, is discarded if the queue is at capacity **qcap**. Each cell corresponds to one positive observation and the remainder in its count c , $c - 1$, corresponds to consecutive negative outcomes (or the *time ‘gap’* between one positive outcome and the next). Thus, the number of positives corresponding to a cell is 1 (a positive observation was made that led to the cell’s creation). Each cell yields one estimate of the proportion, for instance $\frac{1}{c}$, and by combining these estimates, or their counts, from several queue cells, we can attain a more reliable PR estimate, discussed next. Fig. 12(d) shows that, in effect, queues of different items with different occurrence probabilities, correspond to different lengths of history, the lower the PR, the longer the history (but the same maximum number, qcap, of positive observations).

5.4 Extracting PRs from the Queue Cells

The process that yields the final count of a completed queue cell is equivalent to repeatedly tossing a two-sided coin with an unknown but positive heads probability $p^* > 0$, and counting the tosses until and including the toss that yields the first heads (positive) outcome. Here, we first assume p^* does not change (the stationary case). The expected number of tosses until the first heads is observed is $1/p^*$. We are interested in the reverse estimation problem: Assuming the observed count of tosses, until and including the first head, is c , the reciprocal estimator $\frac{1}{c}$ is a *biased*, upper estimator of p^* , for $p^* < 1$, also known to be the MLE. The positive bias can be shown by looking at the expectation expression

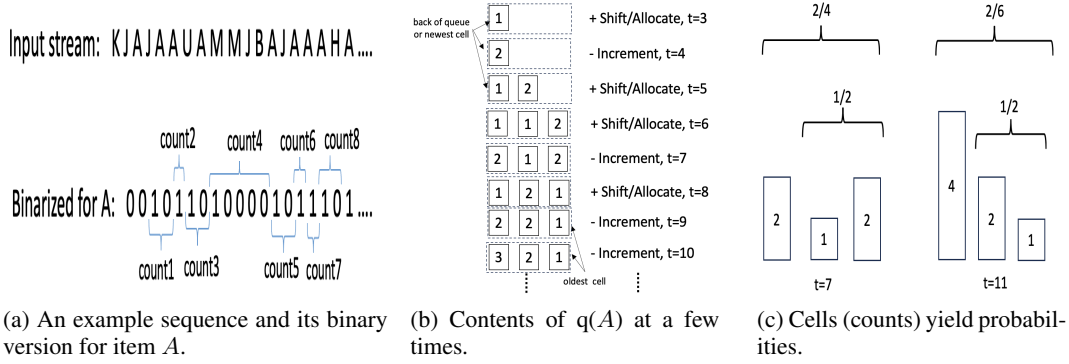


Figure 9: Illustrating the workings of the Qs predictor for tracking the probability of a single item: An example sequence (top, (a)), made binary for item A (bottom), *i.e.* whenever A occurs, the entry in the binarized sequence is a 1, leading to a positive update of the queue for A , otherwise it is a 0, leading to a negative update (once the queue is allocated). Part (b) shows another view of the queue for A upon queue creation and the first few updates (horizontal at each time point, left (newest cell, cell0) to right-most (oldest, cellk). At $t = 3$ when the first A is observed (the first positive update), the queue for A is created with cell0 (newest cell of the queue), initialized with count 1. At time $t = 4$ a negative update is performed and cell0 (its counter) is incremented. At $t = 5$, another positive update, existing cell0 (its count content) is shifted one position to right, and a new cell0 is allocated with value 1, becoming the back of the queue. More generally, on positive updates, existing cells shift to right and a new cell0 with an initial count of 1 is allocated, and on negative updates, the existing cell0 is incremented. At $t = 8$, the value in cellk is discarded upon another positive update (assuming capacity 3), and so on. (c) Cell counts, shown at two snapshots, can be used to estimate a probability. There are several options for pooling the cells to get a probability. For instance, the back (left-most) partial cell can be ignored (see Section 5.4).

(Appendix C). The (bias) ratio, $\frac{c^{-1}}{p^*}$, gets larger for smaller p^* (as $p^* \rightarrow 0$). See Appendix C which contains derivations and further analyses.

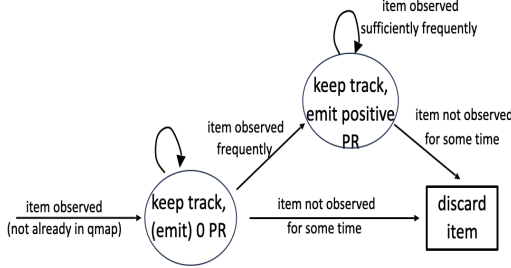
More generally, with k completed cells, $k \geq 2$, cell j having count C_j , we can pool all their counts and define the statistic (random variable) $G_k = \frac{k-1}{\sum_{1 \leq j \leq k} C_j - 1}$. G_k is shown to be the *minimum variance unbiased estimator* of p^* [49], meaning in particular that $\mathbb{E}(G_k) = p^*$. The powerful technique of Rao-Blackwellization is a well-known tool²⁵ in mathematical statistics, used to derive an improved estimator (and possibly optimal, in several senses) starting from a crude estimator, and to establish the minimum-variance property [55, 59, 8, 37, 11]. Note that we need at least two completed cells for appropriately using this estimator. Appendix C.2 contains further description of how Rao-Blackwellization is applied here.

The back cell, cell0, of the queue, with count C_0 , is incomplete, and the reciprocal estimator $\frac{1}{C_0}$ can generally be even higher (worse) than the simple biased MLE estimator derived from a completed cell. However, as we explain, due to non-stationarity, in our implementation of PR estimation via the Qs method, we use cell0 as well (function **GetPR**(q) in Fig. 8), thus we use $k/(\sum_{0 \leq j \leq k} C_j - 1)$ (where the queue has $k+1$ total cells, and the count in the denominator includes *all* queue cells). We have found that with small capacity $qcap$, using an extra cell (even if often incomplete) can noticeably lower the variance of the estimate. More importantly, in the presence of non-stationarity, the estimate $\frac{1}{C_0}$ is crucial for providing an upper bound estimate on PR: imagine p^* has a sudden (discrete) drop from 0.1 to 0. It is only cell0 that would reflect this reduction over time: the other completed cells are unaffected no matter how many subsequent negative observations take place.²⁶ See also Sect. 5.6 on pruning.

With our **GetPR**() function, the Qs technique needs to see two observations of an item, in sufficiently close time proximity, to start outputting positive PRs for the item.

²⁵Many thanks to J. Bowman for pointing us to the paper [49], and describing the proof based on Rao-Blackwellization, in the Statistics StackExchange.

²⁶An alternative for incorporating cell0 is to separate the MLE PR p_0 from cell0 from the MVUE PR p_1 derived from the completed cells, and use p_0 only when it is lower than p_1 , for example, when it is significantly lower according to the binomial-tail test, Sect. 6.1. This is an efficient constant-time test.



PruneQs($qMap$) // Pruning: A heart-beat
 // Parameters: size & count limits s_1, s_2 ,
 // such as $s_1 = 100$ and $s_2 = 10^5$.
 // For any item, C_0 is its count in cell0 .
 Drop any item with $C_0 > s_2$ from $qMap$
 If $|qMap| < 2s_1$:
 Return // Nothing left to do.
 Drop highest C_0 counts until $|qMap|$ is s_1 .

Figure 10: Left: The state changes of an item as it enters the $qMap$. The Qs technique keeps track of any item it sees in its stream (inserts it in $qMap$), for some (minimum, grace-period) time. The item may become salient (positive PR) and stay in that state indefinitely or, eventually or after the grace-period, discarded. Right: The pruning logic: items with large C_0 (count in cell0) are discarded. If the map is too large, it is pruned too (again, rank and remove by descending C_0 , see Sect. 5.6).

5.5 Predicting with SDs

Each queue in $qMap$ provides a PR for its item, but the PRs over all the items in a map may sum to more than 1 and thus violate the SD property. For instance, take the sequence $AAAABBBB$ (several consecutive A s followed by several B s), and assume $qcap = 3$: after processing this sequence, the PR for B is 1.0, while for A is $\frac{2}{6}$. See also Appendix C.3. The SD property is important for down-stream uses of the PRs provided by a method, such as computing expected utilities (and for a fair evaluation under KL() divergence). For evaluations, we apply the FC() function in Fig. 3(a) which works to normalize (scale down) and convert any input map into an SD as long as the map has non-negative values only.

The following properties hold, the proof of which (Lemma 13) along with other properties of the PRs, are in Appendix C.3. Below, $\mathcal{W}()$ is the PR map output of the Qs technique, or $\mathcal{W}(i)$ is the PR obtained from GetPR() when the queue for item i is passed to it.

Lemma 3. For the Qs technique with $qcap \geq 2$, for any item i with a queue $q(i)$, $|q(i)| \leq qcap$, using the PR estimate $\mathcal{W}(i) = (|q(i)| - 1) / (\sum_{0 \leq j < |q(i)|} C_j - 1)$, for any time point $t \geq 1$:

1. $\mathcal{W}^{(t)}(i)$, when nonzero, has the form $\frac{a}{b}$, where a and b are integers, with $b \geq a \geq 1$.
2. If i is observed at t , then $\mathcal{W}^{(t+1)}(i) \geq \mathcal{W}^{(t)}(i)$. If i is not observed at t , then $\mathcal{W}^{(t+1)}(i) < \mathcal{W}^{(t)}(i)$.

5.6 Managing Space Consumption

There can be many infrequent items and the queues map of a predictor can grow unbounded, wasting space and slowing the update times, if a hard limit on the map size is not imposed. The size can be kept in check via removing the least frequent items from the map every so often, for instance via a method that works like a "heart-beat" pattern: map expansion continues until the size reaches or exceeds a maximum allowed capacity $2s_1$, e.g. $s_1 = 100$, remove the items in order of least frequency, i.e. rank by descending count C_0 in cell0 in each queue,²⁷ until the size is precipitously shrunk back to s_1 . When we are interested in modeling (tracking) probabilities down to a smallest PR p_{min} , in general we must have $s_1 > \frac{1}{p_{min}}$ (e.g. with $p_{min} = 0.01$, s_1 needs to be above 100). The higher s_1 , the less likely that we drop salient items, i.e. items with (true) PR above p_{min} (when a true PR exists, under the stationary setting). Note that those queues that are dropped, their PR when normalized, must be below p_{min} whenever $s_1 > \frac{1}{p_{min}}$, and the normalized PR is what we use when we want to use predictions that form a SD. Appendix C.3 explores the maximum possible number of PRs above a threshold before normalizing.

The above periodic pruning logic can also limit the count values within each queue, in particular in cell0, but not in the worst-case: suppose A is seen once, and from then on B is observed for all time. Thus $|qMap| = 2$, and the above pruning logic is never triggered, while the count for A in its cell0 can grow without limit (log of stream size). Thus,

²⁷One could also use estimates from other completed cells as well, such as $\min(\frac{1}{C_0}, \text{GetPR}())$, but only when $\text{GetPR}() > 0$, i.e. this value should be used only when other completed cells exist (otherwise a new item could get dropped prematurely). With nonstationarity, it is possible the estimates from older cells would be outdated, and an item that used to be infrequent may have become sufficiently frequent now.

For predicting at time $t+1$, the Box predictor weighs all items in history from t to $t-K+1$ (size K) equally, $1/K$, and older history is zeroed (forgotten).



(a) How history is weighed by the Box predictor.

```
GetBoxPR(o, q, counts) // Get PR.
  If o ∉ counts: Return 0
  Return counts[o] / q.nc
```

(b) Obtaining PR of an item.

```
UpdateBoxQ(q, counts, o)
  // add item o to queue q and update counts.
  counts[o] ← counts[o] + 1
  q.add(o) // add o to back of queue q.
  // q.nc is the number of cells in queue.
  If q.nc > q.K: // reached max K?
    // Drop the item from front of queue.
    i ← q.pop() // Front (oldest) item.
    counts[i] ← counts[i] - 1
    If counts[i] == 0 :
      // remove from the counts map as well.
      counts.remove(i)
```

(c) Updating a Box predictor.

Figure 11: The Box predictor. (a) The history is weighed by a box function. (b) Obtaining the probability of an item o . (c) Updating is $O(1)$ when a linked-list queue and a counts map is used.

we can impose another constraint that if cell0 C_0 count-value of a queue in the $qMap$ is too large (e.g. $\frac{1}{C_0} \leq 10^{-4}$), such a queue (item) is removed as well. The trigger for the above checks can be periodic, as a function of the update count of the predictor (Fig. 8). The pruning logic is given in Fig. 10 (right).

Fig. 10, left, summarizes the states and state transitions of Qs upon observing an item not already in $qMap$, as it pertains to the item. Any item seen will be kept track of in $qMap$ for some time (assuming $s_1 > 1$). Being tracked does not imply positive PR (salience), however, if the item is seen more in sufficiently close proximity, it becomes salient (we require a minimum of two observations). It may also be discarded without ever becoming salient, or discarded after becoming salient. It may also enter the map and never exit.

5.7 Complexity of the Qs Method

Let $k = qcap$. At each time point, prediction using the $qMap$ and update take the same $O(k|qMap|)$, where we assume $O(1)$ time for summing numbers and taking ratios: queue update involves updating the queue of every item in the map, and the updates, whether positive or negative, take $O(k)$ time. In our experiments, $qcap$ k is small, such as 3 or 5. With a p_{min} of 0.01 and periodic pruning of the map, the size of the queue for each predictor can grow to up to a few 100 entries at most.

Number of time steps required for estimating a PR output for an item with underlying PR p^* (at the start of a new stable period), similar to EMA with harmonic decay (Sect. 4.3), is $\theta(\frac{1}{p^*})$ (time complexity).

5.8 The Box Predictor (a Fixed-Window Baseline), and its Variants

The plain (discrete) Box predictor, also known as the sliding window predictor, keeps a history window of fixed size K , of the last K observations (Fig. 11). The sliding windows idea (of fixed or variable size) is a common tool used in various non-stationary problems [6, 26, 18]. For our setting, the Box SMA can be implemented relatively efficiently via a single queue, and thus it has similarities to the Qs technique (one long queue vs. several small queues). With a hash map of item to observation counts and a linked list queue, updating can be more efficient at $O(1)$ (instead of $O(K)$): This involves adding a cell and possibly dropping one (oldest) cell from the queue, and updating up to two item counts. See Fig. 11. However, the space consumption is a rigid $\Theta(K)$, and unlike the Qs predictor, K could be relatively large such as 100 or 1000, depending on how small one wants to go in tracking PRs. While the worst-case space consumption of Qs predictor is similar, when the input stream has a few salient items with relatively high PR the Qs predictor would be significantly more advantageous. Importantly, the Box predictor may not be sufficiently responsive to non-stationarity: for instance, with $K = 100$, when a new item gets a high PR, it will take 10s of positive observations for the Box predictor to approach the target PR (for the Qs predictor, we would need a handful of positive observations, with a $qcap$ at say 3 or 5). The response time would be slower with increasing K (akin to convergence vs. stability tradeoff when setting the rate of fixed-rate EMA). Thus the box-predictor resembles the fixed-rate EMA, but requires more space. The more dynamic Qs variants react better under non-stationarity.

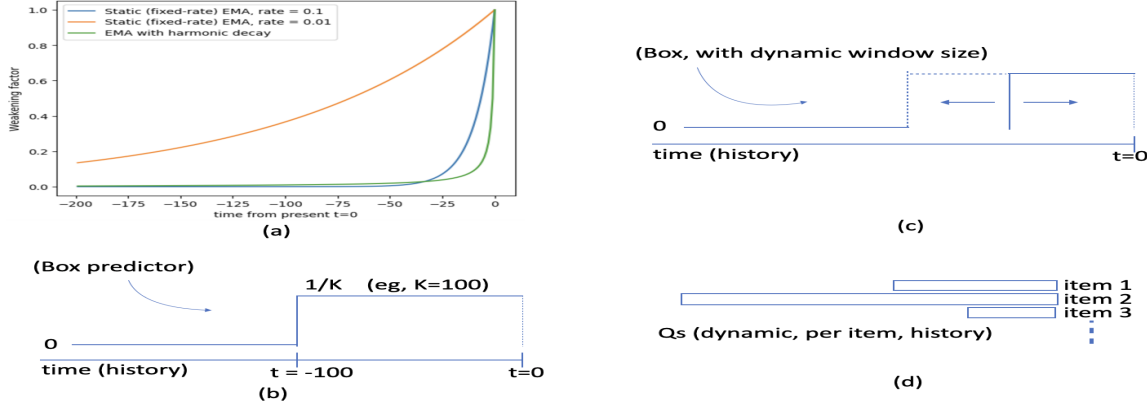


Figure 12: A visualization of how history is weighted by different techniques (in contributing to the present value of the moving average). (a) The EMA variants down-weight the history smoothly (for static EMA, it is $(1 - \beta)^i$ for time $t - i$, i.e. i time points before current time t). (b) For the plain Box predictor history is zeroed (forgotten) beyond the recent window, and otherwise, observations within the window get equal weighting. (c) Dynamic variants of the Box (adaptive windowing) can adjust the window size by trying to detect change (implicitly or explicitly), so that when there is change, more of the irrelevant past is appropriately forgotten (conversely, expand the window when no change, for better estimation). (d) For the Qs SMA, history has a shape similar to that for Box, but a different history (span) is kept for each item: lower probability items require and use longer histories.

There also exist dynamic versions of the Box predictor, or adaptive windowing, where the size of the window is dynamically adjusted, e.g. [6, 50, 64]. The recent probability prediction work of [50], published in the same year as ours, is closest to our work to the best of our knowledge, as the observations are discrete and the task is open-ended. In that work, the algorithm, similar to prior work on adaptive windowing, adjusts the history size k (up to $\log_2(N)$ where N is the stream length). Prior work has focused on other, numeric, data types (e.g. [6, 64]). A challenge in adaptive windowing is how to efficiently pick the window size (which may need to be executed at every time point, or triggered by an efficient change detection method). In our task, we have argued that different items, with different probability ranges (e.g. from 0.1 down to 0.001), in effect require different history sizes. We note that the algorithm of [50] is presented and evaluated in a theoretical context and while the $\log_2()$ can grow with sequence length, it is actually too small, for instance only 10 for 1000 and 20 for 10^5 long sequences, while for PRs around 0.01 say, one requires histories of order 100s.²⁸

Figure 12 gives a visualization of how the history is weighted by several SMAs. In plain EMA updating, the value of an observation at time $t - i$ is multiplied by (weakened) by $(1 - \beta)^i$ with fixed-rate β (powers of 0.9, for $\beta = 0.1$, and 0.99, for $\beta = 0.01$, in the picture). For the harmonic-decay variant, the multiplier (the weakening factor) decreases more rapidly initially, but eventually the exponential decrease of plain EMA yields a lower rate (the crossing is seen for $\beta = 0.1$). The reduction of weight for the EMA variants is smooth, while for Box variants, there is an abrupt change, e.g. from $1/K$ to 0 as shown in the Figure.

6 DYAL: Combining Sparse EMA and Qs

The Qs technique can give us a good roughly unbiased starting point for an estimate of the PR of an item, but it has a high variance (e.g. see Fig. 15(c)) unless we use considerable queue space (many queue cells, and trading off plasticity for stability). With sparse EMA (Sect. 4), and with our assumption that there will be a period of stability when a salient item is observed (stability for that item), one could begin with the Qs estimate and fine tune it to achieve lower variance in the estimation. We next show that these complementary benefits of each approach can indeed be put together, and we call the combination **DYAL**, for *dynamic adjustment of the learning (rate)*, with the mnemonic of *dialing* up and down the learning (rate), shown in Fig. 14.

²⁸One could imagine using multiples of the ceiling $\log_2(N)$ (for small N) but it is not clear how to adjust as stream size N grows, and it appears that the same history span won't work for different PR values (Fig. 12(d) shows that Qs uses different spans). If one were interested in high probabilities, e.g. above 0.1, such Box variants may suffice. The desired theoretical property used to motivate the algorithm is based on total variational loss [50], which is an absolute loss measure. Our arguments on the insensitivity of quadratic loss to smaller probabilities, Sect. A.1, applies to absolute loss too. A remaining challenge is a time-efficient and effective selection of the dynamic box size.

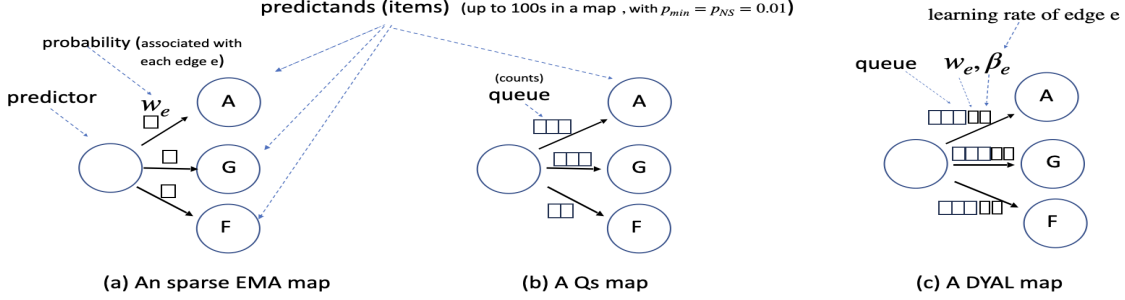


Figure 13: A comparison of the parameters kept with each edge (prediction relation) by the 3 main SMAs of this paper. Each SMA keeps and updates one (logical) map, with one map entry per predictand. Each map entry is viewed as an edge (*i.e.* prediction relation). In this picture 3 predictands are shown in each map (items A, G, and F). (a) For EMA, associated with each edge e is a single weight or PR w_e , that is kept updated. There is one learning-rate β , associated with the entire predictor. (b) For the Qs SMA (center), associated with each edge e is a small queue of counts, integers, up to 3 cells in this picture. There is no (explicit) learning-rate in Qs, and the PRs are derived from the queue contents (Sect. 5). (c) In DYAL, Sect. 6, which combines the two techniques, each edge has its own learning rate β_e , as well as a queue (like Qs) and a PR w_e (like EMA). The learning-rate is dynamic: it is increased from time to time, but the default pattern of change is gradual decay (such as harmonic decay, Sect. 4.3), down to a minimum.

An update in the DYAL SMA has the simple logical structure of the plain EMA, *i.e.* weaken-and-boost (Fig. 6): weaken all existing edges, then boost (strengthen) the edge to the observed item (Sect. 4). However each edge in DYAL, in addition to its weight (a PR, a floating point), also has its own learning rate, which is used for the weakening and boosting of that edge. This is unlike plain EMA, wherein a single rate is used for all edges of a predictor. Fig. 13 shows the parameters kept with each edge, for the three main SMAs of this paper. Associated with each DYAL edge, there is also a queue, and during weakening or boosting an edge, it is possible that the queue estimates are used (a PR as well as a learning rate, both derived from the queue). We refer to this possibility as *listening* to the queue (Sect. 6.1). Each learning rate is decayed, via harmonic decay (Sect. 4.3), after an edge update. For a visualization of the change patterns in learning rates, see Fig. 15(e) and (f) and Fig. 21. The queues are also used for deciding when an item should be discarded. Thus the queues are used as “gates”, the interface to the external observed stream, playing a major role in determining what is kept track of and what is discarded, and providing rough initial estimates, of the PR and β , whenever the PR of an item needs to substantially change. Note that in the pseudo code of Fig. 14 we use three maps (*EmaMap*, *rateMap*, *qMap*), while in the picture of Fig. 13(c) they are combined into one logical graph.

Prediction in DYAL is as in plain EMA, and the *EmaMap* is output. Like EMA, DYAL ensures that *EmaMap* remains a SD after updating. When updating, all the three maps are updated in general, as given in the `UpdateDyal()` function. Upon each observation o , first the queues information on o is obtained. This is the current queue probability qPR (possibly 0) on o , and the $qcount$ (invoke `GetCount()`). Then *qMap* is updated (a Qs-type update). Finally, all the edges in the EMA map, except for o , are weakened. If there was no queue for o , *i.e.* when qPR is 0, o must be new, or NS in general, and nothing more is done, *i.e.* no (EMA) edge strengthening is done (note that a queue is allocated for o upon the *qMap* update). Weakening, for each edge, is either a plain EMA weakening, or the queue estimates are used, which we cover next. Similarly, for strengthening, the condition for listening to the queue is examined, as described next, and the appropriate strengthening action, plain EMA strengthening or listening to the queue, is taken.

6.1 When and How to Listen (Switch) to the Queue Estimates: Statistical (Binomial-Tail) Tests

The queue for each item provides two numbers, the number of cells of the queue is the implicit number of positives observed recently, and the total count across the queue cells is the number of trials (roughly, the `GetCount()` function). A PR estimate qPR is derived from these numbers (`GetProb()`). We also have an estimate of PR, $emaPR$, from the EMA weights *EmaMap*, which we expect to be generally more accurate with lower variance than qPR , but specially in the face of non-stationarity, from time to time this estimate could be out-dated and should be discarded. Based on the counts and the queue estimate qPR , we can perform a binomial-tail test that asks whether, when assuming $emaPR$ is the true PR, one can observe the alternative PR qPR in $qcount$ trials, with some reasonable probability. This binomial tail can be approximated (lower and upper-bounded) efficiently in $O(1)$ time when one has the number of trials and the observed PR qPR [2, 3, 42], and it tells us how likely it is that a binary event with assumed true PR $emaPR$ could lead to the counts and the qPR estimate (of the queue). As seen in Fig. 14, the approximation is based on the (binary) KL divergence ($KL(qPR||emaPR)$). When this event is sufficiently unlikely, or, equivalently, when the binomial-tail

```

UpdateDyal(o) // latest observation o.
  // Data structures: qMap, EmaMap, rateMap.
  qPR, qcount ← GetQInfo(qMap, o)
  UpdateQueues(qMap, o)
  free ← WeakenEdges(o) // Weaken, except for o.
  If qPR == 0: // item is currently NS?
    Return
  emaPR ← EmaMap.get(o, 0.0) // 0 if o ∉ Map.
  // listen to queue?
  If Q_SignificantlyHigh(emaPR, qPR, qcount):
    // set initial rate and PR using queue for o.
    rateMap[o] ← qcount-1
    δ ← min(qPR − emaPR, free)
  Else: // EMA update with harmonic decay.
    β ← rateMap[o]
    δ ← min((1 − emaPR) * β, free)
    rateMap[o] ← DecayRate(β) // Sect. 4.3
  EmaMap[o] ← δ + emaPR

Q_SignificantlyHigh(emaPR, qPR, qcount)
  // Parameter: sig_thrsh (significance threshold).
  If emaPR == 0: // when 0, listen to Qs.
    Return True
  If qPR ≤ emaPR: Return False
  Return qcount * KL(qPR, emaPR) ≥ sig_thrsh

Q_SignificantlyLow(emaPR, qPR, qcount)
  // Parameter: sig_thrsh (significance threshold).
  If emaPR ≤ qPR: Return False
  Return qcount * KL(qPR, emaPR) ≥ sig_thrsh

WeakenEdges(o)
  // Weaken weights and return available PR mass.
  // Data structures: qMap, EmaMap, rateMap.
  // Parameter: pmin.
  // Weaken all except for o. Returns the free mass.
  used ← 0
  For each item and learning-rate, i, β in rateMap:
    If i == o: // Don't weaken o
      used ← used + EmaMap[o]
      Continue
    // Possibly listen (switch) to the queue.
    qPR, qcount ← GetQInfo(qMap, i)
    // if too low, drop i
    If max(EmaMap[i], qPR) < pmin:
      EmaMap.delete(i) & rateMap.delete(i)
      Continue // remove item and go to next.
    If Q_SignificantlyLow(EmaMap[i], qPR, qcount):
      EmaMap[i] ← qPR // Set to q info.
      rateMap[i] ← qcount-1
    Else: // weaken as usual
      EmaMap[i] ← (1 − β) * EmaMap[i]
      rateMap[i] ← DecayRate(β)
  used ← used + EmaMap[i]
  Return 1.0 − used // The free (available) mass

GetQInfo(qMap, o)
  If o ∉ qMap: // no queue for o?
    Return 0, 0
  q ← qMap.get(o)
  Return GetPR(q), GetCount(q)

```

Figure 14: Pseudo code for DYAL, an extension of EMA, where the overall weaken-and-boost update structure remains the same. Here each predictand entry, or edge, has a small queue and its own learning rate, in addition to the PR estimate (a weight) (see Fig. 13), and during weakening and boosting, the queue estimates could be used to reset the edge weight and its learning rate.

score is sufficiently high, DYAL switches to the queue estimate and sets the new rate β accordingly too (see Sect. 4.3 explains the connection between rate β and counts). By default we use a score threshold of 5, corresponding to 99% confidence (meaning 0.01 probability of a false-positive, that is no change and the EMA estimate should have been kept). In a few experiments, we report on the sensitivity of DYAL to the choice of the binomial threshold.

As mentioned in Sect. 4.3, specially now that each edge has its own rate, the rate $rateMap[i]$ can be used as a measure of the predictor's uncertainty around the PR estimate $EmaMap[i]$. Initially, when set to the queue estimate, the rate can be relatively high, and is lowered over time via harmonic decay.

6.2 SD Maintenance and Convergence

We can verify from the logic of DYAL, *i.e.* the weakenings and strengthening of the weights and the bounding of δ (the PR to add) by the *free* variable (the available, or unallocated, PR mass), that the *EmaMap* of DYAL always corresponds to an SD: the PR values kept are positive and never sum to more than 1.0. In the stationary setting, the properties of plain EMA apply and the PRs should converge to the true PRs, except there is some low probability that once in a while switching (listening) to the queue may occur with a more variant estimate (a false-positive switch). We leave a more formal analysis to future work.

6.3 Pruning (Space Management) and Asymptotic Complexity

The pruning logic for the three maps of DYAL is identical to the logic for pruning for the Qs method of Sect. 5.6 except that when an entry is deleted from the queue, its corresponding entries (key-value pairs) in *rateMap* and *EmaMap* are also deleted when they exist. Thus the set of keys in the *qMap* of the predictor will always be a superset of the key sets in *rateMap* and *EmaMap* (note: the keysets in *rateMap* and *EmaMap* are always kept identical). The size of *EmaMap* does not exceed $O(\frac{1}{p_{min}})$ as it is a SD, and *qMap* is pruned periodically as well. Updating time cost for DYAL is similar to Qs: each edge (predictand) is examined and the corresponding queue and possibly EMA weights and learning rate are updated, each test and update (weakening and boosting) take $O(1)$ (per edge) where we assume *qcmap* is constant, and update and prediction take $O(|qMap|)$ time.

deviation threshold \rightarrow	1.5	2	1.5	2
	Qs, 5 (qcap of 5)		Qs, 10 (qcap of 10)	
$p^* = 0.10$	0.385 ± 0.026	0.129 ± 0.020	0.191 ± 0.029	0.026 ± 0.010
$p^* = 0.05$	0.405 ± 0.034	0.142 ± 0.028	0.211 ± 0.044	0.035 ± 0.016
	static EMA, 0.01 (β of 0.01)		static EMA, 0.001 (β of 0.001)	
$p^* = 0.10$	0.075 ± 0.021	0.013 ± 0.006	0.113 ± 0.020	0.071 ± 0.012
$p^* = 0.05$	0.211 ± 0.034	0.050 ± 0.019	0.118 ± 0.029	0.072 ± 0.016
	harmonic EMA, 0.001 (β_{min} of 0.001)		DYAL, 0.001 (β_{min} of 0.001)	
$p^* = 0.10$	0.006 ± 0.007	0.002 ± 0.003	0.018 ± 0.015	0.008 ± 0.006
$p^* = 0.05$	0.012 ± 0.013	0.005 ± 0.005	0.028 ± 0.023	0.014 ± 0.012

Table 4: Synthetic single-item stationary: Deviation rates, for two deviation thresholds $d \in \{1.5, 2\}$, averaged over 200 randomly generated sequences of 10000 binary events (0 or 1), for target probability $p^* \in \{0.05, 0.1\}$. As an example, for $p^* = 0.1$, about 10% of the items will be 1, the rest are 0s in the sequence, and the SMA predicts a probability $\hat{p}^{(t)}$ at every time point t for $o^{(t)} = 1$ (then updates), and we observe from the table that about 38% of time, $\max(\frac{\hat{p}^{(t)}}{p}, \frac{p}{\hat{p}^{(t)}}) > 1.5$ (i.e. $\hat{p}^{(t)} > 0.15$ or $\hat{p}^{(t)} < \frac{0.1}{1.5}$), for the Qs SMA with qcap 5 (top left). The lower the deviation rates the better. In this stationary setting, we see improvements with larger queue capacities (as expected), and a lower β_{min} of 0.001 performs best for the EMA variants. For Qs, with qcap = 10, compare to Table 3, $t_p = 10$.

7 Experiments

We begin with the synthetic experiments, wherein we generate sequences knowing the true SDs $\mathcal{P}^{(t)}$. At any time point, for evaluation, the FC() function of Fig. 3 is applied to the output of all predictors, with $p_{NS} = p_{min} = 0.01$. The default parameters for DYAL are qcap of 3 and binomial-tail threshold of 5, and we report the performance of DYAL for different β_{min} , often set at 0.001. We are interested in $\beta_{min} \leq 0.001$ because our target range is learning PRs in $[0.01, 1.0]$ well. For static EMA, we report the (fixed) β used, for harmonic EMA, the β_{min} , and for Qs, the qcap. The NS-marker used is described in 3.7 (default $c_{NS} = 2$). All code is implemented in Python, and we report timing for several of the experiments (those taking longer than a few minutes).

7.1 Tracking a Single Item, Stationary

All the prediction techniques are based on estimating the probability (PR) for each item separately (treating all other observations as negative outcomes), so we begin with assessing the quality of the predictions for a single item in the binary stationary setting of Sect. 2.1.3. Thus, when $p^* = 0.1$, about 10% of the sequence is 1, the rest 0. Table 4 presents the deviation rates of Qs, EMA, and DYAL, under a few parameter variations, and for $p^* \in \{0.1, 0.05, 0.01\}$. Sequences are each 10k time points long, and deviation rates are averaged over 200 such sequences.²⁹

Under this stationarity setting, higher qcap helps the Qs technique: Qs with qcap 10 does better than qcap of 5, but, specially for $d = 1.5$, both tend to substantially lag behind the best of the EMA variants. EMA with harmonic decay, with an appropriately low β_{min} , does best across all p^* . If we anticipate that the useful items to predict will have PRs in the 0.01 to 1.0 range, in a stationary world, then setting β_{min} for harmonic EMA to a low value, $\frac{0.01}{k}$, where $k \geq 10$, is adequate.³⁰ In this stationary and binary setting, the complexity of DYAL is not needed, and harmonic EMA is sufficient. Still DYAL is the second best. Static EMA is not flexible enough, and one has to anticipate what p^* is and set the rate appropriately. For instance, when $p^* = 0.01$, EMA with the same $\beta = 0.01$ is not appropriate, resulting in too much variance. Finally, we observe that the deviation rates, as well as the variances, for any method, degrade (increase) somewhat as p^* is lowered from 0.1 to 0.01. In ten thousand draws (during sequence generation), there are fewer positive observations with lower p^* , and estimates will have higher variance (see also Appendix C.1).

7.2 Tracking a Single Item, Non-Stationary

We continue with tracking a single item as above, as we report deviation rates when estimating a single p^* , but now the predictors face non-stationarity. As in the above, sequences of 10000 items are generated in each trial. We report on two main settings for non-stationarity: In the first setting, p^* oscillates between, 0.25 and 0.025, thus an abrupt or

²⁹The methods keep track of the probabilities of all the items they deem salient, in this case, both 0 and 1, but we focus on the PR estimates $\hat{p}^{(t)}$ for item 1.

³⁰In the stationary setting, one can set $\beta_{min} = 0$.

deviation threshold \rightarrow	1.5	2	1.5	2
change type and $O_{min} \downarrow$	Qs, 5		Qs, 10	
$0.025 \leftrightarrow 0.25, 10$	0.423 ± 0.029	0.189 ± 0.023	0.395 ± 0.021	0.234 ± 0.014
$0.025 \leftrightarrow 0.25, 50$	0.382 ± 0.038	0.131 ± 0.028	0.222 ± 0.039	0.062 ± 0.017
$\mathcal{U}(0.01, 1.0), 10$	0.443 ± 0.030	0.234 ± 0.042	0.468 ± 0.028	0.284 ± 0.035
$\mathcal{U}(0.01, 1.0), 50$	0.380 ± 0.050	0.173 ± 0.080	0.247 ± 0.060	0.102 ± 0.076
	static EMA, 0.01		static EMA, 0.001	
$0.025 \leftrightarrow 0.25, 10$	0.510 ± 0.024	0.357 ± 0.020	0.996 ± 0.006	0.760 ± 0.043
$0.025 \leftrightarrow 0.25, 50$	0.255 ± 0.045	0.129 ± 0.028	0.705 ± 0.032	0.560 ± 0.023
$\mathcal{U}(0.01, 1.0), 10$	0.686 ± 0.030	0.477 ± 0.035	0.818 ± 0.038	0.693 ± 0.054
$\mathcal{U}(0.01, 1.0), 50$	0.397 ± 0.056	0.209 ± 0.045	0.775 ± 0.085	0.602 ± 0.099
	harmonic EMA, 0.01		harmonic EMA, 0.001	
$0.025 \leftrightarrow 0.25, 10$	0.502 ± 0.025	0.351 ± 0.021	0.957 ± 0.021	0.668 ± 0.053
$0.025 \leftrightarrow 0.25, 50$	0.247 ± 0.046	0.123 ± 0.028	0.606 ± 0.031	0.494 ± 0.018
$\mathcal{U}(0.01, 1.0), 10$	0.684 ± 0.033	0.476 ± 0.034	0.813 ± 0.036	0.683 ± 0.050
$\mathcal{U}(0.01, 1.0), 50$	0.395 ± 0.056	0.204 ± 0.043	0.761 ± 0.079	0.592 ± 0.097
	DYAL, 0.01		DYAL, 0.001	
$0.025 \leftrightarrow 0.25, 10$	0.480 ± 0.029	0.332 ± 0.025	0.586 ± 0.066	0.408 ± 0.061
$0.025 \leftrightarrow 0.25, 50$	0.251 ± 0.048	0.150 ± 0.031	0.099 ± 0.066	0.053 ± 0.037
$\mathcal{U}(0.01, 1.0), 10$	0.560 ± 0.035	0.351 ± 0.054	0.529 ± 0.052	0.313 ± 0.045
$\mathcal{U}(0.01, 1.0), 50$	0.320 ± 0.11	0.189 ± 0.128	0.246 ± 0.081	0.128 ± 0.083

Table 5: Synthetic single-item non-stationary: Deviation-rates on sequences where p^* oscillates back and forth between 0.025 and 0.25, or drawn uniformly at random from the interval $[0.01, 1.0]$ ($p^* \sim \mathcal{U}(0.01, 1.0)$). Each sequence is 10k observations long, and the deviation-rate is averaged over 500 such sequences. For the case of $0.025 \leftrightarrow 0.25$, each subsequence (wherein p^* is constant) is roughly same length: 400 long for $O_{min} = 10$, and 2k for $O_{min} = 50$. For the rows with $\mathcal{U}(0.01, 1.0)$, each subsequence only has to meet the O_{min} constraint (see 7.2 text for details). In this non-stationary setting, focused on one changing item, the Qs SMAs do best perhaps, but DYAL variants do equally well or come close (in terms of both their best-case and worst-case performance).

substantial change (10x) is guaranteed to occur and frequently. This oscillation is shown as $0.25 \leftrightarrow 0.025$ in Table 5. In the second ‘uniform’ setting, each time p^* is to change, we draw a new p^* uniformly at random from the interval $[0.01, 1.0]$, shown as $\mathcal{U}(0.01, 1.0)$, and in this setting, some changes are large, others small and could be viewed as drifts. The stable period, during which p^* cannot change (to allow time for learning), is set as follows. For both settings, within a stable period, the target item (item 1) has to be observed at least O_{min} times before p^* is eligible to change, where results for $O_{min} \in \{10, 50\}$ are shown in Table 5. Additionally, we impose a general minimum-length constraint (not just on positive observations) for the $0.25 \leftrightarrow 0.025$ setting: each stable period has to be $\frac{O_{min}}{\min(0.025, 0.25)}$, so that the different periods would have similar length (expected 400 time points when $O_{min} = 10$, and 2000 when $O_{min} = 50$). In this way, subsequences corresponding to $p^* = 0.25$ would not be too short (otherwise, deviation-rate performance when $p^* = 0.025$ dominates). Thus, with $0.25 \leftrightarrow 0.025$, we get an expected 25 stable subsequences (or changes in p^*) in 10k long sequences with $O_{min} = 10$, and 5 switches in p^* when $O_{min} = 50$. For the uniform setting, we did not impose any extra constraint, and respectively with O_{min} of 10 and 50, we get around 200 and 50 stable subsequences in 10k time points. In this setting, performances in periods when p^* is low do dominate the deviation rates (see also Table 16 where the deviation-rates improve when we impose an overall minimum-length constraint for the uniform setting too).

Compared to the results of Table 4, here the Qs predictor excels, specially when we consider deviation-rates when $O_{min}=10$. With such non-stationarity, $qcap=5$ can even work better than $qcap=10$ (unlike the previous section). In this non-stationary setting, DYAL is the 2nd best, and performs substantially better than the other EMA variants. O_{min} of 10 may still be considered on the low side (*i.e.* relatively high non-stationarity). With $O_{min} = 50$, first off, every technique’s deviation-rate improves, compared to $O_{min}=10$ setting. DYAL, with $\beta_{min}=0.001$, performs best for the $0.25 \leftrightarrow 0.025$ and Qs, $qcap=10$, works best with uniform p^* , DYAL remaining second best. When picking from uniform, the change in p may not be high, Qs can pick up such change faster, and more naturally, than DYAL, which performs explicit tests and may or may not raise its learning rate depending on the extent of change. However, Qs with 10, despite its simplicity, does require significant extra memory (and we’ll find that in the multiple items settings, no setting for Qs works better than DYAL).

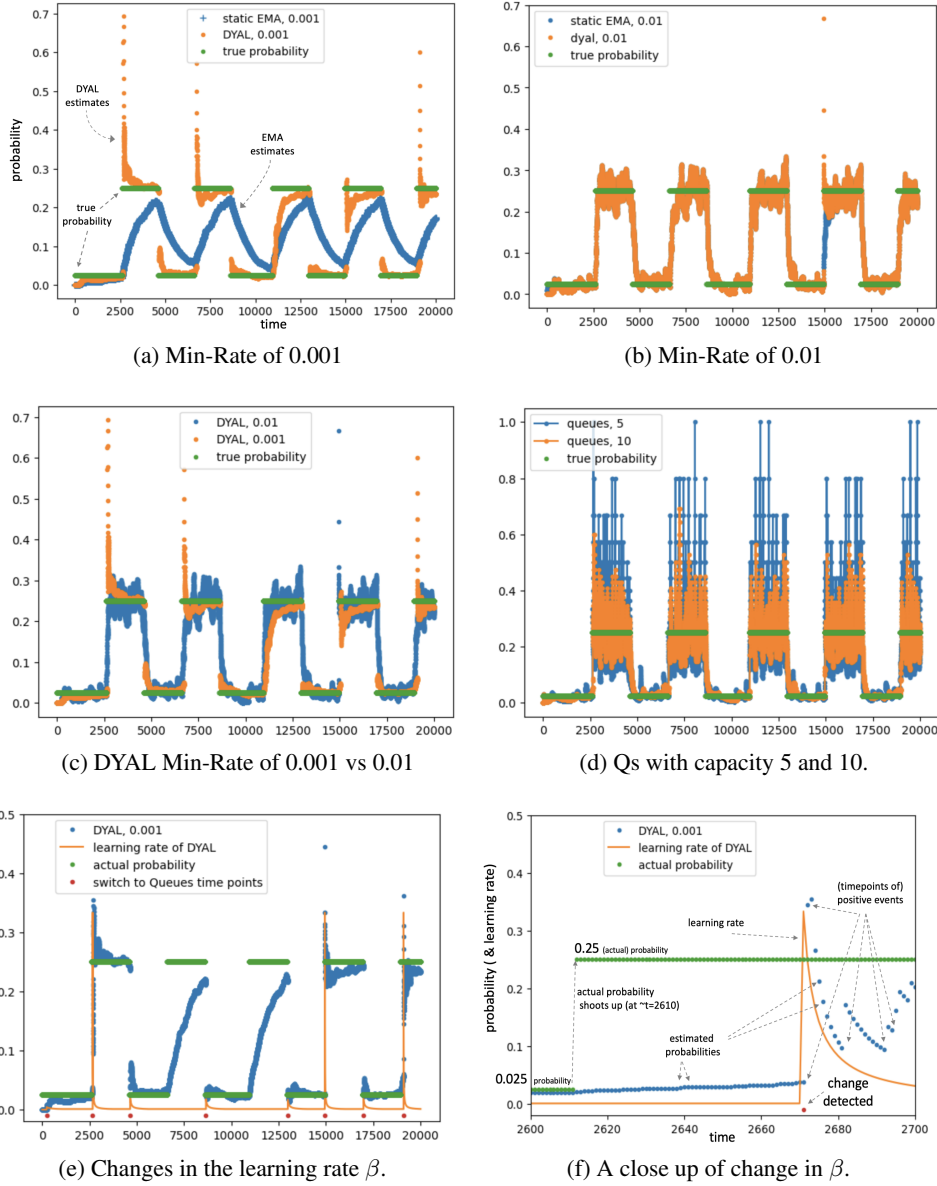


Figure 15: Synthetic single-item oscillation experiments, $0.025 \leftrightarrow 0.25$, on a single sequence. Parts (a) to (d) show the estimates of the three predictors, EMA, Qs, and DYAL, blue and orange colors, around the true probability (green, up-down steps). We can assess convergence speed and variance. Parts (e) and (f) also show evolution of the learning rate and the rate spikes as the probability of a single event is tracked via DYAL.

Figs. 15 shows plots of the output estimates $\hat{p}^{(t)}$, along one of the oscillating sequences ($0.25 \leftrightarrow 0.025$). As expected, we observe that the Qs technique leads to high variance during stable periods, qcap of 5 substantially higher than qcap of 10 (Fig. 15(d)). Similarity for both (static) EMA and DYAL, the rate of 0.01 exhibits higher variance than 0.001 (Figs. 15(b) and (c)). Static EMA and DYAL with 0.01 are virtually identical in Fig. 15(b), except that DYAL can have discontinuities when p^* changes (when it listen to its queue estimates, as discussed next), and converges from both sides of the target p^* , while static EMA converges from one side.

Fig. 15(e) shows the evolution of the learning rate of DYAL, and in particular when DYAL detects a (substantial or sufficiently significant) change (shown via red dots close to the x-axis). At the scale shown, rate increases look like pulses: they go up (whenever DYAL listens to a queue) and then with harmonic decay, they fairly quickly come back down (resembling spikes at the scale of a few hundred time points, for PRs in $[0.01, 1.0]$). We also note that this

rate increase can happen when a high probability (0.25) changes to a low probability (0.025) as well, though the rate increase is not as large, as would be expected. We also note that DYAL is not perfect in the sense that not all the changes are captured (via switching to its queues' estimates), in particular, there are a few "false negatives" (misses), when a change in p^* occurs in the sequence and DYAL continues to use its existing learning rates and adapt its existing estimates. This may suffice when the β at the time is sufficiently high or when the estimate is close. In particular, we can observe in Figs. 15(b) and (c) that a higher rate, $\beta_{min} = 0.01$, leads to fewer switches compared to 0.001, and in Figs. 15(b) we observe that DYAL behaves almost identically to static EMA when both have 0.01 (there appears to be one switch only at $t = 15000$ for DYAL).

Fig. 15(f) presents a close up of when a (significant) change is detected and a switch does occur, from a low true probability of $p^* = 0.025$ to $p^* = 0.25$ in the picture. Note that before the switch, the estimates (the blue line) start rising, but this rise may be too slow. Once sufficient evidence is collected, both the estimate and the learning rate are set to the queues' estimate, which is seen as a more abrupt or discontinuous change in the picture. The estimates then more quickly converge to the new true PR of 0.25. While we have not shown the actual negative and positive occurrences in the picture, it is easy to deduce where they are from the behavior of $\hat{p}^{(t)}$ (specially after the switch, where the estimates are high): the positives occur when there is an increase in the estimate $\hat{p}^{(t)}$ (from t to $t + 1$). Fig. 21 and Fig. 30 show additional patterns of change in the learning rate in multi-item real sequences.

Appendix E reports on a few additional variations in parameters and settings, *e.g.* Qs with $qcap = 3$, and deviation threshold $d = 1.1$, as well as imposing a minimum-length constraint for the uniform setting (Tables 15 and 16).

There are additional challenges (*e.g.* of setting appropriate parameters), when a predictor has to predict multiple items well, with different items having different probabilities and exhibiting different non-stationarity patterns. This is the topic of the next section and the rest of the paper.

7.3 Synthetic, Non-Stationary, Multi-Item

```

GenSequence(desiredLen,  $O_{min}$ ,  $L_{min}$ )
  // Create & return a sequence of subsequences.
  seq  $\leftarrow$  [] // A sequence of items.
  prevSD  $\leftarrow$  {}
  While len(seq) < desiredLen:
    // Extend existing sequence
     $\mathcal{P} \leftarrow$  GenSD(prevSD) // get new SD.
    seq.extend(GenSubSeq( $\mathcal{P}$ ),  $O_{min}$ ,  $L_{min}$ )
    prevSD  $\leftarrow$   $\mathcal{P}$ 
  Return seq

GenSubSeq( $\mathcal{P}$ ,  $O_{min}$ ,  $L_{min}$ )
  // Generate a (stationary) subsequence, via repeated
  // sampling iid from SD  $\mathcal{P}$ . It should be long enough
  // so that every item in  $\mathcal{P}$  occurs  $\geq O_{min}$  times in it.
  counts  $\leftarrow$  {} // An observation counter map.
  seq  $\leftarrow$  [] // A sequence of items.
  While min(counts) <  $O_{min}$  or len(seq) <  $L_{min}$ :
    o  $\leftarrow$  DrawItem( $\mathcal{P}$ ) // item o drawn.
    seq.append(o)
    // Update counts only for salient items.
    If o  $\in \mathcal{P}$ : // increment o's observed count.
      counts[o]  $\leftarrow$  counts.get(o, 0) + 1
  Return seq

GenSD(prevSD) // Generate a new SD.
  // Parameters: recycle,  $p_{min}$ ,  $P_{max}$ ,  $p_{NS}$ .
  probs  $\leftarrow$  [] // PRs of the SD.
  // Repeat while unallocated mass is sufficient.
  While u(probs) >  $p_{NS} + p_{min}$ : // sample PRs.
     $p_{max} \leftarrow$  min(left -  $p_{NS}$ ,  $P_{max}$ )
     $p \sim \mathcal{U}([p_{min}, p_{max}])$  // uniformly at random.
    probs.append(p) // add p to SD.
  If recycle: // reuse items '1', '2', ..
    Random.shuffle(probs) // random permute
    // item '1' gets probs[0], '2' gets probs[1], etc.
  Return MakeMap(probs)
Else: // Allocate new items (unused ids).
  Return MakeNewSDMap(probs, prevSD)

DrawItem( $\mathcal{P}$ ) // Return a salient or noise item.
  sump  $\leftarrow$  0.0 // via sampling.
   $p \sim \mathcal{U}([0, 1.0])$  // Uniformly at random.
  For o, prob  $\in \mathcal{P}$ :
    sump  $\leftarrow$  sump + prob
  If p  $\leq$  sump:
    Return o // Done.
  Return UniqueNoiseItem() // a unique noise id.

```

Figure 16: Pseudocode for generating a sequence of subsequences. Each subsequence corresponds to a stable period, subsequence $j \geq 1$ being the result of drawing iid from the j th SD, $\mathcal{P}^{(j)}$.

Fig. 16 provides pseudocode of the main functions for generating item sequences under non-stationarity. As in the above, we think of a non-stationary sequence as a concatenation of "stable" (stationary) subsequences, subsequence j , $j \geq 1$, corresponding to one SD $\mathcal{P}^{(j)}$. The subsequence is long enough (drawn iid from $\mathcal{P}^{(j)}$) so that $\min_{i \in \mathcal{P}^{(j)}} \text{count}(i) \geq O_{min}$, where $\text{count}(i)$ is the number of occurrences of item i in the subsequence. We may have a minimum (overall) length requirement as well, $L_{min} \geq 0$. Each $\mathcal{P}^{(j)}$ is created using the **GenSD** function.

In **GenSD**, some probability, p_{NS} , is reserved for noise, the NS items. Probabilities are drawn uniformly from what probability mass is available, initially $1 - p_{NS}$, with the constraint that each drawn probability p should be sufficiently

large, $p \geq p_{min}$. Optionally, we may impose a maximum probability P_{max} constraint as well ($P_{max} < 1$). Assume we get the set $S = \{p_1, p_2, \dots, p_k\}$, once this loop in GenSD is finished, then we will have $\sum_{p_i \in S} p_i \leq 1 - p_{NS}$, and each PR p_k satisfies the minimum and maximum constraints.

	1.5any	1.5obs	logloss	1.5any	1.5obs	logloss	opt. loss
new items ↓	Qs, 5			Qs, 10			
$O_{min} = 10$	0.94	0.24	1.17	0.88	0.17	1.19	1.040 ± 0.11
$O_{min} = 50$	0.92	0.22	1.13	0.78	0.10	1.09	1.028 ± 0.22
	static EMA, 0.01			static EMA, 0.001			
10	0.86	0.20	1.26	1.00	0.95	2.33	1.040
50	0.80	0.06	1.07	0.70	0.32	1.44	1.028
	harmonic EMA, 0.01			harmonic EMA, 0.001			
10	0.86	0.19	1.25	0.98	0.88	2.25	1.040
50	0.80	0.06	1.07	0.62	0.23	1.34	1.028
	DYAL, 0.01			DYAL, 0.001			
10	0.94	0.09	1.11	0.89	0.09	1.14	1.040
50	0.89	0.05	1.05	0.59	0.03	1.06	1.028
recycle items ↓	Qs, 5			Qs, 10			
$O_{min} = 10$	0.91	0.23	1.16	0.83	0.13	1.14	1.040 ± 0.11
$O_{min} = 50$	0.91	0.22	1.12	0.76	0.10	1.08	1.028 ± 0.22
	static EMA, 0.01			static EMA, 0.001			
10	0.87	0.16	1.16	1.00	0.73	1.65	1.040
50	0.80	0.06	1.06	0.77	0.26	1.28	1.028
	harmonic EMA, 0.01			harmonic EMA, 0.001			
10	0.87	0.15	1.15	0.98	0.66	1.54	1.040
50	0.80	0.05	1.05	0.71	0.18	1.18	1.028
	DYAL, 0.01			DYAL, 0.001			
10	0.91	0.10	1.11	0.83	0.16	1.18	1.040
50	0.88	0.05	1.04	0.56	0.04	1.06	1.028

Table 6: Synthetic multi-item experiments: Deviation rates and log-loss, averaged over 50 sequences, $\sim 10k$ length each, O_{min} of 10 and 50, uniform SD generation vis GenSD(): $P_{max} = 1.0$, $p_{min} = p_{NS} = 0.01$ for GenSD(), and change the SD \mathcal{P} whenever *all* salient items in \mathcal{P} are observed $\geq O_{min}$ times. In top half, items are new when underlying SD changes, and in the bottom half, items are ‘recycled’ (Sect. 7.3).

Once the set S of k PRs is generated, GenSD() then makes a SD from S . Under the **new-items** setting (when *recycle* = 0), new item ids, $|S|$ such, are generated, *e.g.* an item id count is incremented and assigned, and the items are assigned the probabilities (and all the old items, salient in $\mathcal{P}^{(j-1)}$, get zeroes, so discarded). Thus, as an example, the first few SDs could be $\mathcal{P}^{(1)} = \{1:0.37, 2:0.55, 3:0.065\}$, $\mathcal{P}^{(2)} = \{4:0.75, 5:0.21, 6:0.01, 7:0.017\}$, and $\mathcal{P}^{(3)} = \{8:0.8, 9:0.037, 10:0.15\}$.

Under the **recycle** setting, with k PRs generated, items 1 through k are assigned from a random permutation³¹ $\pi()$ of S : $\mathcal{P}(i) \leftarrow p_{\pi(i)}$ (thus item 1 may get p_3 , etc.). For example, with the previous PRs, we could have $\mathcal{P}^{(1)} = \{1:0.065, 2:0.37, 3:0.55\}$ (and 0.015 is left for NS items), $\mathcal{P}^{(2)} = \{1:0.75, 2:0.01, 3:0.21, 4:0.017\}$ (a new item is added), $\mathcal{P}^{(3)} = \{1:0.037, 2:0.8, 3:0.15\}$. Thus, under the *recycle* setting, in addition to changes in probability, the support of the underlying SD \mathcal{P} may expand (one or more new items added), or shrink, with every change (*i.e.* from one stable subsequence to the next one).

During drawing from a SD \mathcal{P} , when a NS item is to be generated we generate a unique NS id. This is one simple extreme, which also stress tests the space consumption of the maps used by the various methods on long sequences. Another extreme is to reuse the same NS items, so long as the condition that their true probabilities remain below (but close to) the boundary p_{min} is met.³² For simplicity, we present results on the former unique NS setting (pure noise). We have seen similar patterns of accuracy performance in either case.

³¹As the PR generation process tends to generate smaller PRs with each iteration of the loop, this random shuffling ensures that the same items are not assigned consistently high or low PRs.

³²Specially when NS item probabilities are borderline and close p_{min} , there can be some windows or subsequences on which the proportion goes over p_{min} .

We note that there are a variety of options for SD and sequence generation. In particular, we also experimented with the option to change only one or a few items, once they become eligible (their observation count reaching O_{min}), and we obtained similar results. Because this variation requires specifying the details of how an item’s PR is changed (*e.g.* how it is replaced by zero or more new or old items), for simplicity, we use GenSD(), *i.e.* changing all items’ PRs, and only when all become eligible. Note that, under the *reuse*=1 setting, some items’ probabilities may not change much, simulating a no-change for some items. Experiments on real streams provide further settings (Sect. 8).

Table 6 presents deviation rates (generalized to multiple items) as well as log-loss of various methods. We next describe how the deviation-rates as well the *optimal loss* (lowest achievable log-loss) are computed. To define all these measures, we need the sequence of underlying true distributions, $[\mathcal{P}]_1^N$ ($\mathcal{P}^{(t)}$ was used to generate $o^{(t)}$), which we have access to in these synthetic experiments.

The optimal (lowest achievable) loss (log-loss) at time t is defined as follows: given item $o^{(t)}$ is observed and $\mathcal{P}^{(t)}$ is the underlying distribution (at time t), then if $o^{(t)} \in \mathcal{P}^{(t)}$ ($o^{(t)}$ is salient), the optimal loss at t is $-\ln(\mathcal{P}^{(t)}(o^{(t)}))$, and if $o^{(t)}$ is NS ($o^{(t)} \notin \mathcal{P}^{(t)}$), then the loss is $-\ln(1 - \text{sum}(\mathcal{P}^{(t)}))$. The optimal log-loss is simply the average of this measure over the entire sequence. Note that if a single SD \mathcal{P} generated $[o]_1^N$, what we described is an empirical estimate of the SD entropy, *i.e.* the expectation:³³ $-(1 - \text{sum}(\mathcal{P})) \ln(1 - \text{sum}(\mathcal{P})) + \sum_{i \in \mathcal{P}} \mathcal{P}(i) - \ln(\mathcal{P}(i))$. Reporting the optimal log-loss allows us to see how close the various methods are getting to the lowest loss possible. Note that optimal loss, as seen in Table 6, does not change whether we use new items or recycle items. We use the same 50 sequences for the different methods, so the corresponding optimal losses are identical as well.

The (multi-item) deviation-rate, given the sequence of underlying SDs $[\mathcal{P}]_1^N$, is defined as:

$$\text{dev}([W]_1^N, [o]_1^N, [\mathcal{P}]_1^N, d) = \frac{1}{N} \sum_{t=1}^N \text{multidev}(o^{(t)}, \mathcal{W}^{(t)}, \mathcal{P}^{(t)}, d) \quad (\text{multi-item deviation}),$$

where for the multidev() function, we explored two options: under the more lenient ‘obs’ setting, we score based on the observation o at time t only: $\text{multidev}_{\text{obs}}(o, \mathcal{W}, \mathcal{P}, d) = \text{deviates}(\mathcal{W}(o), \mathcal{P}(o), d)$. Under the more demanding ‘any’ setting, we count as deviation if any estimate in \mathcal{W} having high deviation: $\text{multidev}_{\text{any}}(o, \mathcal{W}, \mathcal{P}, d) = \max_{i \in \mathcal{P}} \text{deviates}(\mathcal{W}(i), \mathcal{P}(i), d)$ (o is not used). $\text{multidev}_{\text{obs}}()$ is closer to log-loss, as it only considers the observation, and like log-loss, is therefore more sensitive to items with higher PR in the underlying \mathcal{P} . $\text{multidev}_{\text{any}}()$ is a more strict performance measure. Table 6 shows both rate types with $d = 1.5$.

Table 6 shows performance results when GenSD is used with $P_{max} = 1.0$, $p_{min} = 0.01$, and two O_{min} settings. With such generation settings, we get on average just under 17 SD changes, or subsequences (stability periods), when $O_{min}=10$, and just under 4 SD changes, when $O_{min}=50$. The support size (number of positive entries in an SD) was around 5. All performances, even for Qs with $qcap=5$, improve as O_{min} is increased from 10 to 50, and the performance of Qs with $qcap=10$ is better than $qcap=5$, even for high non-stationarity $O_{min}=10$, as we change the underlying SD \mathcal{P} only when *all* salient items of SD \mathcal{P} pass the O_{min} threshold. Nevertheless, even with $qcap$ of 10, Qs often trails the best of the EMA variants significantly. As in the previous section, harmonic EMA can slightly outperform static EMA, but both underperform DYAL at its best. In particular DYAL is not as sensitive to setting the (minimum) rate to a low value, as seen in Fig. 17 for several settings and rate values. We also note that while the log-loss values can seem close, the deviation rates can explain or reveal better why DYAL often does perform better.

We can also pair two methods and count the number of wins and losses, based on log-loss over each of the same 50 sequences, and perform statistical sign tests. With $O_{min}=50$ and the new-items setting, pairing DYAL with $\beta_{min} = 0.01$ (best or near best of DYAL) against all other techniques, EMA static or harmonic (with β in $\{0.001, 0.01, 0.02, 0.05, 0.1\}$) or Qs, DYAL gets lower a log-loss on *all* 50 sequences. If we lower the β_{min} rate for DYAL to 0.001, we still get dominating performance by DYAL, but harmonic can win on a few one or two sequences. With $O_{min}=10$ and again the new-items setting, pairing DYAL with $\beta_{min} = 0.01$ against all others, again we obtain the same dominating results for DYAL.

With the item-recycle setting, the differences between the best of the EMA variants and DYAL variants shrinks somewhat. For instance, with $O_{min}=50$, harmonic EMA with $\beta_{min} = 0.01$ gets 9 wins (DYAL, $\beta_{min} = 0.01$, gets the remaining 41 wins), and if we use $\beta_{min} = 0.001$ for DYAL, DYAL loses 42 times to harmonic EMA with $\beta_{min} = 0.01$. Similarly, with $O_{min}=10$, in the recycle setting, we need to set $\beta_{min} = 0.02$ to get a dominating performance by DYAL, and setting it lower to $\beta_{min} = 0.01$ (which worked well for $O_{min}=50$) yields mixed performance. Thus, the choice of rate β_{min} for DYAL can make a difference, although the operating range or the sensitivity to β_{min} is substantially lower for DYAL than for other EMA variants (Fig. 17), in particular when setting β_{min} to a low value. We observe this improved sensitivity on other data sources and settings as well.

³³When the underlying SD \mathcal{P} changes from time to time, the computed optimal log-loss is the weighted average of the entropies, weighted by the length of the subsequence each SD was responsible for.

DYAL, 0.01 vs. Box, 100	$O_{min} = 10$, recycle	10, new	$O_{min} = 50$, recycle	50, new
losses, wins of DYAL	7, 43	0, 50	8, 42	0, 50
LogLossNS, opt: 1.064 and 0.988	1.120, 1.108	1.182, 1.113	1.013, 1.008	1.025, 1.010

Table 7: Number of losses and wins, based on LogLossNS, of DYAL, with $\beta_{min} = 0.01$, pairing it against Box with window size 100 (which performed better than 50 or 200), under the recycle (item-recycle) and new-items settings, with $O_{min} = 10$ and 50, on 50 sequences of 10k each (the setting of Table 6). Thus DYAL has the lower loss on 43 of 50 sequences in the recycle setting with $O_{min} = 10$. Average LogLossNS values are also shown (1st number is Box’s), and average optimal LogLossNS is 1.064 ($O_{min}=10$) and 0.988 ($O_{min}=50$). All wins are highly significant (using the binomial sign test). With the lower $\beta_{min} = 0.001$ for DYAL, it has statistically more wins under the more challenging new-items settings but has mixed performance under the recycle settings.

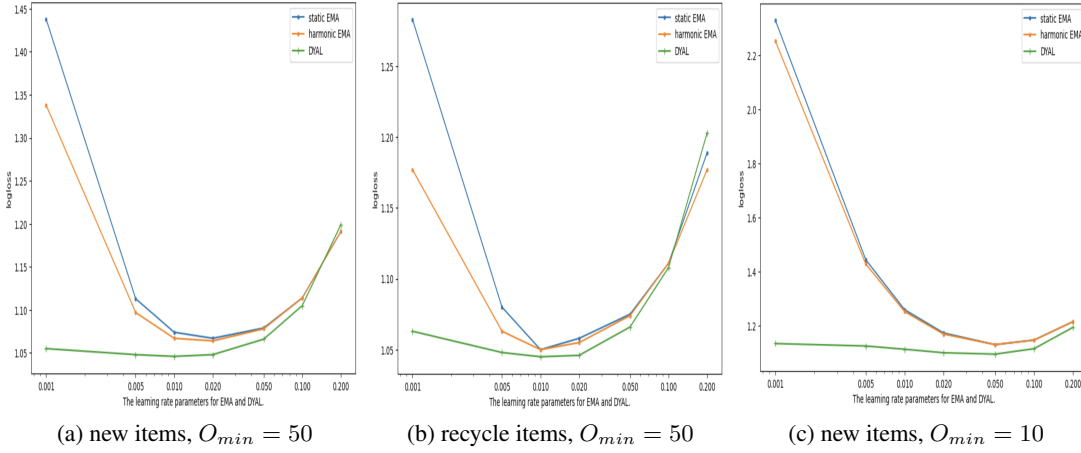


Figure 17: log-loss performance, as the learning rate is changed, in synthetic multi-item experiments, $O_{min} = 50$. (a) new items. (b) recycle items. DYAL is less sensitive to how low β_{min} is set, compared to harmonic and static EMA variants.

The Box SMA (Sect. 5.8) performs somewhat better than static EMA with an appropriate window size, which is about 100 for the setting of Table 6 (50 and 500 are strictly inferior, and 200 is slightly worse, in terms of LogLossNS and other measures). Like EMA, Box is inflexible and requires tuning the fixed window size for different input streams, and unlike EMA its rigid space consumption is prohibitive. Table 7 summarizes paired comparisons with DYAL, under the two recycle and new-item settings and $O_{min} = 10$ and 50. DYAL with $\beta_{min} = 0.01$, consistently outperforms it.

Appendix E.2, Table 17, presents performances for a few additional settings, in particular when P_{max} , for GenSD(), is set to a lower value of 0.1 instead of 1.

8 Experiments On Real-World Data Sources

In real-world datasets, a variety of complex phenomena combine to generate the sequences of observations, and even if we assume stationary distributions generate the data over some stable durations, we do not know the actual underlying probabilities in order to compare methods. In all the sections below, we obtain sequences of observations, in different domains, and report the log-loss performances, in particular AvgLogLossNS (Eq. 8), when comparing different predictors on these (same) sequences.

Table 8 presents the classification of the data sources we use here according to the type of non-stationarity. The sequences obtained from the Expedition system,³⁴ an implementation of ideas in prediction games [41], and described next, exhibit what we have called internal or developmental non-stationarity: new items (concepts) are generated over time by the system itself. If we turn off concept generation and keep predicting at the character level in Expedition, we do not have any non-stationarity, with a static external text corpus and in the way we sample lines, and we report

³⁴We used a text corpus of NSF abstracts in the Expedition experiments [20]. The dataset contains approximately 120k research paper abstracts, yielding 2.5 million English text lines, over 20 million term occurrences, and just under 100 unique characters.

Non-Stationarity →	Internal	External	Number	Median	Minimum	Maximum
Expedition, up to n-grams	✓	–	104	1.2k	75	48k
Expedition, only characters	–	–	Examples of predictors, and seq. lengths: ("ht", 91), ("t s", 75), ("and", 144), ("ron", 189), ("th", 3066), ("t", 25k), (" ", 48k)			
Unix commands	–	✓				

Table 8: Left: Real datasets and types of non-stationarity exhibited in the experiments. Right: Statistics on 104 Expedition sequences, with median sequence size of 1.2k. Blank space is the most frequent character leading to a sequence length of 48k, and 't' is the next most common at 25k.

comparisons in this setting as well (Sect. 8.2), finding that DYAL, developed for non-stationarity, continues to enjoy performance advantages over the others in this setting too. We provide evidence that the sequences in our final task, the Unix commands data sequences (Sect. 8.3), exhibit external non-stationarity: each person’s pattern of command usage changes over days and months, as daily activities and projects change. An example of a task exhibiting both internal and external non-stationarity is feeding the Expedition system one genre or language (*e.g.* French) for some time, followed by another (*e.g.* Spanish). We leave experiments on tasks exhibiting both internal and external non-stationarity to the future.

8.1 Expedition: Up to N-Grams

The Expedition system operates by repeatedly inputting a line of text (on average, about 50 characters in these experiments), *interpreting* it, and learning from the final selected interpretation. The interpretation process consists of search and matching (Fig. 18): it begins at the low level of characters, which we call *primitive concepts*, and ends in the highest-level concepts in its current *concept vocabulary* V that both match the input well and fit with one another well. Initially, this vocabulary V corresponds to the set of characters, around 100 unique such in our experiments, but over many episodes the vocabulary with which the system interprets grows to thousands of concepts and beyond. In our experiments, concepts are *n-grams* (words and words fragments). Higher level n-grams help predict the data stream better, in the sense that bigger chunks of the stream (better predictands) can be predicted in one shot and fewer independence assumptions are made. In the Expedition system, concepts are *both the predictors and the predictands*.

8.1.1 An Overview of Simplified Expedition

In previous work, we developed and motivated an information theoretic concept quality score we named CORE. CORE is a measure of *information gain*, a reward or score that promotes discovering and use, within interpretations, of larger or higher-level (higher reward) concepts [43]. In this work, we ignore the quality of the concepts (the predictands), and focus only on the more “pure” prediction task of better predicting a sequence of (unit-reward) items in the face of non-stationarity. We also leave it to future work to carefully assess the impact of better prediction algorithms on the learning and development of the entire system, *i.e.* the performance of the overall system with multiple interacting parts. Here and in Appendix F, we briefly describe how a simplified Expedition system works, and how we extract sequences, for learning and prediction, and for comparing different predictors. There are three main tasks in Expedition:

1. Interpreting (in every episode): using current concept vocabulary V , segment a line of text (the episode input) and map the segments into highest-level concepts, creating a concept sequence.
2. Predicting and updating (learning) prediction weights (every episode): Using a final selected interpretation s , update prediction weights among concepts in interpretation s .
3. Composing (every so often): Make new concepts out of existing ones (expand V).

In this paper, we focus on the prediction task 2, and to simplify the comparison of different prediction algorithms, we divorce prediction from interpreting and composing, so that the trajectory the system takes, in learning and using concepts, is independent of the predictor (the learner of the prediction weights), and different predictors can be directly compared. Otherwise, one needs to justify the intricacies of interpretation and new concept generation and that such do not unfairly work well with one technique over another. The (simplified) interpretation and composing methods we used, for tasks 1 and 3, are described in Appendix F.

8.1.2 Prediction Tasks, and Collecting Sequences

In every episode, once an interpretation, *i.e.* a final concept sequence, is selected, each concept in the sequence, except the right most, acts as a predictor and updates its weight for predicting what comes immediately after it to the right.

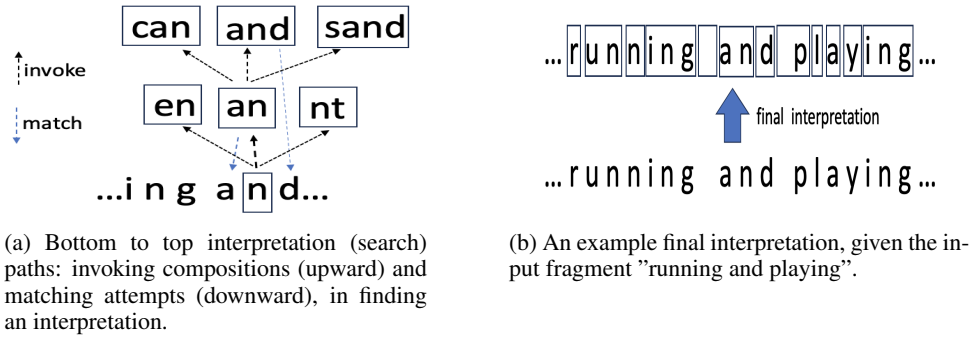


Figure 18: (a) The interpretation search process consists of invoking (“upward”) and matching attempts (“downward”), until no more compositions that match the input remain. (b) The final selected interpretation is a sequence of highest level available concepts, n-grams, that match the given input line well.

For example, in the concept sequence of Fig. 18(b), the predictor (concept) ‘r’ observes the (concept) ‘un’ to its right and updates accordingly, and (the predictor) ‘un’ observes ‘n’ to its right and updates accordingly, and so on. Note that only the final selected interpretation is used for updating prediction weights here, and the interpretation search path leading to it, as well as other search paths leading to unselected final interpretations, are discarded.

We ran the Expedition system for four trials, in each trial starting from scratch and with a different random seed, *i.e.* different sequences of lines are input to the system. Each trial was stopped after 20k to 30k episodes, each taking under an hour. In the course of a trial, thousands of new concepts are generated and used. Id generation for concepts is incremental via a simple counter, and as characters are seen first, before any higher-level n-gram is generated, concepts with lower ids correspond to characters (unigrams) and after id 95 we get bigrams and trigrams.

In each trial, for each of a few arbitrary concept ids being tracked³⁵ (a few below id 20, a few around 100 and 500), we collect and create a sequence from what comes after the corresponding concept in the episodes it is active in, *i.e.* it appears in one or more places in the final selected interpretation. For instance, in one trial, the concept (corresponding to) ‘t’ was tracked, and ‘t’ got a sequence of 25k observations long, each observation being a concept id. Thus ‘t’ was active in up to 25k episodes (in some episodes, ‘t’ may appear more than once). Initially, in the first few 100s of episodes say, ‘t’ will only ‘see’ single characters (unigrams) immediately next to its right (concept ids below 95), and later on, as bigrams and higher n-grams are generated, a mix of unigrams with higher level n-grams is observed. With tracking of a few ids, we collected 104 sequences over the different trials, with median sequence size of 1.2k observations, minimum size of 75, and maximum sequence size of 48k (Table 8). For the less frequent and newer concepts we get shorter sequences. There are nearly 1000 unique concepts (concept ids) in the longest sequences, and 10s of unique concepts in the shorter ones. A few example concepts with their sequence lengths are given in Table 8.

8.1.3 Internal Non-Stationarity in Expedition

Initially, every character (as a predictor) sees single characters in its stream of observations. For instance the character ‘b’, as a predictor, sees ‘a’, or ‘e’, or ‘ ’, etc. immediately occurring afterwards in an episode, for some time. Later on, as the higher level concepts, bigrams and trigram, are generated and used in interpretations, the predictor ‘b’ also sees bigrams and trigrams (new concepts) in its input stream, and sees the unigrams characters less frequently. Furthermore, when concept ‘b’ joins another concept, such as ‘e’, to create a new concept ‘be’, the distribution around ‘b’ changes too, as ‘e’ is not seen to follow ‘b’ as much as before the creation and use of ‘be’: a fraction of the time when ‘b’ occurs in an episode at the lowest level, ‘be’ is observed, at the highest level of interpretation, instead of the unigram ‘b’ followed by ‘e’. We also note that the frequency of the occurrence of a lower-level concept, at the highest interpretation level, tends to decrease over time as higher n-grams, that use that concept as a part, are generated and used.

The input corpus of text as well as the manner in which a text line is sampled (uniformly at random) to generate an episode is not changing here, *i.e.* no change in the occurrence statistics of individual characters, nor in their co-occurrences, or there is no external non-stationarity here, but there is internal non-stationarity, as the interpretations,

³⁵The same character gets different ids in different trials.

	Qs				static		harmonic	DYAL
	2	3	5	10	0.001	0.01	0.01	0.001
logloss	2.65	2.60	2.61	2.70	2.80	2.56	2.71	2.39

Table 9: log-loss of various methods on 104 sequences extracted from Expedition (median sequence size of 1.2k).

DYAL, 0.001 vs. \rightarrow	Qs, 3	static, 0.01	static, 0.005	harmonic, 0.01
$c_{NS} = 3$	1, 103	0, 104	17, 87	0, 104
$c_{NS} = 2$ (default)	1, 103	0, 104	16, 88	0, 104
$c_{NS} = 1$	13, 91	22, 82	13, 91	8, 96
$c_{NS} = 0$	17, 87	13, 91	2, 102	27, 77

Table 10: Number of losses and wins of DYAL, with $\beta_{min} = 0.001$, pairing it against a few other techniques, on the 104 Expedition sequences, as we alter the c_{NS} threshold. If observation count $\leq c_{NS}$ then it is marked NS (Sect. 3.5). Thus DYAL wins over Qs with ($qcap = 3$) on 103 of 104 sequences (top left). The number of wins of DYAL is significant at over 99.9% confidence level in all cases. Also, DYAL wins over static with $\beta \in \{0.01, 0.005\}$, on all the 19 longest sequences, at default $c_{NS} = 2$.

over time, use highest level matching n-grams. Thus, the nature of the prediction task, at the highest interpretation level, can change gradually, even when the external input stream is stationary.

8.1.4 Overall Performance on 104 Expedition Sequences

Table 9 shows the log-loss (AvgLogLossNS()) scores of our 4 predictors, averaged over the 104 Expedition sequences. All the parameters are at their default when not specified, thus DYAL is run with binomial threshold of 5 and a queue capacity of 3. We observe that DYAL does best on average, and as Table 10 shows, pairing and performing sign tests indicates that log-loss of DYAL (with $\beta_{min} = 0.001$) outperforms others (yields the lower loss) over the great majority of the sequences.

Table 10 also changes the c_{NS} to assess sensitivity to what is considered noise. Lowering the c_{NS} makes the problem harder, and we have observed here and in other settings, that log-loss goes up. For instance, the log-loss performance of DYAL goes from 2.93 at $c_{NS} = 0$ down to 2.3 with $c_{NS} = 3$. Of course, with $c_{NS} = 1$, we are expecting a technique to provide a good PR estimate even though the item has occurred only once before! Without extra information or assumptions, such as making the stationarity assumption and assuming that there are no noise items, or using global statistics on similar situations (*e.g.* past items that were seen once), this appears impossible.

We next go over the sensitivity and behavior of different techniques under parameter changes, as well as looking at performance on long *vs.* short sequences (subsets of the 104 sequences).

8.1.5 Sensitivity to Parameters

Fig. 19(a) shows the sensitivity to β_{min} for DYAL and harmonic EMA, and β for static EMA. We observe, as in Sect. 7.3 for the case of multi-item synthetic experiments, that DYAL is less sensitive than both of harmonic and static EMA, while harmonic is less sensitive than static when β is set low (and otherwise, similar performance to static). In particular, for longer sequences, lower rates can be better (see next Section), but for other EMA variants, low rates remain an issue when faced with non-stationarity (*i.e.* new salient items).

Fig. 19(b) shows the sensitivity of DYAL to the choice of the binomial threshold, which controls when DYAL uses the queue estimates. There is some sensitivity, but we posit that at 3 and 5, DYAL performs relatively well. We also ran DYAL using different queue capacities with $\beta_{min} = 0.001$ (default is $qcap = 3$), and obtained similar log-loss results (*e.g.* 2.38 at $qcap = 2$, and 2.4 for $qcap = 5$).

8.1.6 Longer *vs.* Shorter Sequences

Of the 104 sequences, there are 19 sequences with length above 5k, median length being 13k. We averaged the log-loss performances of DYAL, as we change its β_{min} , over these 19, as well as over the sequences with length below 1k, of which there are 46 such, with median of 280 observations. Fig. 20(a) shows that lowering the β_{min} works better or no worse, for longer sequences, as expected, while the best performance for the shorter sequences occurs with higher $\beta_{min} > 0.01$. A similar patterns is also seen in Fig. 20(a) for Qs technique. Larger queue

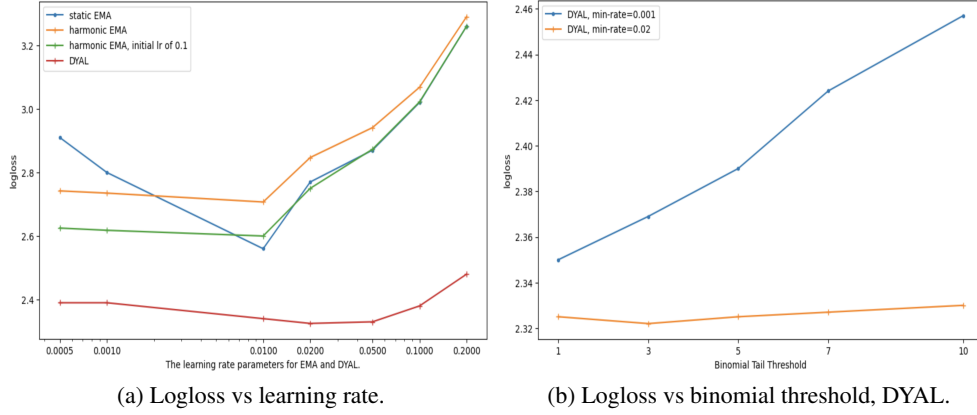


Figure 19: Prediction sequences from Expedition: Changing the learning rate (left), and the binomial threshold (right) in DYAL, and plotting the log-loss (AvgLogLossNS ()) performance.

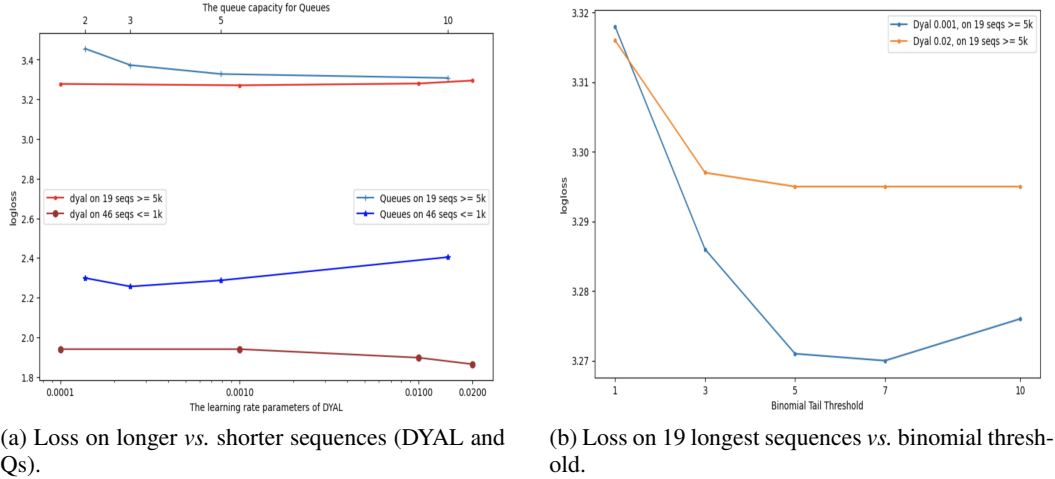


Figure 20: log-loss (a) on 19 longest sequences (above 5k) vs 46 shorter sequences (below 1000). On the longer sequences and lower β_{min} for DYAL, and a higher queue capacity for Qs, helps. (b) loss vs binomial threshold on 19 longest sequences. Setting the value in 3 to 7 works well, and $\beta_{min} = 0.001$ does better than $\beta_{min} = 0.02$ on these sequences.

capacities work better for longer sequences, but because shorter sequences dominate the 104 sequences, overall we get the result that a qcap of 3 works best for this data overall.

We also note that the shorter sequences yield a lower log-loss (both figures of 20). This is expected and is due to our policy for handling NS: for methods that allocate most their initial mass to noise and when this agrees with the NS marker referee, one gets low loss. For instance, at $t = 1$, the NS marker marks the next item as NS, and with a predictor that has all its PR mass unallocated, log-loss is 0 (loglossRuleNS() in Fig. 3(b)). As the sequence grows longer, and more salient items are discovered, the average loss can go up. This is also observed in the next section when we do character-based prediction (Sect. 8.2.1).

8.1.7 Evolution of the Learning Rates, Degrees, etc.

Fig. 21 shows plots of the evolution of maximum (max-rate) and median of the learning rates in the *rateMap* of DYAL for two predictors (two sequences), the concept "ten", with just over 200 episodes, and the concept "I" with over 12000 episodes. The number of entries (edges) in the *rateMap* (and the *EmaMap*), or the out-degree, is also

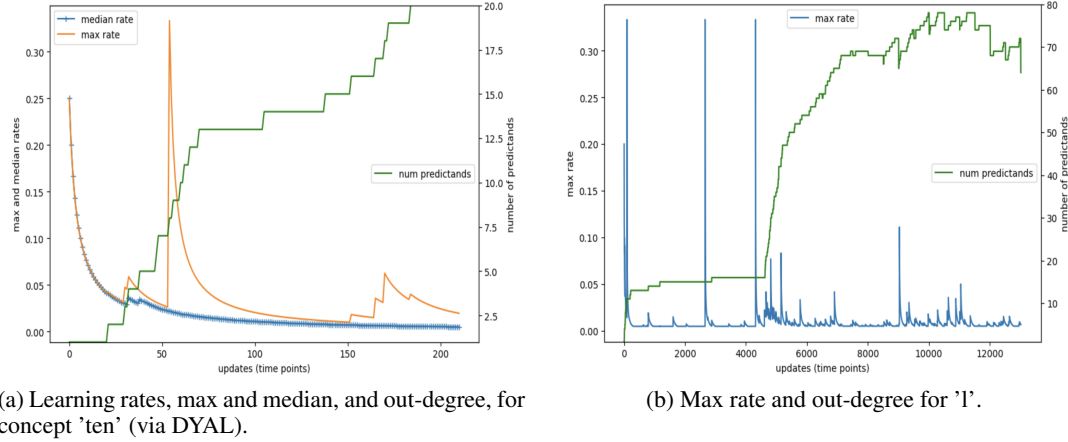


Figure 21: Examples of evolution of the learning rates of DYAL and the number of predictands, or out-degree (number of entries in *EmaMap*), with time. (a) Maximum (max-rate) and median learning rates and number of predictands for the concept 'ten'. (b) Maximum learning rates and number of predictands for the 13k-long sequence for the concept 'l'.

reported. We observe that the maximum over the learning rates contain bursts every so often indicating new concepts need to be learned, while the median rate converges to the minimum, indicating that most predictands at any given time are in a stable state. On the long 12k sequence, we also see the effect of pruning the map every so often: the number of map entries remain below 100 as old and low PR items are pruned (see Sect. 5.6 and 6.3).

Appendix F.4 also includes plots of the max-rate on a few additional sequences (self-concatenations), in exploring evidence for non-stationarity.

8.2 Expedition at the Character level

Here, we do not generate new concepts, thus the prediction task remains at the (primitive) character level. We track all the characters as predictors: each character, when observed, predicts the next character, and, for evaluation, each has its own referee (NS marker). We report log-loss ($\text{AvgLogLossNS}()$) at every time point, meaning that with each input line, from left to right as in the previous section, for each character (predictor), we predict (what character comes to the right) and record the log-loss, then observe and update the predictor. At certain times t , e.g. after observing 1k characters (1000 observe and update events), we report the average of the log-losses upto t . For instance, on the line "abcd", we collect the log-loss performance of the predictors corresponding to 'a', 'b' and 'c' (and after the loss is collected, each predictor updates too³⁶). Thus, in this section, unlike the previous sections, we are reporting an average of the log-loss performance of *different* predictors, over time. Note further that, in this manner of reporting, the more frequent characters (predictors), such as 'e', 'a', and the blank space ' ', will have more of an impact on the reported performance.

In this character-prediction setting, there is neither external nor internal non-stationarity, as described in the previous section, and even though there is no non-stationarity, we find that DYAL out-performs the other predictors, as seen in Table 11 and Fig. 22. Table 11 shows log-loss averaged over 10 runs for a few choices of parameters, where a run went to 1k, 2k and 10k time points (prediction episodes). Fig. 22 shows log-loss performance for a few learning rates, from 10k to 300k time points. We see that DYAL with one choice of $\beta_{min} = 0.001$, does best over all snapshots. The Qs technique does best with the highest capacity of 10 (in this stationary setting), and EMA variants require playing with the learning rate as before, and still lag DYAL. Plain EMA variants, static and harmonic, underperform for a combination of the way we evaluate and their insufficient inflexibility with regards to the learning rate: when an item is seen for the first time, harmonic may give it a high learning rate, but then is punished in subsequent time points, as the item may be a low probability event. Note that in our experiments, we started the harmonic with a initial learning rate of 1.0 (and experimenting with the choice of initial rate β_{max} may improve its performance, see Fig. 23 on Unix commands). Static EMA assigns whatever its fixed learning rate is, to a new item, which could be too low or too high.

³⁶In these experiments, we do not update for the last concept of a line, 'd' in this example, as there is no next character for such, though one could use a special end of line marker.

time ↓	Qs			static (EMA)			harmonic	DYAL
	3	5	10	0.005	0.01	0.02	0.01	0.001
1000	1.69±0.05	1.66	1.64	1.6	1.87	2.24	2.59	1.20
2000	2.01±0.02	1.96	1.93	2.11	2.16	2.34	2.50	1.60
10000	2.39±0.01	2.32	2.27	2.43	2.37	2.41	2.44	2.15

Table 11: log-loss averaged over 10 runs of character-level Expedition (no new concepts generated). DYAL does best over all time snapshots.

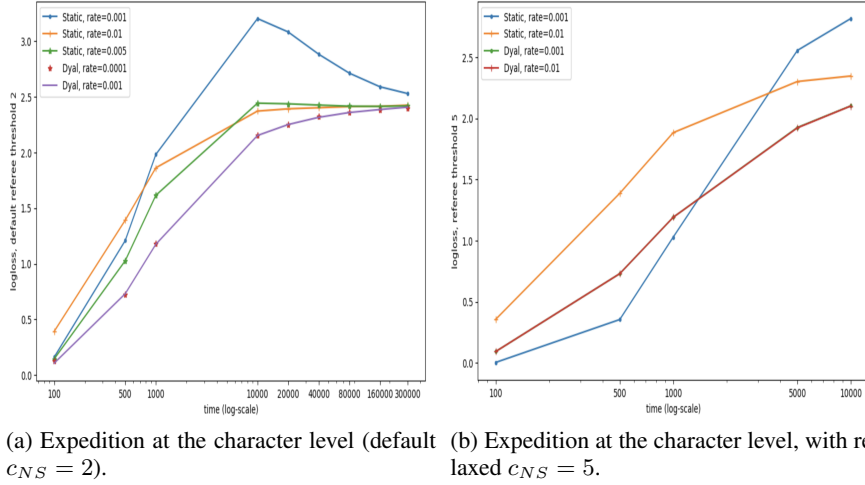


Figure 22: log-loss vs time, for Expedition at the character level. (a) With default $c_{NS} = 2$, each point is average over 5 sequences. (b) With the more relaxed $c_{NS} = 5$ (shown up to 10000) initially all curves improve, lowered log-loss, compared to $c_{NS} = 2$. In particular static EMA with a low rate benefits most, as it only slowly allocates probability to salient items, agreeing more with the relaxed referee. In both cases, DYAL with two different rates ($\beta_{min} \in \{0.0001, 0.001\}$ in (a) and $\beta_{min} \in \{0.001, 0.01\}$ in (b)) results in almost identical losses.

8.2.1 LogLossNS Initially Goes Up

Consistent with our previous observation on lower (better) log-loss performance on shorter vs. longer sequences (Sect. 8.1.6), here, as more seen items become salient (not marked NS), and with the manner we evaluate with a referee, log-loss increases over time for most methods but approaches a plateau and converges. For a ‘slow’ method such as static EMA with a low β , log-loss peaks before it starts going down. DYAL is not slowed down or is not as sensitive to setting the (minimum) rate low (β_{min} set to 0.001 or lower) (in Fig. 22, the plots for DYAL with β_{min} from 0.0001 to 0.01 appear identical), and may actually benefit from a low rate in the long run (Table 12).

We developed the bounded log-loss primarily for comparing different techniques. Here, we observe that the loss may go up on the initial segments of a sequence, which can be counter-intuitive and undesired (loss should go down, in general, with more learning). Appendix A.4 briefly discusses the alternatives we considered. It is also possible that assuming items have rewards and taking into account the rewards may address this issue as well (mentioned as a future direction in Conclusions Sect. 10), and the motivation for the reward-based CORE score in [41].

$\beta_{min} \rightarrow$	0.0001	0.001	0.01	0.05	0.1
log-loss	2.408±0.002	2.398±0.001	2.415±0.000	2.512±0.002	2.652±0.001

Table 12: Character-level Expedition using DYAL over longer runs: log-loss averaged over 5 runs till 300k time points (character predictions). β_{min} of ≥ 0.05 is too high (indicating there are salient predictands with probability below 0.1), while low $\beta_{min} \leq 0.001$ do slightly better than 0.01.

52-scientists (52 sequences)						Masquerade (50 sequences, 5k each)		
sequence length			# unique commands per user			# unique commands per user		
median	min	max	median	min	max	median	min	max
1.8k	205	12k	106	22	359	101	5	138

Table 13: Statistics on Unix commands data. Left: 52-scientists, median sequence length is 1.8k commands, and the median number of unique commands per sequence is 106, while one user (sequence) has 138 unique commands (the maximum). Right: Masquerade, 50 sequences, each 5k long. Median number of unique commands per sequence is 101, while one user used only 5 unique commands (in 5k commands).

8.3 Unix Commands Data

We look at two sequence datasets in the domain of user-entered Unix commands, which we refer to as the *52-scientists* data, a subset of data collected by Greenberg [29], and the Masquerade sequences [63]. These sequences are good examples of high external non-stationarity: for instance, it is observed in our previous work on Greenberg sequences [45] that if the online updates are turned off mid-way during learning, when it appears that the accuracy has plateaued, the prediction performance steadily and significantly declines. Non-stationarity in daily activities can be due to a variety of factors, and changes may be permanent, periodic and so on (project changes, taking vacations, illness, and so on), and timely adaption is important for automated assistants. We also present further evidence of non-stationarity below, as well as in Appendix F.4. The data likely includes a mix of other non-iid phenomena as streaks (repeating commands) and certain hidden periodic behaviors. Table 13 presents basic sequence statistics for the two sources.

8.3.1 Task and Data Description

In our previous work [45], we were interested in the ranking performance, for a recommendation or personalization task, and we used several features of context, mostly derived from previously typed commands, as predictors of the next command. We updated and aggregated the predictions of the features using a variation of EMA that included mistake-driven or margin-based updates, and showed significant performance advantage over techniques such as SVMs and maximum entropy [45]. Here, we are interested in the extent to which the sequences are stable enough to learn probabilities (PRs), and the relative performance of different probabilistic prediction techniques. As the sequences would be relatively short if we focused on individual commands as predictors (100s long for almost all cases), we look at the performance of the “always-active” predictor that tries to learn and predict a “moving prior” of which next command is typed.³⁷ Therefore here, each command in the sequence is an item. For both datasets, we use only the command stubs, *i.e.* Unix commands such as “ls”, “cat”, “more”, and so on, without their arguments (filenames, options, etc.). The Masquerade data has the stubs only, and our experiments with full commands, *vs.* stubs only, on 52-scientists yields similar findings. The sequences have been collected over the span of days to months for both datasets, depending on the level of the activity of a user. For Masquerade, we only use the first 5000 commands entered by each user, as the remainder can have other users’ commands interspersed, designed for the Masquerade detection task³⁸ [63].

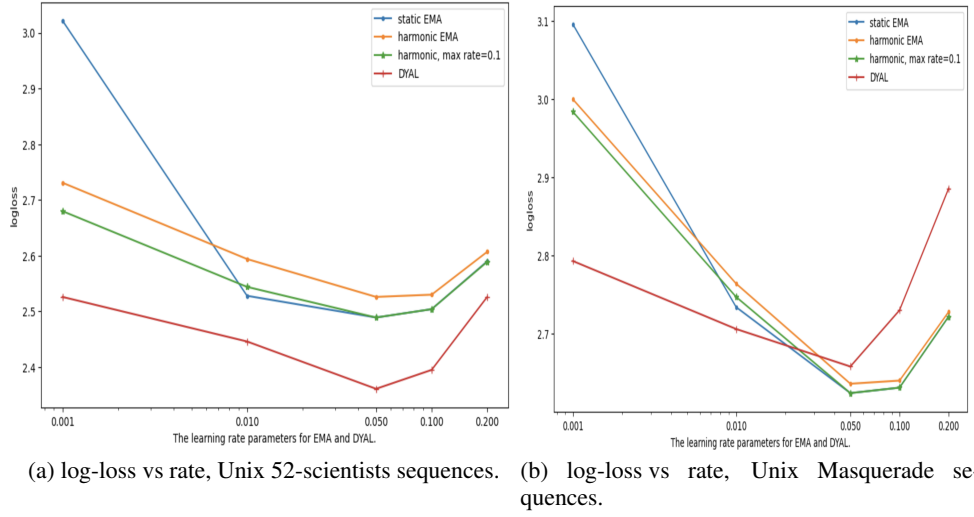
8.3.2 Performance on Unix Data

Fig. 23 shows the performance of EMA variants as a function of the learning rate, and Table 14 reports on Qs performance with a few qcap values, and includes the best of EMA variants. We observe a similar v-shape pattern of performance for static and harmonic EMA, while for DYAL, as before, the plots show less of a dependence on β_{min} compared to other EMA variants. However, the degradation in performance as we lower β_{min} is more noticeable here. DYAL performs better on 52-scientists compared to others, but is beaten by static EMA on Masquerade. Below, we report on paired comparisons and the effect of changing the referee threshold c_{NS} .

We note these data indeed have higher non-stationarity compared to previous ones when we consider a few indicators: the best performance occurs when β_{min} is relatively high at ≈ 0.05 , larger than our previous datasets (Fig. 23). Table 14 also shows that Qs does best here with smaller qcap values. Appendix F.4 presents additional experiments showing further evidence of external non-stationarity.

³⁷The Greenberg data has 3 other user types, but the sequences for all the other types are shorter. We obtained similar results on the next collection of long sequences, *i.e.* ‘expert-programmers’, and for simplicity only include the 52-scientists subset.

³⁸It may be fruitful to develop an application of the online predictors we have developed, to the Masquerade detection task and compare to other methods.

Figure 23: log-loss performances (AvgLogLossNS()) vs. β parameters: (a) 52-scientists (b) Masquerade.

52-Scientists					Masquerade				
Qs				DYAL	Qs				static
2	3	5	10	0.05	2	3	5	10	0.05
2.581±0.28	2.586	2.629	2.686	2.361	2.769±0.5	2.735	2.754	2.830	2.624

Table 14: On Unix sequences, Qs log-loss performance, and the best of EMA variants. Lower qcaps work better, suggesting significant non-stationarity.

8.3.3 Pairing and Sign-Tests on Unix Sequences

We compare DYAL to static EMA as harmonic and static behave similarly. At β of 0.05, best for both DYAL and static EMA, on the 52-scientist sequences, we get 46 wins for DYAL over static (lower log-loss for DYAL), and 6 wins for static. On average, 13% of a sequence is marked NS by the referee. As we raise the referee threshold c_{NS} from 2 to 3 to 4, we get additional wins for DYAL and the log-loss performances improve for all methods, and the fraction of sequence marked NS goes up, reaching to 18% at $c_{NS} = 4$. Conversely if we lower the referee threshold to 1, we get fewer 34 wins for DYAL over static EMA (and 11% marked NS).

On Masquerade’s 50 sequences, we get only 10 wins for DYAL vs. 40 for static, again at $\beta_{min} = 0.05$, where both do their best, which is statistically highly significant. With the default of $c_{NS} = 2$ only 5% of a sequence is marked NS on average. As in the case of 52-scientists, when we increase the referee threshold from 2 to 3 to 4, we get additional wins for DYAL, and at $c_{NS} = 4$, DYAL has 37 wins over 13 wins for static (8% marked NS with $c_{NS} = 4$). Similar to the above 52-scientists case, lowering the threshold to 1 leads to more wins for static. Importantly, if use a referee that is based on a short window of the last 200 (rather than our simple unlimited window size) and require seeing an item at least twice in the last 200 timepoints to mark it as salient (not NS), again DYAL becomes superior (47 wins for DYAL, and 9% marked NS).

Why a fixed and relatively high learning rate of 0.05 does relatively well here compared to the more dynamic DYAL, on Masquerade sequences? Any assumption behind the design of DYAL, in particular the sufficient stability assumption, may be partially failing here. For many items, their PR, or appearance frequency, may be high once they appear, but their stability period may be too short, and a simple high learning-rate of 0.05 may work just as well, compared to the slow two-tiered approach of first detection and estimation via the Qs technique, and at some point, switching to the queues estimate. As we increase the referee threshold c_{NS} , we focus or bias the evaluation further on the more stable items in the sequence, and we get better relative results for DYAL. This observation gives more credence to the stability explanation.

9 Related Work

Our problem lies in the areas of online learning [33], non-stationarity and learning under concept drift [18, 26, 31], change detection [72, 18], probability forecasting and assessing quality of output probabilities (propriety, calibration) [22, 71, 9, 28, 14], (non-parametric) density estimation or distribution learning [50, 51, 10], with connections to streaming data structures and algorithms [24, 25] and time-series analysis [73, 48]. To the best of our knowledge, this combination of open-ended categorical (nominal) probability prediction under non-stationarity, with attention to practical efficiency, has not been studied before. We provided pointers on relevant work for the tools and techniques we used throughout the paper. In this section, we further situate our work within the broader context of similar tasks and problem domains, and provide a short history.

Our task and the DYAL solution involves a kind of *implicit* change detection (CD) [26, 18, 80]: Two main categories of adaptation strategy to change are blind (or implicit) and informed (or explicit) [26, 18]. In all of Qs, EMA (static or harmonic-decay), and Box, adaptation to non-stationarity is done automatically or without explicit detection. DYAL comes closest to explicit detection, and it uses the implicit Qs to do so. In our task, the system need only adjust its output probabilities in a timely manner. In some tasks, such as monitoring for safety and potential attacks, explicitly pinpointing the (approximate) time of change can be important too [18, 58]. Change detection is a diverse subject studied in several fields such as system monitoring, psychology (*e.g.* within human vision) and image processing and time series analysis (*e.g.* [58, 69, 72, 4]). Here, we seek a (timely) response and adaptation to a change. Many variants of moving averages are also used in time-series analysis (*e.g.* the ARMA model). There, the observations are ordinal (such as counts) even if discrete (*e.g.* [73, 48]), and stationarity or limited non-stationarity is typically assumed. Similarly, much past work, *e.g.* on variable window sizes, has addressed numeric data, for instance tracking means and variances [6, 64] (Sect. 5.8). It has been observed that CD is understudied for categorical data [58], and the authors develop efficient model-based explicit CD techniques for streaming data: the set of items is known and fixed in this work (a multinomial distribution). Their evaluation is based on measuring change-detection rates (*e.g.* true-positive rates for an acceptable fixed false-positive rate).

The online observe-update cycle, updating a semi-distribution, has a resemblance to online (belief) state estimation, *e.g.* in Kalman filters and partially observed Markov models for control and decision making, in particular with a discrete state space [15, 11]. Here, the goal is pure prediction (*vs.* action selection or control), though some of the techniques developed in this work may be useful to that setting, specially when one faces a changing external world. Extensions of the Kalman filter with dynamic window sizes (for numeric sequences) has proved useful for adapting supervised and unsupervised learning techniques, such as Naive Bayes, to non-stationarity [6, 79]. More generally, streaming algorithms aim to compute useful summary statistics, such as unique counts and averages, while being space and time efficient, in particular often requiring a single pass over a large data set or sequence, such as the count-min sketch algorithm [24, 25]. Here, we have been interested in computing recent proportions in a non-stationary setting, for continual prediction, implemented by each of many (severely) resource-bounded predictors. Learning finite state machines in a streaming manner shares similar philosophy and a similar subproblem of change detection (in particular, Fig. 1, “system for continuous learning” [5]).

Non-parametric density estimation techniques are often based on kernels or keeping track of specific instances and assume stationarity (*e.g.* [10, 17]). Recent work, in computational-learning theory, comes closest to ours and extends the density estimation task to an open-ended, in particular with infinite-support, non-stationary setting [50], but (space) efficiency and empirical performance of the predictor is not a focus, and the kept history grows logarithmically in stream length. Furthermore, absolute loss (total-variational distance) is used to assess the theoretical quality of algorithms (limiting applicability to estimate only high probabilities well, above say 0.1, see Sect. 5.8).

This paper extends our ongoing work on developing large-scale online multiclass learning techniques, for lifelong continual learning when the set of classes is not known apriori, and often large and dynamic (*i.e.* open-ended) [46, 47], in particular in the framework of Prediction Games for learning a growing networked vocabulary of concepts [43, 40, 41]. In online (supervised) learning, *e.g.* [33, 60, 39], the focus is often on the interaction of the predictors (features) and, for example, on learning a good weighting combination for a linear model, while we have focused on learning good *independent* probabilistic predictors, akin to the (multiclass) Naive Bayes model [38], but in an unsupervised (or self-supervised) setting, as well as the counting techniques for n-gram language models [61], but in a non-stationary setting. Another avenue of work is calibrating classifiers after training (trained on a ranking or accuracy-related objective) [22], and there may be extensions applicable to our non-stationary open-ended and online setting. Similarly, investigating online techniques for learning good mixing weights, but also handling the non-stationarities, may prove a fruitful future direction, for instance in the mold of (sleeping) experts algorithms [23, 33, 13].

Learning-rate decay has been shown beneficial for training on backpropagation-based neural networks, and there is research work at explaining the reasons [78, 67]. Here, we motivated decay variants in the context of sparse EMA updates and learning good probabilities fast, and motivated keeping predictand-specific rates.

10 Summary and Future Directions

Dynamic worlds require dynamic learners: often there is change, but we typically cannot predict what will change (or when). In the context of online open-ended probabilistic categorical prediction, we presented a number of sparse moving average (SMA) techniques for resource-bounded (finite-memory) predictors. We described the challenges of assessing probability outputs and developed a method for evaluating the probabilities, based on bounding log-loss, under noise and non-stationarity. We showed that different methods work best for different regimes of non-stationarity, but provided evidence that in the regime where the probabilities can change substantially but only after intermittent periods of stability, the DYAL SMA which is a combination of the sparse EMA and the Qs technique, is more flexible and has advantages over either of the simpler methods: the Qs predictor has good sensitivity to abrupt changes (can adapt fast), but also has higher variance, while plain EMA is slower but is more stable, and combining the two, with predictand-specific learning rates, leads to faster more robust convergence in the face of non-stationarities. The use of per-predictand rates can also serve as indicators of current confidence in the prediction estimates.

This work originated from the problem of assimilating new concepts (patterns), within the Prediction Games framework, where concepts serve as both the predictors and the predictands in the learning system. In particular, here we made a distinction that even if the external world is assumed stationary, the development of new concepts, explicitly represented in the system, results in internal, in particular developmental, non-stationarity, for the many learners within the system. This means sporadic abrupt changes in the co-occurrence probabilities among the activated concepts as the system changes and evolves (over many episodes) its interpretations of the raw input stream. However, we expect that the rate of the generation of new concepts, which should be controllable, can be such that there would be stability periods, long enough to learn the new probabilities, both to predict well and to be predicted well. Still, we strive for predictors that are fast in adapting to such intermittent patterns of change.

We plan to further evaluate and develop the SMAs within the Prediction Games framework, in particular under longer time scales and as the concept generation and interpretation techniques are advanced, and we seek to better understand the interaction of the various system components. We touched on a variety of directions in the paper. For instance, it may be fruitful to take into account item (predictand) rewards when rewards are available, and this may lead to different and interesting design changes in the prediction algorithms, or how we evaluate.

Acknowledgments

Many thanks to Jana Radhkrishnan for granting the freedom conducive to this work at Cisco, and to Tom Dean’s SAIRG reading group, including Brian Burns, Reza Eghbali, Gene Lewis, and Justin Wang, for discussions and valuable pointers and feedback: we hope to crack portions of the hippocampal and frontal neocortex code and loops! Many thanks to James Tee for his assistance, and discussions on online learning and state estimation. I am grateful to John Bowman for providing me the valuable pointer and a proof sketch based on Rao-Blackwellization.

References

- [1] W. C. Abraham and A. V. Robins. Memory retention – the synaptic stability versus plasticity dilemma. *Trends in Neurosciences*, 28:73–78, 2005.
- [2] R. Arratia and L. Gordon. Tutorial on large deviations for the binomial distribution. *Bulletin of Mathematical Biology*, 51:125–131, 1989.
- [3] R. B. Ash. *Information Theory*. Dover Publications, 1990.
- [4] A. M. Atto, F. Bovolo, and L. Bruzzone. *Change Detection and Image Time Series Analysis 1: Unsupervised Methods*. Wiley-ISTE, 2021.
- [5] B. Balle, J. Castro, and R. Gavaldà. Adaptively learning probabilistic deterministic automata from data streams. *Machine Learning*, 96:99–127, 2014.
- [6] A. Bifet and R. Gavaldà. Learning from time-changing data with adaptive windowing. In *SDM*, 2007.
- [7] Albert Bifet, Gianmarco De Francisci Morales, Jesse Read, Geoff Holmes, and Bernhard Pfahringer. Efficient online evaluation of big data stream classifiers. *Proceedings of the 21th ACM SIGKDD International Conference on Knowledge Discovery and Data Mining*, 2015.

- [8] D. Blackwell. Conditional expectation and unbiased sequential estimation. *The Annals of Mathematical Statistics*, 1947.
- [9] G. W. Brier. Verification of forecasts expressed in terms of probability. *Monthly Weather Review*, 1950.
- [10] D. Cohen, A. Kontorovich, and G. Wolfer. Learning discrete distributions with infinite support. *arXiv: Statistics Theory*, 2020.
- [11] Wikipedia Contributors. The Rao-Blackwell-Kolmogorov Theorem, Jensen’s Inequality, Negative Binomial Distribution, Moving average, Efficiency (statistics), Kalman Filter, and Change Detection. In *Wikipedia, The Free Encyclopedia*. 2024. <https://en.wikipedia.org/wiki/>.
- [12] T. M. Cover and J. A. Thomas. *Elements of Information Theory*. John Wiley & Sons, 1991.
- [13] V. Dani, O. Madani, D. Pennock, S. Sanghai, and B. Galebach. An empirical comparison of expert aggregation techniques. In *UAI*, 2006.
- [14] A. P. Dawid. Present position and potential developments: Some personal views: statistical theory: the prequential approach. *Journal of the Royal Statistical Society: Series A (General)*, 147(2), 1984.
- [15] T. L. Dean and M. P. Wellman. *Planning and Control*. Morgan Kaufmann, 1991.
- [16] J. L. Devore. *Probability and Statistics for Engineering and the Sciences*. 9th Edition, Cengage, Boston, 2016.
- [17] L. Devroye and L. Györfi. Nonparametric density estimation : the L1 view. *J. of the American Statistical Association*, 82:344, 1987.
- [18] G. Ditzler, M. Roveri, C. Alippi, and R. Polikar. Learning in nonstationary environments: A survey. *IEEE Computational Intelligence Magazine*, 10, 2015.
- [19] H. Du. Beyond strictly proper scoring rules: The importance of being local. *Weather and Forecasting*, 2020.
- [20] D. Dua and C. Graff. UCI machine learning repository. University of California, Irvine, School of Information and Computer Sciences, 2017. <https://archive.ics.uci.edu/dataset/134/nsf+research+award+abstracts+1990+2003>.
- [21] P. Dupont, F. Denis, and Y. Esposito. Links between probabilistic automata and hidden markov models: probability distributions, learning models and induction algorithms. *Pattern Recognition*, 2005.
- [22] T. Silva Filho, H. Song, M. Perello-Nieto, R. Santos-Rodriguez, M. Kull, and P. Flach. Classifier calibration: a survey on how to assess and improve predicted class probabilities. *Machine Learning*, 112:3211–3260, 2021.
- [23] Y. Freund, R. Schapire, Y. Singer, and M. Warmuth. Using and combining predictors that specialize. In *STOC*, 1997.
- [24] M. M. Gaber, A. Zaslavsky, and S. Krishnaswamy. Mining data streams: A review. *SIMOD Record*, 34(2), June 2005.
- [25] J. Gama, J. S. Aguilar-Ruiz, and R. Klinkenberg. Knowledge discovery from data streams. In *Intelligent Data Analysis*, 2009.
- [26] João Gama, Indrė Žliobaitė, Albert Bifet, Mykola Pechenizkiy, and A. Bouchachia. A survey on concept drift adaptation. *ACM Computing Surveys (CSUR)*, 2014.
- [27] T. Gneiting, F. Balabdaoui, and A. E. Raftery. Probabilistic forecasts, calibration and sharpness. *Journal of the Royal Statistical Society Series B: Statistical Methodology*, 69(2):243–268, 2007.
- [28] I. J. Good. Rational decisions. *J. of the Royal Statistical Society: Series B (Methodological)*, 1952.
- [29] S. Greenberg. Using unix: collected traces of 168 users. Technical report, University of Calgary, Alberta, 1988.
- [30] D. P. Helmbold and P. M. Long. Tracking drifting concepts using random examples. In *Annual Conference Computational Learning Theory*, 1991.
- [31] F. Hinder, V. Vaquet, and B. Hammer. One or two things we know about concept drift - a survey on monitoring evolving environments. *ArXiv*, abs/2310.15826, 2023.
- [32] R. V. Hogg, J. W. McKean, and A. T. Craig. *Introduction to Mathematical Statistics*. 8th Edition, Pearson, Boston, 2018.
- [33] S. C. H. Hoi, D. Sahoo, J. Lu, and P. Zhao. Online learning: A comprehensive survey, 2018.
- [34] T. Ingold. *The Perception of the Environment: Essays on Livelihood, Dwelling and Skill*. Routledge, 2000. (See, for instance, chapter 11 on the temporality of the landscape.).
- [35] A. Kuh, T. Petsche, and R. L. Rivest. Learning time-varying concepts. In *Neural Information Processing Systems*, 1990.

- [36] S. Kullback and R. A. Leibler. On information and sufficiency. *Ann. Math. Stat.*, 1951.
- [37] E. L. Lehmann and H. Scheffé. Completeness, similar regions, and unbiased estimation:. *The Indian Journal of Statistics*, 1950.
- [38] D. D. Lewis. Naive (Bayes) at forty: The independence assumption in information retrieval. In Claire Nédellec and Céline Rouveirol, editors, *Proceedings of ECML-98, 10th European Conference on Machine Learning*, number 1398, pages 4–15, Chemnitz, DE, 1998. Springer Verlag, Heidelberg, DE.
- [39] N. Littlestone. Learning quickly when irrelevant attributes abound: A new linear-threshold algorithm. *Machine Learning*, 2(4):285–318, 1988.
- [40] O. Madani. Prediction games in infinitely rich worlds. In *AAAI Fall Symposium*, 2007. Yahoo! Research Technical Report, available at: www.omadani.net/publications.html.
- [41] O. Madani. Expedition: A system for the unsupervised learning of a hierarchy of concepts. *ArXiv*, 2021.
- [42] O. Madani. Text analysis via binomial tails. In *Document Intelligence Workshop at KDD*. 2021.
- [43] O. Madani. An information theoretic score for learning hierarchical concepts. *Frontiers in Computational Neuroscience*, 17, 2023.
- [44] O. Madani. <https://github.com/omadaniTet/sparse-moving-averages/blob/main/README.txt>, 2024.
- [45] O. Madani, H. Bui, and E. Yeh. Efficient online learning and prediction of users’ desktop behavior. In *IJCAI*, 2009.
- [46] O. Madani, M. Connor, and W. Greiner. Learning when concepts abound. *J. of Machine Learning Research (JMLR)*, 10, 2009.
- [47] O. Madani and J. Huang. On updates that constrain the number of connections of features during learning. In *ACM KDD*, 2008.
- [48] Raju Maiti and Atanu Biswas. Coherent forecasting for stationary time series of discrete data. *AStA Advances in Statistical Analysis*, 2015.
- [49] J. Marengo and D. L. Farnsworth. A geometric approach to conditioning and the search for minimum variance unbiased estimators. *Open Journal of Statistics*, 2021.
- [50] A. Mazzetto. An improved algorithm for learning drifting discrete distributions. In *International Conference on Artificial Intelligence and Statistics*, 2024.
- [51] Alessio Mazzetto and Eli Upfal. Nonparametric density estimation under distribution drift. In *International Conference on Machine Learning*, 2023.
- [52] M. Merleau-Ponty. *The Phenomenology of Perception*. Gallimard, 1945. (Translation & copy-right 1958, Routledge & Kegan Paul, and another translation by Colin Smith.).
- [53] M. Mermillod, A. Bugaiska, and P. Bonin. The stability-plasticity dilemma: investigating the continuum from catastrophic forgetting to age-limited learning effects. *Frontiers in Psychology*, 4, 2013.
- [54] M. Mohri and A. M. Medina. New analysis and algorithm for learning with drifting distributions. In *International Conference on Algorithmic Learning Theory*, 2012.
- [55] M. S. Nikulin. Rao-Blackwell-Kolmogorov theorem. In *Encyclopedia of Mathematics*. EMS Press, 2001 (1994). https://encyclopediaofmath.org/wiki/Rao-Blackwell-Kolmogorov_theorem.
- [56] A. Painsky and G. W. Wornell. On the universality of the logistic loss function. *2018 IEEE International Symposium on Information Theory (ISIT)*, 2018.
- [57] E. A. Di Paolo, T. Buhrmann, and X. E. Barandiaran. *Sensorimotor Life: An enactive proposal*. Oxford University Press, 2017.
- [58] J. Plasse and N. M. Adams. Multiple changepoint detection in categorical data streams. *Statistics and Computing*, 2019.
- [59] C. R. Rao. Information and accuracy attainable in the estimation of statistical parameters. *Bulletin of the Calcutta Mathematical Society*, 1945.
- [60] F. Rosenblatt. The perceptron: A probabilistic model for information storage and organization in the brain. *Psychological Review*, 65(6):386–408, 1958.
- [61] R. Rosenfeld. Two decades of statistical language modeling: Where do we go from here? *IEEE*, 88(8), 2000.
- [62] Jeffrey C. Schlimmer and Richard Granger. Incremental learning from noisy data. *Machine Learning*, 1986.

- [63] M. Schonlau, W. DuMouchel, W.-H. Ju, A. F. Karr, M. Theusan, and Y. Vardi. Computer intrusion: Detecting masquerades. *Statistical Science*, 2001.
- [64] R. Sebastião, J. Gama, P. P. Rodrigues, and J. Bernardes. Monitoring incremental histogram distribution for change detection in data streams. In *KDD Workshop on Knowledge Discovery from Sensor Data*, 2008.
- [65] R. Selten. Axiomatic characterization of the quadratic scoring rule. *Experimental Economics*, 1998.
- [66] G. Shafer and V. Vovk. *Probability and Finance: It's Only a Game!* John Wiley & Sons, 2001.
- [67] L. N. Smith. A disciplined approach to neural network hyper-parameters: Part 1 - learning rate, batch size, momentum, and weight decay. *ArXiv*, 2018.
- [68] R. Sutton and A. Barto. *Reinforcement Learning: An Introduction*. The MIT Press, 1998.
- [69] A. Tartakovsky, I. Nikiforov, and M. Basseville. *Sequential Analysis: Hypothesis Testing and Changepoint Detection*. Chapman and Hall/CRC, Boca Raton, 2014.
- [70] M. Toda. Measurement of subjective probability distribution. Technical report, State College, Pennsylvania, Institute for Research, Division of Mathematical Psychology, 1963.
- [71] H. Tyralis and G. Papacharalampous. A review of probabilistic forecasting and prediction with machine learning. *ArXiv*, abs/2209.08307, 2022.
- [72] G. J. J. van den Burg and C. K. I. Williams. An evaluation of change point detection algorithms. *ArXiv*, 2022.
- [73] C. H. Weiß. *An Introduction to Discrete-Valued Time Series*. 2018.
- [74] C. H. Weiß. Continuously monitoring categorical processes. *Qual. Technology. Quant. Manag.*, 2012.
- [75] G. Widmer and M. Kubát. Learning in the presence of concept drift and hidden contexts. *Machine Learning*, 1996.
- [76] D. Williams. *Probability with Martingales*. Cambridge University Press, 1991.
- [77] R. L. Winkler. Scoring rules and the evaluation of probability assessors. *J. of the American Statistical Association*, 1969.
- [78] K. You, M. Long, and M. I. Jordan. How does learning rate decay help modern neural networks. *arXiv*, 2019.
- [79] G. Ziffer, A. Bernardo, E. Della Valle, and A. Bifet. Kalman filtering for learning with evolving data streams. *2021 IEEE International Conference on Big Data (Big Data)*, 2021.
- [80] Giacomo Ziffer, Alessio Bernardo, Emanuele Della Valle, and Albert Bifet. Fast incremental naive bayes with kalman filtering. *2020 International Conference on Data Mining Workshops (ICDMW)*, 2020.

A Further Material for the Evaluation Section

In this section, we provide proofs and further details for the evaluation section 3. We begin with quadratic loss and its insufficient sensitivity (to estimating low probabilities), and we develop properties that point to the near propriety of `LogLossNS()` in Sect. A.3, including extensions of `KL()` to SDs and how scaling and shifting SDs affects optimality of SDs under KL scoring. Sect. A.4 discusses a few alternatives that we considered for evaluating sequence prediction when using log-loss and handling noise (NS) items.

A.1 The Quadratic Loss, and its Insensitivity to PR Ratios

The Quadratic loss (Brier score) of a candidate SD, \mathcal{L}_2 , is defined as:

$$\mathcal{L}_2(\mathcal{W}|\mathcal{P}) := \mathbb{E}_{o \sim \mathcal{P}}(\text{QRule}(\mathcal{W}, o)), \text{ where } \text{QRule}(\mathcal{W}, o) := \sum_{i \in \mathcal{I}} (\delta_{i,o} - \mathcal{W}(i))^2, \quad (10)$$

where $\delta_{i,o}$ denotes the Kronecker delta, *i.e.* $\delta_{i,o} = 1$ when $o = i$ and 0 otherwise ($\delta_{i,o} = 0$ for $i \neq o$) and an equivalent expression is $\text{QRule}(\mathcal{W}, o) = (1 - \mathcal{W}(o))^2 + \sum_{i \in \mathcal{I}, i \neq o} \mathcal{W}(i)^2$. Note that at each time point t , to compute the value of $\text{QRule}()$ (the loss or cost over an observation), we go over all the items in \mathcal{I} , and we have $0 \leq \text{QRule}(\mathcal{W}, o) \leq 2.0$. One can view the scoring rule $\text{QRule}()$ as taking the (squared) Euclidean distance between two vectors: the *Kronecker vector*, *i.e.* the vector with Kronecker delta entries (all 0, except the dimension corresponding to observed item o), and the probability vector corresponding to the SD \mathcal{W} .

In particular, for instance in [65], when both \mathcal{P} and \mathcal{W} are DIs, it is established that the \mathcal{L}_2 score is equivalent to (squared) Euclidean distance to the true probability distribution, where the distance is defined as:

$$\text{QuadDist}(\mathcal{W}_1, \mathcal{W}_2) := \sum_{i \in \mathcal{I}} (\mathcal{W}_1(i) - \mathcal{W}_2(i))^2 \quad (\text{defined for SDs } \mathcal{W}_1 \text{ and } \mathcal{W}_2)$$

The equivalence is in the following strong sense (extended to SDs):

Lemma 4. (*sensitivity of \mathcal{L}_2 to the magnitude of PR shifts only*) Given DI \mathcal{P} and SD \mathcal{W} , defined over the same finite set \mathcal{I} , then $\mathcal{L}_2(\mathcal{W}|\mathcal{P}) = \text{QuadDist}(\mathcal{W}, \mathcal{P})$

Proof. This property has been established when both are DIs (*i.e.* when $a(\mathcal{W}) = 1$) [65], and similarly can be established for SDs by writing the expectation expressions, rearranging terms, and simplifying. We give a proof by reducing to the DI case: when \mathcal{W} is a strict SD, we can make a DI variant of \mathcal{W} , call it \mathcal{W}' , via adding an extra element j to \mathcal{I} with remainder PR $\mathcal{W}'(j) = u(\mathcal{W})$ (note: $\mathcal{P}(j) = 0$). Observing the following 3 relations establishes the result: 1) $\text{QuadDist}(\mathcal{P}, \mathcal{W}) = \text{QuadDist}(\mathcal{P}, \mathcal{W}') - \mathcal{W}'(j)^2$, 2) $\mathcal{L}_2(\mathcal{W}'|\mathcal{P}) = \text{QuadDist}(\mathcal{W}', \mathcal{P})$ (as both are DIs), and 3) $\mathcal{L}_2(\mathcal{W}'|\mathcal{P}) = \mathcal{L}_2(\mathcal{W}|\mathcal{P}) + \mathcal{W}'(j)^2$, as with every draw from \mathcal{P} we incur the additional cost of $\mathcal{W}'(j)^2$ compared to the cost from \mathcal{W} : by definition, we have, $\mathcal{L}_2(\mathcal{W}'|\mathcal{P}) = \sum_{i \in \mathcal{I}, i \neq j} \mathcal{P}(i) (\mathcal{W}'(j)^2 + (1 - \mathcal{P}(i))^2 + \sum_{u \in \mathcal{I}, u \neq i, u \neq j} \mathcal{P}(u)^2) = \sum_{i \in \mathcal{I}, i \neq j} \mathcal{P}(i) \mathcal{W}'(j)^2 + \sum_{i \in \mathcal{I}, i \neq j} \mathcal{P}(i) ((1 - \mathcal{P}(i))^2 + \sum_{u \in \mathcal{I}, u \neq i, u \neq j} \mathcal{P}(u)^2) = \mathcal{W}'(j)^2 + \mathcal{L}_2(\mathcal{W}|\mathcal{P})$ (the last equality in part follows from $\sum_{i \in \mathcal{I}, i \neq j} \mathcal{P}(i) = 1$). \square

Examining the distance version of the loss, we first note that \mathcal{L}_2 has a desired property of symmetry when \mathcal{W} is also a DI, *i.e.* $\mathcal{L}_2(\mathcal{W}_1|\mathcal{W}_2) = \mathcal{L}_2(\mathcal{W}_2|\mathcal{W}_1)$ (for two DIs \mathcal{W}_1 and \mathcal{W}_2). We can also observe that \mathcal{L}_2 is only sensitive to the magnitude of shifts in PRs:

Corollary 2. (*sensitivity of \mathcal{L}_2 to the magnitude of PR shifts only*) With DI \mathcal{P} and SD \mathcal{W} (on the same items \mathcal{I}), let $\Delta_i := \mathcal{P}(i) - \mathcal{W}(i)$. Then $\mathcal{L}_2(\mathcal{W}|\mathcal{P}) = \sum_{i \in \mathcal{I}} \Delta_i^2$.

\mathcal{L}_2 is not sensitive to the size of the source (or destination) of the original probabilities of items those quantities are transferred from: it does not particularly matter if a positive PR is reduced to 0 in going from \mathcal{P} to \mathcal{W} . For instance, assume $\mathcal{P} = \{1:0.9, 2:0.1\}$. Consider the two candidate SDs $\mathcal{W}_1 = \{1:0.8, 2:0.1\}$, $\mathcal{W}_2 = \{1:0.9, 2:0.0\}$ (\mathcal{W}_i differing from \mathcal{P} only on item i). In terms of violating a deviation threshold (Sect. 3), \mathcal{W}_2 violates all ratio thresholds on item 2, and the log-loss (Sect. 3.4) is rendered infinite on it, while SD \mathcal{W}_1 has a relatively small violation. However, for both cases $\Delta = 0.1$, and we have $\mathcal{L}_2(\mathcal{W}_1|\mathcal{P}) = \mathcal{L}_2(\mathcal{W}_2|\mathcal{P}) = 0.1^2$, and \mathcal{W}_1 and \mathcal{W}_2 would have similar empirical losses using the \mathcal{L}_2 score.

Compared to the log-loss, the Brier score can be easier to work with, as there is no possibility of “explosion”, *i.e.* unbounded values (see Sect. 3.4). However, in our application we are interested in probabilities that can widely vary, for instance, spanning two orders of magnitude ($\mathcal{P}(i) \geq 0.1$ for some i , and $\mathcal{P}(j)$ near 0.01 for other items), and as mentioned above, different items are associated with different rewards and we are interested in optimizing expected rewards. Thus confusing a one-in-twenty event with a substantially lower probability event, such as a zero probability event, can incur considerable underperformance (depending on the rewards associated with the items). The utility of a loss depends on the application. For instance, for clustering DIs, symmetry can be important, and thus quadratic loss may be preferable over log-loss. In our prior work, in an application where events were binary, and PRs were concentrated near 0.5 (outcomes of two-team professional sports games), quadratic loss was adequate [13].

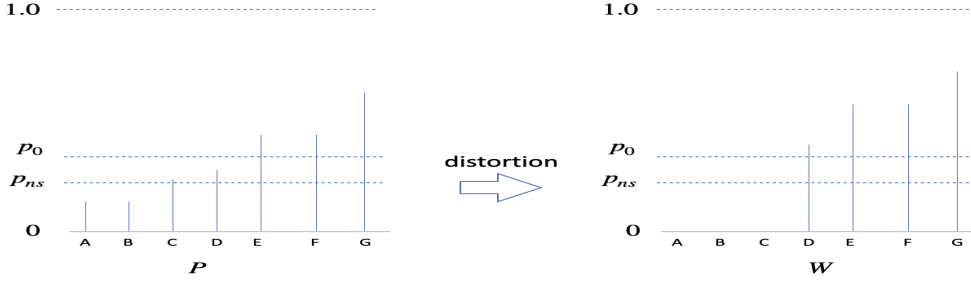


Figure 24: When using $FC()$ and $\text{loglossRuleNS}()$, *distortion* can occur, *i.e.* a SD \mathcal{W} may obtain a lower loss than the true generating SD \mathcal{P} (due to filtering, scaling, and bounding the loss). Sections A.3 through A.3.6 shed light on the conditions for distortion and its extent. In particular, Lemma 8 characterizes the properties of a minimizing SD \mathcal{W}^* : smaller items in \mathcal{P} (those with lower PR, such as A , B and C above) may be zeroed, and have their PR mass transferred (spread, proportionately) onto higher items in an optimal \mathcal{W}^* .

A.2 The Sensitivity of log-loss

The following corollary to Lemma 1 (on the connection of log-loss to relative entropy) highlights and quantifies the sensitivity (or bias) of log-loss towards larger PRs (where, without loss of generality, we are using items, or dimensions, 1 and 2):

Corollary. (*LogLoss is much more sensitive to relative changes in larger PRs*) Let \mathcal{P} be a DI over two or more items ($\mathcal{I} = \{1, 2, \dots\}$, $|\mathcal{I}| \geq 2$), with $\mathcal{P}(1) > \mathcal{P}(2) > 0$, and let the multiple $m = \frac{\mathcal{P}(1)}{\mathcal{P}(2)}$ (thus $m > 1$). Consider two SDs \mathcal{W}_1 and \mathcal{W}_2 , with \mathcal{W}_1 differing with \mathcal{P} on item 1 only ($\forall i \in \mathcal{I}$ and $i \neq 1$, $\mathcal{W}_1(i) = \mathcal{P}(i)$), and assume moreover $\mathcal{P}(1) > \mathcal{W}_1(1) > 0$, and let $m_1 = \frac{\mathcal{P}(1)}{\mathcal{W}_1(1)}$ (thus, $m_1 > 1$). Similarly, assume \mathcal{W}_2 differs with \mathcal{P} on item 2 only, and that $\mathcal{P}(2) > \mathcal{W}_2(2) > 0$, and let $m_2 = \frac{\mathcal{P}(2)}{\mathcal{W}_2(2)}$. We have $\text{LogLoss}(\mathcal{W}_2|\mathcal{P}) < \text{LogLoss}(\mathcal{W}_1|\mathcal{P})$ for any $m_2 < m_1^m$.

Proof. We write the difference Δ in the losses and simplify: $\Delta = \text{LogLoss}(\mathcal{W}_1|\mathcal{P}) - \text{LogLoss}(\mathcal{W}_2|\mathcal{P}) = \mathcal{P}(1) \ln \frac{\mathcal{P}(1)}{\mathcal{W}_1(1)} - \mathcal{P}(2) \ln \frac{\mathcal{P}(2)}{\mathcal{W}_2(2)}$ (all other terms are 0, *e.g.* $\mathcal{W}_1(2) = \mathcal{P}(2)$, and the entropy terms cancel). We thus have $\Delta = m\mathcal{P}(2) \ln(m_1) - \mathcal{P}(2) \ln(m_2)$, or we have $\Delta > 0$ as long as $\ln(m_1^m) - \ln(m_2) > 0$, or whenever $m_1^m > m_2$. \square

A.3 On the (Near) Propriety of LogLossNS()

In the iid generation setting based on SD \mathcal{P} , when using a perfect NS-marker and using $FC()$ parameterized by $p_{NS} = p_{min} > 0$, we explore and establish how $KL()$ comparisons change under various transformations. Under a few assumptions such as small p_{NS} , we describe when \mathcal{P} remains optimal or near optimal, and for any \mathcal{W} scoring near or better than \mathcal{P} (using $\text{LogLossNS}()$), when we can expect that such a SD must remain close to \mathcal{P} . See Fig. 24. We note that there are two related but distinct questions, when using $\text{LogLossNS}()$: (1) how far the loss of \mathcal{P} is from the minimum loss $\text{LogLossNS}(\mathcal{W}^*|\mathcal{P})$ (or **distortion in the loss**), and (2) how far can any minimizer \mathcal{W}^* be from \mathcal{P} (item distortion). When comparing different candidate SDs, we care about distortion in items (*i.e.* the second sense³⁹). There can be multiple minimizers and we can have no distortion in loss but some distortion in items. We will focus on distortion on items. There are 4 causes or sources of distortion: filtering, capping, bounding the loss, and use of an imperfect NS-marker. At the end of this section, we briefly discuss the last cause, that of an imperfect practical NS-marker (Sect. A.3.6).

Below we explain that $\text{LogLossNS}()$ is equivalent to a *bounded* quasi-divergence denoted $KL_{NS}()$, similar to plain log-loss being equivalent to plain KL divergence: the quasi-divergence $KL_{NS}()$ is based on transformations of SDs (scaling and filtering, augmenting). In particular, first we define *augmentation* of an SD to a corresponding DI that has one extra item with all remaining PR mass. This allows us to draw from \mathcal{P} (as if it were DI, in particular for the

³⁹As comparisons converge onto or prefer a minimizer \mathcal{W}^* , and we want to see how different a \mathcal{W}^* can be from the true \mathcal{P} .

purpose of evaluating $\text{LogLossNS}()$: We show computing $\text{LogLossNS}(\mathcal{W}|\mathcal{P})$ is equivalent to computing a bounded $\text{KL}()$ on the augmented versions of \mathcal{P} and $\text{FC}(\mathcal{W})$ (Lemma 5).

Definition 3. *Definitions of augmenting an SD to a DI, and bounded KL corresponding to $\text{LogLossNS}()$:*

- Given a non-empty SD \mathcal{P} defined on $\mathcal{I} = \{1, \dots, k\}$, $k \geq 1$, its augmentation (operation), denoted $\text{DI}(\mathcal{P})$, is a corresponding DI \mathcal{P}' , where \mathcal{P}' is defined on \mathcal{I}' , $\mathcal{I}' = \mathcal{I} \cup \{0\}$, $\mathcal{P}'(0) = u(\mathcal{P})$, and $\mathcal{P}'(i) = \mathcal{P}(i)$, $\forall i \in \mathcal{I}$.

- **(Bounded KL)** For non-empty SD \mathcal{P} and SD \mathcal{W} :

$$\text{KL}_b(\mathcal{P}||\mathcal{W}) := \sum_{i \in \text{sup}(\mathcal{P})} \mathcal{P}(i) \ln\left(\frac{\mathcal{P}(i)}{\max(\mathcal{W}(i), p_{NS})}\right) \quad (\text{where } p_{NS} \in [0, 1], \text{ bounded when } p_{NS} > 0).$$

- **(KL() for LogLossNS)** $\text{KL}_{NS}(\mathcal{P}||\mathcal{W}) := \text{KL}_b(\text{DI}(\mathcal{P})||\text{DI}(\text{FC}(\mathcal{W})))$ (where the p_{NS} of $\text{FC}()$ is used in $\text{KL}_b()$).

For a DI \mathcal{P} , $\text{DI}(\mathcal{P}) \equiv \mathcal{P}$ in the sense that all positive PRs match,⁴⁰ and for two SDs \mathcal{P} and \mathcal{W} , $\mathcal{P} \neq \mathcal{W} \Leftrightarrow \text{DI}(\mathcal{P}) \neq \text{DI}(\mathcal{W})$. Unlike $\text{KL}()$, $\text{KL}_b()$ is bounded when $p_{NS} > 0$ (no greater than $-\ln(p_{NS})$), and both $\text{KL}_b(\mathcal{P}||\mathcal{W})$ and $\text{KL}_{NS}(\mathcal{P}||\mathcal{W})$ can be negative even when both \mathcal{P} and \mathcal{W} are DIs (the minimum is not 0 any more), and so they are not divergences, but we argue still useful for scoring and comparisons. In particular, $\text{KL}_{NS}(\mathcal{P}||\mathcal{P})$ is not necessarily 0, as $\text{FC}()$ used on the 2nd parameter of KL_{NS} , here \mathcal{P} , can alter \mathcal{P} , i.e. can filter and scale it, while \mathcal{P} provided as first parameter is only augmented. Furthermore, $\text{KL}_b(\mathcal{P}||\mathcal{P})$ can grow unbounded in the negative direction: imagine \mathcal{P} being the uniform distribution with k items, each item with PR $\frac{1}{k}$ contributing $\frac{1}{k} \ln(\frac{1}{kp_{NS}})$, then $\text{KL}_b(\mathcal{P}||\mathcal{P}) = -\ln(kp_{NS})$ (with $kp_{NS} > 1$), and with k growing, $\text{KL}_b(\mathcal{P}||\mathcal{P}) \rightarrow -\infty$. The same condition holds for $\text{KL}_{NS}()$ ($\text{FC}()$ does not change this), but as the lemma below shows, the addition of the positive entropy counteracts this growth and $\text{LogLossNS}()$ is always in $[0, -\ln(p_{NS})]$.

We also note that there is another distinct way of obtaining a DI from a strict SD \mathcal{P} , that of scaling it, to $\alpha\mathcal{P}$, where $\alpha = \frac{1}{a(\mathcal{P})}$. Both operations are useful, and used below.

Lemma 5. *For any two SDs \mathcal{P} and \mathcal{W} defined on $\mathcal{I} = \{1, \dots, k\}$, where \mathcal{P} is non-empty, and using a perfect NS-marker, $\text{isNS}_{\mathcal{P}}()$, wrt to \mathcal{P} :*

$$\text{LogLossNS}(\mathcal{W}|\mathcal{P}) = H(\text{DI}(\mathcal{P})) + \text{KL}_{NS}(\mathcal{P}||\mathcal{W}).$$

Proof. We first explain the different parts of $\text{LogLossNS}(\mathcal{W}|\mathcal{P})$, i.e. $\mathbb{E}_{o \sim \mathcal{P}}(\text{loglossRuleNS}(o, \mathcal{W}, \text{isNS}_{\mathcal{P}}(o)))$, to show that it is equivalent to comparing two augmented DIs under $\text{KL}()$.

Let $\mathcal{W}' = \text{FC}(\mathcal{W})$ and $\mathcal{P}' = \text{DI}(\mathcal{P})$. An item $o \sim \mathcal{P}$ (drawn from \mathcal{P}), is salient with probability $a(\mathcal{P})$ ($o \in \text{sup}(\mathcal{P})$), and otherwise is marked NS by $\text{isNS}_{\mathcal{P}}()$ (perfect NS-marker), and it is important to note that o does not occur in \mathcal{I} when marked NS ($\mathcal{W}'(o) = \mathcal{W}(o) = \mathcal{P}(o) = 0$ when $\text{isNS}_{\mathcal{P}}(o)$ is true), with our uniqueness assumption when generating NS items. When we use $\text{loglossRuleNS}()$, the score in the NS case is $-\ln(u(\mathcal{W}'))$. This case occurs $u(\mathcal{P})$ of the time, and a salient item i , $i \in \mathcal{I}$, occurs $\mathcal{P}(i)$ of the time, thus $\text{LogLossNS}(\mathcal{W}|\mathcal{P}) = -u(\mathcal{P}) \ln(u(\mathcal{W}')) - \sum_{i \in \mathcal{I}} \mathcal{P}(i) \ln(\max(\mathcal{W}'(i), p_{NS}))$. We have that $u(\mathcal{W}') \geq p_{NS}$ (from the scaling down in $\text{FC}()$), or $\max(u(\mathcal{W}'), p_{NS}) = u(\mathcal{W}')$. Adding and subtracting $H(\mathcal{P}')$ establishes the equivalence:

$$\begin{aligned} \text{LogLossNS}(\mathcal{W}|\mathcal{P}) &= -u(\mathcal{P}) \ln(u(\mathcal{W}')) - \sum_{i \in \mathcal{I}} \mathcal{P}(i) \ln(\max(\mathcal{W}'(i), p_{NS})) - H(\mathcal{P}') + H(\mathcal{P}') \\ &= -u(\mathcal{P}) \ln(u(\mathcal{W}')) - \sum_{i \in \mathcal{I}} \mathcal{P}(i) \ln(\max(\mathcal{W}'(i), p_{NS})) + \sum_{i \in \mathcal{I}'} \mathcal{P}'(i) \ln(\mathcal{P}'(i)) + H(\mathcal{P}') \\ &= u(\mathcal{P}) \ln \frac{u(\mathcal{P})}{u(\mathcal{W}')} + \sum_{i \in \mathcal{I}} \mathcal{P}(i) \ln \frac{\mathcal{P}(i)}{\max(\mathcal{W}'(i), p_{NS})} + H(\mathcal{P}') \\ &= \text{KL}(\mathcal{P}'||\text{DI}(\mathcal{W}')) + H(\mathcal{P}') = \text{KL}_{NS}(\mathcal{P}||\mathcal{W}) + H(\text{DI}(\mathcal{P})). \end{aligned}$$

The 2nd to 3rd line follow from $H(\mathcal{P}') = -\sum_{i \in \mathcal{I}'} \mathcal{P}'(i) \ln(\mathcal{P}'(i)) = -u(\mathcal{P}) \ln(u(\mathcal{P})) - \sum_{i \in \mathcal{I}} \mathcal{P}(i) \ln(\mathcal{P}(i))$. \square

⁴⁰We are abusing notation in using $\text{DI}()$ to also denote the augmentation operator applied to a SD \mathcal{P} to make a distribution, in addition to the related notion of referring to a distribution.

The following example describes a case when \mathcal{P} may not minimize $\text{LogLossNS}()$ even when $\mathcal{P} = \text{FC}(\mathcal{P})$ (i.e. even when \mathcal{P} is not altered by $\text{FC}()$). Let the underlying $\mathcal{P} := \{A:0.78, B:0.02\}$, thus 0.2 of the time, a noise item is generated. Then with $p_{\min} = p_{NS} = 0.01$ in $\text{FC}()$, \mathcal{P} scores at $\text{LogLossNS}(\mathcal{P}|\mathcal{P}) = -0.78 \ln(0.78) - 0.02 \ln(0.02) - 0.2 \ln(0.20) \approx 0.594$, while $\mathcal{W}_1 = \{A:0.78\}$ and $\mathcal{W}_2 = \{A:0.8\}$ have a lower loss: $\text{LogLossNS}(\mathcal{W}_1|\mathcal{P}) = -0.78 \ln(0.78) - 0.02 \ln(0.01) - 0.2 \ln(0.22) \approx 0.589$, and similarly $\text{LogLossNS}(\mathcal{W}_2|\mathcal{P}) = -0.78 \ln(0.8) - 0.02 \ln(0.01) - 0.2 \ln(0.20) \approx 0.588$. An intuitive reason is that when $\mathcal{P}(B)$ is sufficiently close to p_{NS} , then it is advantageous to move that mass to A or to the allocation to noise (or spread a portion on both), and the penalty from this reduction (and transfer) is not as much as the reduced loss (the gain) of a higher PR for A or for the noise allotment. This can be seen more clearly when $\mathcal{P}(B) \leq p_{NS}$ (i.e. right at or below the boundary). Section A.3.2 develops this near boundary property. We first need the (scaling) properties developed next.

A.3.1 Properties of $\text{KL}()$ on SDs (Under Scaling and Other Transformations)

We now show how plain $\text{KL}()$ comparisons (defined for SDs in Defn. 7) are affected by scaling one or both SDs. This is useful in seeing how $\text{FC}()$, with its scaling and filtering, can alter the minimizer of $\text{KL}_{NS}()$, and to see when distortion can happen when using $\text{KL}_b()$. Recall that, as in Sect. 3.3, we assume that the set \mathcal{I} over which both \mathcal{P} and \mathcal{W} are defined is finite, e.g. the union of the supports of both. We have defined $\text{KL}()$ for sds \mathcal{P} and \mathcal{W} (definition 7), and for the following lemma, we can extend the definition of $\text{KL}()$ to non-negative valued \mathcal{P} and \mathcal{W} (no constraint on the sum, unlike plain SDs), or assume α is such that $\alpha\mathcal{W}$ and $\alpha\mathcal{P}$ remain a SD.

Lemma 6. (plain $\text{KL}()$ under scalings) For any non-empty SD \mathcal{P} and SDs \mathcal{W} , and any $\alpha > 0$:

1. $\text{KL}(\mathcal{P}||\alpha\mathcal{W}) = \text{KL}(\mathcal{P}||\mathcal{W}) + \ln(\alpha^{-1})a(\mathcal{P})$.
2. $\text{KL}(\alpha\mathcal{P}||\mathcal{W}) = \alpha\text{KL}(\mathcal{P}||\mathcal{W}) + \alpha\ln(\alpha)a(\mathcal{P})$.
3. $\text{KL}(\alpha\mathcal{P}||\alpha\mathcal{W}) = \alpha\text{KL}(\mathcal{P}||\mathcal{W})$.

Proof. The α multiplier comes out, in all cases, yielding a fixed off-set for first 2 cases, and a positive multiplier for the 2nd and 3rd cases:

$$\begin{aligned} \text{KL}(\mathcal{P}||\alpha\mathcal{W}) &= \sum_{i \in \mathcal{I}} \mathcal{P}(i) \ln\left(\frac{\mathcal{P}(i)}{\alpha\mathcal{W}(i)}\right) = \sum_{i \in \mathcal{I}} \mathcal{P}(i) \ln\left(\frac{\mathcal{P}(i)}{\mathcal{W}(i)} \frac{1}{\alpha}\right) = \sum_{i \in \mathcal{I}} \mathcal{P}(i) (\ln\left(\frac{\mathcal{P}(i)}{\mathcal{W}(i)}\right) + \ln(1/\alpha)) \\ &= \sum_{i \in \mathcal{I}} \mathcal{P}(i) \ln\left(\frac{\mathcal{P}(i)}{\mathcal{W}(i)}\right) + \ln(\alpha^{-1}) \sum_{i \in \mathcal{I}} \mathcal{P}(i) = \text{KL}(\mathcal{P}||\mathcal{W}) + \ln(\alpha^{-1})a(\mathcal{P}). \\ \text{KL}(\alpha\mathcal{P}||\mathcal{W}) &= \sum_{i \in \mathcal{I}} \alpha\mathcal{P}(i) \ln\left(\frac{\alpha\mathcal{P}(i)}{\mathcal{W}(i)}\right) = \alpha \left(\sum_{i \in \mathcal{I}} \mathcal{P}(i) \ln\left(\frac{\mathcal{P}(i)}{\mathcal{W}(i)}\right) + \ln(\alpha) \sum_{i \in \mathcal{I}} \mathcal{P}(i) \right). \\ \text{KL}(\alpha\mathcal{P}||\alpha\mathcal{W}) &= \sum_{i \in \mathcal{I}} \alpha\mathcal{P}(i) \ln\left(\frac{\alpha\mathcal{P}(i)}{\alpha\mathcal{W}(i)}\right) = \alpha \sum_{i \in \mathcal{I}} \mathcal{P}(i) \ln\left(\frac{\mathcal{P}(i)}{\mathcal{W}(i)}\right) = \alpha\text{KL}(\mathcal{P}||\mathcal{W}). \end{aligned}$$

□

As a consequence of the above lemma, we conclude that scaling does not change $\text{KL}()$ comparisons, e.g. with $\alpha > 0$, if $\text{KL}(\mathcal{P}||\mathcal{W}_1) < \text{KL}(\mathcal{P}||\mathcal{W}_2)$ then $\text{KL}(\mathcal{P}||\alpha\mathcal{W}_1) < \text{KL}(\mathcal{P}||\alpha\mathcal{W}_2)$, and we can use the above lemma and the properties of $\text{KL}()$ to conclude the following *proportionate* properties. These help inform us on how a best scoring SD, under scaling and filtering, is related to the SD generating the sequence:

Corollary 3. Scaling and spreading (adding or deducting mass) should be proportionate to SD \mathcal{P} to minimize $\text{KL}(\mathcal{P}||\cdot)$:

1. (\mathcal{P} is the unique minimizer over appropriate set) Given non-empty SD \mathcal{P} , $\text{KL}(\mathcal{P}||\mathcal{P}) = 0$, and for any $\mathcal{W} \neq \mathcal{P}$ with $a(\mathcal{W}) \leq a(\mathcal{P})$, $\text{KL}(\mathcal{P}||\mathcal{W}) > 0$.
2. (same minimizer for \mathcal{P} and its multiple) Let non-empty SDs \mathcal{P}_1 and \mathcal{P}_2 be such that $\mathcal{P}_1 = \alpha\mathcal{P}_2$ for a scalar $\alpha > 0$, and consider any non-empty set S of SDs. For any two SDs $\mathcal{W}_1, \mathcal{W}_2 \in S$, $\text{KL}(\mathcal{P}_1||\mathcal{W}_1) < \text{KL}(\mathcal{P}_1||\mathcal{W}_2) \Leftrightarrow \text{KL}(\mathcal{P}_2||\mathcal{W}_1) < \text{KL}(\mathcal{P}_2||\mathcal{W}_2)$ (thus, a SD $\mathcal{W} \in S$ is a minimizer for both or for neither).
3. Given a non-empty SD \mathcal{P} , among SD \mathcal{W} such that $a(\mathcal{W}) = s$, the one that minimizes $\text{KL}(\mathcal{P}||\mathcal{W})$ is proportionate to (or a multiple of) \mathcal{P} , i.e. $\forall i \in \mathcal{I}, \mathcal{W}(i) = \frac{s}{a(\mathcal{P})} \mathcal{P}(i)$ (when $s = 0$ this becomes vacuous).

Proof. (part 1) When \mathcal{P} is a DI, among $\mathcal{W} \neq \mathcal{P}$ that are DI too, the property $\text{KL}(\mathcal{P}||\mathcal{W}) > 0$ holds [12]. If \mathcal{W} is a strict SD, on at least one item i , $\mathcal{W}(i) < \mathcal{P}(i)$, and we can repeat increasing all such $\mathcal{W}(i)$ in some order until $\mathcal{W}(i) = \mathcal{P}(i)$ or \mathcal{W} becomes a DI (finitely many such i), lowering the distance (the log ratio $\frac{\mathcal{P}(i)}{\mathcal{W}(i)}$). We conclude for any $\mathcal{W} \neq \mathcal{P}$, $\text{KL}(\mathcal{P}||\mathcal{W}) > \text{KL}(\mathcal{P}||\mathcal{P}) = 0$. When \mathcal{P} is a nonempty strict SD: We have $\text{KL}(\mathcal{P}||\mathcal{P}) = \sum \mathcal{P}(i) \ln \frac{\mathcal{P}(i)}{\mathcal{P}(i)} = 0$. We can scale \mathcal{P} by $\alpha = \frac{1}{a(\mathcal{P})}$ to get a DI, and from the property of $\text{KL}(\mathcal{P}||\cdot)$ for DI \mathcal{P} , and using Lemma 6, we conclude that for any other SD $\mathcal{W} \neq \mathcal{P}$, with $a(\mathcal{W}) \leq a(\mathcal{P})$ (and thus $\alpha\mathcal{W}$ remains a SD), must yield a higher (positive) $\text{KL}(\mathcal{P}||\mathcal{W})$: $\text{KL}(\mathcal{P}||\mathcal{W}) = \frac{\text{KL}(\alpha\mathcal{P}||\alpha\mathcal{W})}{\alpha} > 0$ (using Lemma 6, and $\text{KL}(\alpha\mathcal{P}||\alpha\mathcal{W}) > 0$, from first part of this claim).

(part 2) Let $\Delta_1 := \text{KL}(\mathcal{P}_1||\mathcal{W}_1) - \text{KL}(\mathcal{P}_1||\mathcal{W}_2)$ and $\Delta_2 := \text{KL}(\mathcal{P}_2||\mathcal{W}_1) - \text{KL}(\mathcal{P}_2||\mathcal{W}_2)$. $\Delta_1 = \text{KL}(\alpha\mathcal{P}_2||\mathcal{W}_1) - \text{KL}(\alpha\mathcal{P}_2||\mathcal{W}_2) = \alpha(\text{KL}(\mathcal{P}_2||\mathcal{W}_1) - \text{KL}(\mathcal{P}_2||\mathcal{W}_2))$ (from part 2, Lemma 6, $\alpha \ln(\alpha) \ln(a(\mathcal{P}_2))$ canceling). Therefore, $\Delta_1 < 0 \Leftrightarrow \Delta_2 < 0$.

(part 3) This is a consequence of parts 1 and 2 where the set S includes \mathcal{P}_1 , where \mathcal{P}_1 is proportionate to \mathcal{P}_2 , and \mathcal{P}_1 minimizes $\text{KL}()$ to itself among $\mathcal{W} \in S$ (part 1). \square

We note that in part 1 above, if there is no constraint on $a(\mathcal{W})$, then due to the functional form of $\text{KL}()$, multiples of \mathcal{P} (and other \mathcal{W}) can score better than \mathcal{P} and obtain negative scores. In this and related senses, $\text{KL}()$ on SDs is not a divergence in a strict technical sense (even if we generalize the definition of statistical divergence to non-distributions). If we constrain the set of SDs $\text{KL}()$ is applied to, for instance to $a(\mathcal{W}) = s$, then $\text{KL}(\mathcal{P}||\cdot)$ can enjoy certain divergence properties (such as having a unique minimizer). Our main aim is to show such losses and distances remain adequate for comparing predictors. In part 2 above, we consider the set S SDs to be general: it may not yield a minimizer (consider open sets), or may have many (e.g. disjoint closed sets).

A.3.2 All-Or-Nothing Removals and Other Properties of $\text{KL}_b()$

When using $\text{KL}_b(\mathcal{P}||\cdot)$ with $p = p_{NS} > 0$, in changing \mathcal{P} to get a \mathcal{W}^* that minimizes $\text{KL}_b(\mathcal{P}||\cdot)$, where $a(\mathcal{W}^*) = a(\mathcal{P})$, we show that we have all-or-nothing deductions, and when not deducting, we may increase the mass, shifting from small to larger items, i.e. those with higher PRs:

Definition 4. With respect to given threshold p_{NS} , $p_{NS} \in (0, 1)$, the SD \mathcal{P} is called **non-degenerate** if $a(\mathcal{P}) > p_{NS}$, otherwise, it is **degenerate** (wrt p_{NS}).

Lemma 7. (Minimizer existence for the degenerate case) Given threshold p_{NS} , $p_{NS} \in (0, 1)$, if a nonempty SD \mathcal{P} is degenerate, then for any SD \mathcal{W} with $a(\mathcal{W}) \leq a(\mathcal{P})$ (including \mathcal{P} and the empty SD), $\text{KL}_b(\mathcal{P}||\mathcal{W}) = -a(\mathcal{P}) \ln(p_{NS})$ (all such SDs are minimizers).

Proof. For any such \mathcal{W} , $\text{KL}_b(\mathcal{P}||\mathcal{W}) = \sum_{i \in \text{sup}(\mathcal{P})} -\mathcal{P}(i) \ln(p_{NS})$ (as $\forall i, \mathcal{W}(i) \leq a(\mathcal{W}) \leq p_{NS}$), thus $\text{KL}_b(\mathcal{P}||\mathcal{W}) = -a(\mathcal{P}) \ln(p_{NS})$ \square

If \mathcal{P} is non-degenerate, we show that a minimizer must exist, but we first show some of the properties it must have (see also Fig. 24).

Lemma 8. For any $p_{NS} \in (0, 1)$ and any non-degenerate SD \mathcal{P} , where we want to minimize $\text{KL}_b(\mathcal{P}||\mathcal{W})$ over the set S of SDs \mathcal{W} such that $a(\mathcal{W}_1) \leq a(\mathcal{P})$ (and wlog we need only consider $\text{sup}(\mathcal{W}) \subseteq \text{sup}(\mathcal{P})$):

1. (all positive PR items are above p_{NS}) For any $\mathcal{W}_1 \in S$, if there is an item i where $\mathcal{W}_1(i) \in (0, p_{NS}]$, then there is a SD $\mathcal{W}_2 \in S$, such that $\forall i \in \text{sup}(\mathcal{W}_2), \mathcal{W}_2(i) > p_{NS}$, and $\text{KL}_b(\mathcal{P}||\mathcal{W}_2) < \text{KL}_b(\mathcal{P}||\mathcal{W}_1)$. Therefore, in minimizing $\text{KL}_b(\mathcal{P}||\cdot)$, we need only consider the set $S_2 = \{\mathcal{W} | \mathcal{W} \in S, a(\mathcal{W}) = a(\mathcal{P}), \text{and } \forall i \in \text{sup}(\mathcal{W}), \mathcal{W}(i) > p_{NS}\}$ (S_2 is not empty as \mathcal{P} is non-degenerate).
2. (existence and proportionate increase) The set $S^* \subseteq S_2$ of minimizers of $\text{KL}_b(\mathcal{P}||\cdot)$ is not empty, and for any $\mathcal{W}^* \in S^*$, and for some fixed multiple $r \geq 1$, $\forall i \in \text{sup}(\mathcal{W}^*), \mathcal{W}^*(i) = r\mathcal{P}(i)$.
3. (order is respected) For any minimizer \mathcal{W}^* and any two items i and j , when $\mathcal{P}(i) < \mathcal{P}(j)$, if $\mathcal{W}^*(i) > 0$, then $\mathcal{W}^*(j) > 0$ (and, from part 2, $\mathcal{W}^*(j) > \mathcal{W}^*(i)$).

Proof. (part 1) Say \mathcal{W}_1 has one or more items with low PR $\leq p_{NS}$, call the set $\mathcal{I}_2, \mathcal{I}_2 := \{i | \mathcal{W}_1(i) \leq p_{NS}\}$, with total PR b (thus $b := \sum_{i \in \mathcal{I}_2} \mathcal{W}_1(i)$). We can also assume $a(\mathcal{W}_1) = a(\mathcal{P})$ (if less, we can also shift the difference onto receiving item j in this argument). Then if \mathcal{W}_1 also has an item j with PR above p_{NS} , shift all the mass b to item j . Otherwise, shift all the mass b to a single item j in \mathcal{I}_2 (pick any item). In either case, we have $\text{KL}_b(\mathcal{P}||\mathcal{W}_2) <$

$\text{KL}_b(\mathcal{P}||\mathcal{W}_1)$: In the first case, the cost (*i.e.* $-\mathcal{P}(i) \ln(\frac{\mathcal{P}(i)}{\max(Q(i), p_{NS})})$) is not changed for items in \mathcal{I}_2 ($-b \ln(p_{NS})$), while for item j the cost is lowered. In the second case, we must have $b > p_{NS}$ (\mathcal{P} is non-degenerate), and the cost for the receiving item i improves (as we must have $Q_2(i) > p_{NS}$), while for others in \mathcal{I}_2 it is not changed.

(part 2) The set S_2 (from part 1), can be partitioned into finitely many subsets (ie disjoint sets whose union is S_2), each partition member corresponding to a non-empty subset of $\text{sup}(\mathcal{P})$. For instance all those that have positive PR on item 1 only (greater than p_{NS} by definition of S_2) (support of size 1) define one partition subset (we get $|\text{sup}(\mathcal{P})|$ such subsets corresponding to singletons). The size of the support set k of a SD in S_2 , $k \leq |\text{sup}(\mathcal{P})|$, can be large to the extent that $\frac{a(\mathcal{P})}{k} \geq p_{NS}$ is satisfied ($k = 1$ works, but larger k may yield valid SDs in S_2 as well). On each such partition set \mathcal{S}_k , $\text{KL}_b(\mathcal{P}||\cdot)$ becomes equivalent to $\text{KL}(\mathcal{P}||\cdot)$, in the following sense: If \mathcal{S}_k is a partition, then $\forall \mathcal{W}_1, \mathcal{W}_2 \in \mathcal{S}_k$, $\text{KL}_b(\mathcal{P}||Q_1) - \text{KL}_b(\mathcal{P}||Q_2) = \text{KL}(\mathcal{P}||Q_1) - \text{KL}(\mathcal{P}||Q_2)$. From Corollary 3, the total mass from elements that are zeroed (if any), *i.e.* $\text{sup}(\mathcal{P}) - \text{sup}(\mathcal{W}_1)$, is spread proportionately on $\text{sup}(\mathcal{W}_1)$ to minimize $\text{KL}(\mathcal{P}||\cdot)$ over a partition subset. Since we have a finitely many partitions (the size of a powerset at most), and each yields a well-defined minimizer of $\text{KL}_b(\mathcal{P}||\cdot)$, we obtain one or more minimizers for the entire S_2 and therefore S .

(part 3) Wlog consider items 1 and 2, $p_1 = \mathcal{P}(1)$ and $p_2 = \mathcal{P}(2)$, where $p_1 < p_2$, and assume in SD $\mathcal{W}_1 \in S_2$ (with support size $|\text{sup}(\mathcal{W}_1)| \geq 1$), item 1 has an allocation $T > p_{NS}$ (as $\mathcal{W}_1 \in S_2$), while $\mathcal{W}_1(2) < \mathcal{W}_1(1)$. We need only consider the case $\mathcal{W}_1(2) = 0$: if $\mathcal{W}_1(2) > 0$, then $\mathcal{W}_1(2) > p_{NS}$ as $\mathcal{W}_1 \in S_2$, and proportionate increase from part 2 establishes the result. Assuming $\mathcal{W}_1(2) = 0$, we can 'swap' items 1 and 2, to get SD $\mathcal{W}_2 \in S_2$, and swapping improves $\text{KL}_b(\cdot)$, *i.e.* letting $\Delta := \text{KL}_b(\mathcal{P}||\mathcal{W}_1) - \text{KL}_b(\mathcal{P}||\mathcal{W}_2)$, we must have $\Delta >$

$$\begin{aligned} \Delta &= (p_2 \ln \frac{p_2}{p_{NS}} + p_1 \ln \frac{p_1}{T}) - (p_1 \ln \frac{p_1}{p_{NS}} + p_2 \ln \frac{p_2}{T}) \quad (\text{all other terms cancel}) \\ &= -p_2 \ln(p_{NS}) - p_1 \ln(T) + p_1 \ln(p_{NS}) + p_2 \ln(T) = (p_2 - p_1)(\ln(T) - \ln(p_{NS})) > 0 \end{aligned}$$

0:

The last step (conclusion) follows from our assumptions that $p_2 > p_1$ and $T > p_{NS}$. Note that \mathcal{W}_2 can further be improved by a proportionate spread (the allotment T to item 2 increased). \square

The lemma implies that the minimizer is unique if no two items in $\text{sup}(\mathcal{P})$ have equal PRs (due to proportionate spread). It also suggests a sorting algorithm to find an optimal allocation: With $k = 1, 2, \dots, |\text{sup}(\mathcal{P})|$, use the highest k items (highest $\mathcal{P}(i)$), and spread $a(\mathcal{P})$ proportionately onto the k items, yielding \mathcal{W}_k , and compute $\text{KL}(\mathcal{P}||\mathcal{W}_k)$. One of $\mathcal{W}_1, \mathcal{W}_2, \dots$ is the minimizer. The algorithm can be stopped early if $\frac{a(\mathcal{P})}{k} \leq p_{NS}$ and also when proportionate spread leaves an item with $\text{PR} \leq p_{NS}$. One could also start with smallest item, spreading it on remainder, and repeating. The threshold p_0 described next determines when this algorithm should stop (see also Lemma 10).

Some items can have such a large PR that they are safe from being zeroed (in a minimizer \mathcal{W}^*). The next two sections derive the threshold $p_0 > p_{NS}$, specifying when a PR can be above p_{NS} but sufficiently close to it for the possibility of being zeroed or distortion (its PR shifted to higher items to yield lower losses). Note that even if a $\text{PR} \leq p_{NS}$, it may not be zeroed in the minimizer because shifts from smaller items may raise its mass to above p_0 . The smallest item i , with $\mathcal{P}(i) < p_0$, is guaranteed to be zeroed (in some minimizer \mathcal{W}^* , Lemma 9 below).

A.3.3 The Case of Two Items (and Threshold p_0)

Suppose the DI \mathcal{P} has two items, with PRs p and $1 - p$, *i.e.* $\mathcal{P} = \{1:p, 2:1-p\}$, where $p \leq 1 - p$, and $p > p_{NS}$, and we want to see how high p can be and yet distortion remains possible, *i.e.* item 1 is zeroed and its mass shifted to item 2, and $\Delta := \text{KL}_b(\mathcal{P}||\mathcal{P}) - \text{KL}_b(\mathcal{P}||\mathcal{W}) > 0$: how high p , $p > p_{NS}$, can be and yet we can get $\Delta > 0$. $\Delta = 0 - (p \ln \frac{p}{p_{NS}} + (1-p) \ln \frac{1-p}{1})$, thus $\Delta > 0$, when $p \ln(p_{NS}) > p \ln(p) + (1-p) \ln(1-p)$, or $p_{NS} > p(1-p)^{\frac{1-p}{p}}$.

Thus the threshold p_0 is such that $p_{NS} = p_0(1-p_0)^{\frac{1-p_0}{p_0}}$. Now, with $r := (1-p_0)^{\frac{1-p_0}{p_0}}$, $r > 1 - p_0$ for $p_0 > 0.5$ ($r \rightarrow 1.0$ as $p_0 \rightarrow 1$), and $r < 1 - p_0 < 1$ when $p_0 < 0.5$ (and $r = 1 - p_0 = p_0 = 0.5$ when $p_0 = 0.5$) (note that in our set up, $p_0 \leq 0.5$). Thus, indeed $p_{NS} < p_0$. We can set p_0 and see how low p_{NS} should be (or, otherwise, solve for p_0). Considering the ratio $\frac{p_{NS}}{p_0} = \frac{p_0(1-p_0)^{(1-p_0)/p_0}}{p_0} = r$, where we have defined $r = (1-p_0)^{\frac{1-p_0}{p_0}}$, and as $p_0 \rightarrow 0$, $\frac{p_{NS}}{p_0} \rightarrow \frac{1}{e}$ (e denotes the base of the natural logarithm), while as $p_0 \rightarrow 0.5$, $\frac{p_{NS}}{p_0} \rightarrow \frac{1}{2}$, or:

$$2p_{NS} \leq p_0 \leq ep_{NS} \approx 3p_{NS}. \quad (11)$$

Thus, as a rule of thumb, as long as $p \geq 3p_{NS}$, p is not zeroed. With $p_{NS} = 0.01$, we can get a positive distortion for $p < p_0 \approx 0.027$ (no distortion if $p \geq 0.0270$). With $p_{NS} = 0.001$, no distortion if $p \geq p_0 \approx 0.00272$, and with $p_{NS} = 0.1$, the threshold $p_0 \approx 0.24$ (no distortion if $p \geq p_0 = 0.24$).

When \mathcal{P} is a strict SD, the possibility of distortion becomes more limited: assume again that \mathcal{P} has two items with equal probability $p, p > p_{NS}$, then $\Delta > 0$ (defined above) implies $0 - (p \ln \frac{p}{p_{NS}} + p \ln \frac{p}{2p}) > 0$, or $\ln(p_{NS}) > \ln(p/2)$, or $2p_{NS} = p_0$, implying distortion possibility only when $p \leq 0.02$ with $p_{NS} = 0.01$.

A.3.4 More Items (and Threshold p_0)

The case of more items is similar to two items, and yields the same distortion threshold p_0 : given DI \mathcal{P} assume all its items have PR above p_{NS} , and $\Delta := \text{KL}_b(\mathcal{P}||\mathcal{P}) - \text{KL}_b(\mathcal{P}||\mathcal{W}^*) = 0 - \text{KL}_b(\mathcal{P}||\mathcal{W}^*)$, and we are wondering about the relation of say $p_1 = \mathcal{P}(1)$ and p_{NS} when $\Delta > 0$.

$$\begin{aligned} \Delta &= - \left(p_1 \ln(p_1/p_{NS}) + \sum_{i \geq 2} p_i \ln(p_i/(p_i + \frac{p_i}{1-p_1}p_1)) \right) \\ &\quad \text{(the above is the proportionate spread of } p_1 \text{ onto others in } \mathcal{W}^*) \\ &= p_1 \ln(p_{NS}) - p_1 \ln(p_1) - \sum_{i \geq 2} p_i \ln(p_i) + \sum_{i \geq 2} p_i \ln(p_i + \frac{p_i}{1-p_1}p_1) \\ &= p_1 \ln(p_{NS}) - \sum_{i \geq 1} p_i \ln(p_i) + \sum_{i \geq 2} p_i \ln(\frac{p_i}{1-p_1}) \\ &= p_1 \ln(p_{NS}) - \sum_{i \geq 1} p_i \ln(p_i) + \sum_{i \geq 2} p_i \ln(p_i) - \ln(1-p_1) \sum_{i \geq 2} p_i \\ &= p_1 \ln(p_{NS}) - \ln(1-p_1) \sum_{i \geq 1} p_i - p_1 \ln(\frac{p_1}{1-p_1}) = p_1 \ln(p_{NS}) - \ln(1-p_1) - p_1 \ln(\frac{p_1}{1-p_1}) \end{aligned}$$

And $\Delta > 0$ implies $p_1 \ln(p_{NS}) > \ln(1-p_1) + p_1 \ln(\frac{p_1}{1-p_1})$, or when p_1 is low enough such that $p_{NS} > p_1(1-p_1)^{\frac{1-p_1}{p_1}}$. This is the same bound or threshold as the two-item case, and we summarize the properties in the following lemma.

Lemma 9. *With a DI \mathcal{P} and $p_{NS} \in (0, 1)$, if item i has PR $\mathcal{P}(i) \geq p_0$, where p_0 is such that $p_{NS} = p_0(1-p_0)^{\frac{1-p_0}{p_0}}$, then $\mathcal{W}^*(i) \geq \mathcal{P}(i)$ (item i is not zeroed) in any minimizer \mathcal{W}^* of $\text{KL}_b(\mathcal{P}||\cdot)$. If $i \in \text{sup}(\mathcal{P})$ has the smallest PR in $\text{sup}(\mathcal{P})$ and $\mathcal{P}(i) < p_0$, then i is zeroed in some minimizer \mathcal{W}^* ($\mathcal{W}^*(i) = 0$) and if it is the unique minimum, then $\mathcal{W}^*(i) = 0$ in any minimizer \mathcal{W}^* .*

Proof. The result follows from the above derivation and the ordering properties specified in Lemma 8. \square

For the analysis of extent of distortion below, we can assume \mathcal{P} is a DI, as when using $\text{KL}_{NS}()$ the first argument is augmented to a distribution. However, we expect the above analysis and bound can be extended to strict SDs as well.

A.3.5 Extent of Distortion

Lemma 9 and 8 explain which items are zeroed, and the following lemma specifies extent of increase in an item's PR in any minimizer of $\text{KL}_b(\mathcal{P}||\cdot)$, and further characterizes the properties of a minimizer.

Lemma 10. *Given any DI \mathcal{P} and $p_{NS} \in (0, 1)$, and any DI \mathcal{W} with $\text{sup}(\mathcal{W}) \subseteq \text{sup}(\mathcal{P})$ and with proportionate spread according to \mathcal{P} , let $Z := \text{sup}(\mathcal{P}) - \text{sup}(\mathcal{W}^*)$ (the zeroed items or the difference of the two support sets), and $p_z(\mathcal{W}) := \sum_{i \in Z} \mathcal{P}(i)$, thus $p_z(\mathcal{W})$ is the total mass of the zeroed items (the shifted mass), $p_z(\mathcal{W}) \geq 0$. **(part 1)** We have for any $i \in \text{sup}(\mathcal{W})$, $\mathcal{W}(i) = \frac{\mathcal{P}(i)}{1-p_z(\mathcal{W})}$. **(part 2)** Furthermore, let S_g be the set of all such proportionate \mathcal{W} with $\min_{i \in \text{sup}(\mathcal{W})} \mathcal{P}(i) \geq p_0$. Then any minimizer DI \mathcal{W}^* of $\text{KL}_b(\mathcal{P}||\cdot)$ is in S_g , and has the largest support and the smallest shifted mass among such (i.e. $p_z(\mathcal{W}^*) \leq p_z(\mathcal{W})$ and $|\text{sup}(\mathcal{W}^*)| \geq |\text{sup}(\mathcal{W})|$ for any $\mathcal{W} \in S_g$).*

Proof. For a DI \mathcal{W} , let p_z denote $p_z(\mathcal{W})$, and let $s := \sum_{i \in \text{sup}(\mathcal{W})} \mathcal{P}(i)$. From the definition of proportionate spread, we add $\frac{\mathcal{P}(i)}{s}p_z$ to $\mathcal{P}(i)$. We have $s = 1 - p_z$, therefore, $\mathcal{W}(i) = \mathcal{P}(i) + \frac{\mathcal{P}(i)}{1-p_z}p_z = \mathcal{P}(i)(1 + \frac{p_z}{1-p_z}) = \frac{\mathcal{P}(i)}{1-p_z}$. **(proof of part 2)** From Lemma 8, p_z is proportionately spread onto non-zeroed items in \mathcal{W}^* as well. Consider \mathcal{Q}_1 and \mathcal{W}^* , both in S_g , and assume $\text{sup}(\mathcal{W}_1) > \text{sup}(\mathcal{W}^*)$ (proof by contradiction). By shifting the lowest PR in S_1 to remaining (higher PR) items in the support, and repeating, we should get to \mathcal{W}^* (or an equivalent, in case of ties). But each shift results in an inferior \mathcal{W} because of our assumption that all PRs are $\geq p_0$ and the shifts only increase the PR on items that remain (non-zeroed items). \square

We now have the tools for understanding the types and extents of distortion from using $\text{KL}_{NS}(\text{DI}(\mathcal{P})||.)$ under different scenarios. We know that an item with PR below p_0 can be zeroed, *i.e.* completely distorted, in \mathcal{W}^* . From the outset, working with finite-space predictors, we have accepted the possibility of poor or no estimation of small PRs beyond a point. Certain such low-PR items may have their PR multiplied by many folds in \mathcal{W}^* (yielding a high distortion ratio $\frac{\mathcal{W}^*(i)}{\mathcal{P}(i)}$): imagine the uniform DI \mathcal{P} with k items, each with PR $1/k$. A few of these items attain a high PR of p_0 or higher ($\approx 3p_{NS}$) in \mathcal{W}^* (a fixed $\approx \frac{1}{3p_{NS}}$ such non-zeroed items). For instance, with $p_{NS} = 0.01$, the number of non-zeroed items is fixed at $\approx \frac{1}{0.03} \approx 33$. The original total PR mass on these items (in \mathcal{P}) is $\frac{33}{k}$, shrinking with increasing k . Thus, as we imagine increasing k , the mass $p_z, 1 - \frac{33}{k}$, shifting from the zeroed items to non-zeroed items increases, approaching 1, and using Lemma 10, the relative increase in the PR of non-zeroed items grows unbounded: $\frac{\mathcal{W}^*(i)}{\mathcal{P}(i)} = \frac{1}{1-p_z} \rightarrow \infty$. Note also that $\text{FC}()$ does not alter \mathcal{W}^* in this example by much (so our argument holds for both $\text{KL}_b()$ and $\text{KL}_{NS}()$). This example showing large distortion ratio on small items (items with tiny PR below p_{NS}) holds when we use a perfect marker (we explain how using a practical imperfect marker affects distortion in the next section, in particular, see Lemma 11).

When the total PR shift p_z is small, the increase $\frac{1}{1-p_z}$ in PR of any non-zeroed item is also small. Let S_g be the set of items in $\text{DI}(\mathcal{P})$ (including item 0) with PR above p_0 (*i.e.* well above $p_{NS} = p_{min}$), and let $p_g := \sum_{i \in S_g} \mathcal{P}(i)$. By Lemma 9, no item in S_g is zeroed (no mass from it is shifted), so $p_z \leq 1 - p_g$. For example, a p_g value of 0.9 means $p_z \leq 0.1$, and therefore no item is increased by no more than $\frac{1}{0.9} \approx 1.1$. In particular, if there are one or more items in \mathcal{P} with PR above $p_0 > p_{NS}$, and the remaining is unallocated and $1 - \mathbf{a}(\mathcal{P}) = \mathbf{u}(\mathcal{P}) \geq p_{NS}$, *i.e.* there is no normalizing and removal in FC , then \mathcal{P} remains the unique optimal (minimizer) of $\text{KL}_{NS}(\mathcal{P}||\text{FC}(.))$ (and of $\text{KL}_b(\mathcal{P}||.)$). For instance, this is the case for SD $\mathcal{P} = \{1 : 0.5, 2 : 0.1\}$ (with $p_{NS} = 0.01$) ($\text{FC}()$ does not change \mathcal{P} in this example). If $\mathbf{u}(\mathcal{P}) < p_{NS}$, then some normalizing will occur. However, if the normalizing factor doesn't change (reduce) the PRs by much, the distortion will remain low. For example, with the SD $\mathcal{P} = \{1 : 0.5, 2 : 0.1, 3 : 0.4\}$, $\text{FC}(\mathcal{P}) = 0.99\mathcal{P} = \{1 : 0.495, 2 : 0.099, 3 : 0.396\}$, and \mathcal{P} remains optimal for $\text{KL}_{NS}(\mathcal{P}||\text{FC}(.))$, and so are the close multiples of \mathcal{P} , $\alpha\mathcal{P}$ for $\alpha \in [0.99, 1]$ ($\text{KL}_{NS}(\mathcal{P}||\mathcal{P}) = \text{KL}_{NS}(\mathcal{P}||\alpha\mathcal{P})$ as long as $\alpha \geq 0.99$). In this example, there are multiple minimizers for $\text{KL}_{NS}(\mathcal{P}||\text{FC}(.))$ but a unique one for $\text{KL}_{NS}(\mathcal{P}||.)$ ($\text{FC}()$ maps them to one unique minimizer).

Note also that an SD \mathcal{W} can have more distance from \mathcal{P} than the minimizer \mathcal{W}^* , and still score lower than \mathcal{P} itself (*i.e.* \mathcal{W}^* does not determine the largest distance from \mathcal{P} under the constraint of scoring better). We have focused on the distance of a minimizer because of our intended use of $\text{KL}_{NS}()$ for comparisons (where a minimizer \mathcal{W}^* is preferred).

A.3.6 Imperfect NS-marker and Setting the p_{NS} threshold

We have assumed a perfect NS-marker (referee) in all the above. Assuming $p_{min} = 0.01$, a simple practical NS-marker, *e.g.* keeping a history of the last 100 time points (a box predictor), will have some probability of making false positive markings (a salient item marked NS) and false negative errors (items below p_{min}). The error probability goes down as an item becomes more salient or more noisy (its PR gets farther from the p_{NS} threshold), and for items with PR near the boundary, the loss would be similar whether or not $\ln(p_{NS})$ is used. We assume such a box predictor as a practical NS-marker here. Note also that, just as in the case for the prediction algorithms, there is a tradeoff here on the size of the horizon used for the practical NS-marker: change and non-stationarity motivate shorter history. We also note that with a practical marker, marking items with PR below p_{NS} as NS with high probability, the example of previous section with tiny items yielding high $\frac{\mathcal{W}^*(i)}{\mathcal{P}(i)}$ ratio would not occur: if a DI \mathcal{P} has all its items well below p_{NS} , the best scoring \mathcal{W}^* is the empty SD ($\mathbf{u}(\mathcal{W}^*) = 1$), with a practical NS-marker. We formalize the extent of increase in this imperfect setting next.

Given a SD \mathcal{P} on $\mathcal{I} = \{1, 2, \dots\}$, the *ideal-threshold* NS-marker, or the **threshold marker** for short, marks an item i NS iff $\mathcal{P}(i) \leq p_{NS}$. Considering how $\text{LogLossNS}()$ (or $\text{loglossRuleNS}()$) works when the threshold marker is used, the marker in effect converts a SD \mathcal{P} to a DI \mathcal{P}' where for any item i with $\mathcal{P}(i) \leq p_{NS}$, its PR, together with $\mathbf{u}(\mathcal{P})$, is transferred to item 0 when computing $\text{KL}_{NS}(\mathcal{P}'||.)$ (recall that $\text{DI}(\mathcal{P})$, in definition 3, only transferred $\mathbf{u}(\mathcal{P})$ to item 0). Thus \mathcal{P}' is a DI where $\forall i \in \text{sup}(\mathcal{P}')$ if $i \neq 0$, then $\mathcal{P}'(i) > p_{NS}$. It is possible that $\mathcal{P}'(0) < p_{NS}$, but as we use $\text{FC}()$, we could limit our analysis to DI \mathcal{P}' where $\forall i \in \text{sup}(\mathcal{P}')$, $\mathcal{P}'(i) \geq p_{NS}$.

The next lemma shows that the distortion ratio $\frac{\mathcal{W}^*(i)}{\mathcal{P}(i)}$ is upper bounded by about 3 in this setting where the PRs are above p_{NS} .

Lemma 11. *Given any DI \mathcal{P} with $\min_{i \in \text{sup}(\mathcal{P})} \mathcal{P}(i) \geq p_{NS}$, for any minimizer \mathcal{W}^* of $\text{KL}_b(\mathcal{P}||.)$, the distortion ratio*

$$\frac{\mathcal{W}^*(i)}{\mathcal{P}(i)} \leq \frac{p_0}{(1-p_0)p_{NS}} < \frac{3}{(1-p_0)}.$$

Proof. Let m be the mass of non-zeroed items in \mathcal{P} ($m = 1 - p_z(\mathcal{P})$, p_z was also used in Lemma 10), then we need to bound the distortion ratio $\frac{1}{m}$ which is the ratio by which each item i in $\text{sup}(\mathcal{W}^*)$ goes up by ($\frac{\mathcal{W}^*(i)}{\mathcal{P}(i)}$). Let j be any item that is zeroed (at least one such item exists, otherwise the distortion ratio is 1). Let $x := \mathcal{P}(j)$, and we have $x \geq p_{NS}$. Then spreading 1.0 over one additional item, $\text{sup}(\mathcal{W}^*) \cup \{j\}$, proportionately, would fail to take the PR of j to p_0 (by Lemma 10, \mathcal{W}^* would not be optimal). Proportional allocation over $\text{sup}(\mathcal{W}^*) \cup \{j\}$ yields $\frac{x}{x+m}$ for item j and we must have $\frac{x}{x+m} < p_0 \Rightarrow x < p_0 x + p_0 m \Rightarrow \frac{(1-p_0)x}{p_0} < m$ and as $x > p_{NS}$, we get $\frac{1}{m} < \frac{p_0}{(1-p_0)x} \leq \frac{p_0}{(1-p_0)p_{NS}}$. \square

When $p_{NS} = 0.01$, then $p_0 < 0.03$, or $(1 - p_0)^{-1} < 1.031$, and the distortion ratio is bounded by 3.1. A practical marker can be viewed as a noisy version of the (ideal) threshold marker.

Given threshold $p_{NS} > 0$, if we find that the predictions $\mathcal{W}^{(t)}$ have mostly unallocated mass or PRs close to p_{NS} , then p_{NS} and p_{min} may need to be lowered (e.g. from 0.01 to 0.001) for evaluation as well as better (finer) prediction. For example, with $p_{min} = p_{NS} = 0.01$, we may find that many learned PRs are below 0.05. Or may observe that a sizeable portion of the predicted SDs is unallocated ($u(\mathcal{W}^{(t)})$ well above p_{NS}). This lowering of thresholds can lead to extra space consumption by the predictor. It does not guarantee that further salient items will be learned, as any remaining salient items may have probability well below the new p_{NS} that we set, or all that is left could be truly pure noise (measure 0). All this depends on the input stream (rate of change, rate of pure noise,...), in addition to the quality of the predictor.

A.4 Alternative Scoring Schemes for Noise

We have considered a few other options for handling NS items (when using log-loss), including not having a referee: One possibility is reporting two numbers for each prediction method: the number of items it treated as NS on a given sequence (assigned 0 or sufficiently small probability), and otherwise average the LogLoss on the remainder of the input sequence. A method is inferior if it marks a large fraction of items as NS compared to others, but if the fractions are close, one looks at the LogLoss numbers. However, we thought that comparing methods with two numbers would be difficult, and it is also hard to combine two very different numbers to get a single understandable number to base comparisons on. Another no-referee option is to pair two methods (or multiple methods) and specify a policy when they disagree (on items deemed NS by one but not the other). Here, one needs to specify a scoring policy handling disagreements. This option does not provide a single understandable quality score for a method in isolation (making it hard to pick parameters when improving a single algorithm as well), and may not easily generalize to comparing more than two methods.

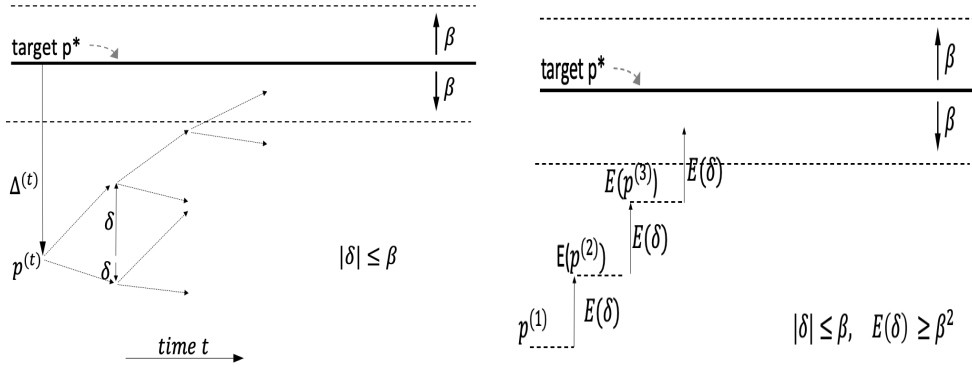
We could also use a referee, but ignore (skip) the NS items when averaging the loss. This measure can provide insights, and we have looked at it in some experiments, but it can also lead to impropriety (incentive incompatibility or deviations from truth-telling): a method that puts all of its PR mass toward salient items, than leaving some for the noise portion of the stream, would score better. Assume the portion of noise items in the stream is 0.2 (20% of the times a noise item appears), and otherwise a salient item, say A , occurs with 0.8 probability. If we ignore NS items during evaluation, the method that shifts the 0.2 PR mass over the salient items, in this case always outputting A with PR 1, would score better than the honest method that reports A with its true PR of 0.8.

B Convergence Properties of Sparse EMA

Lemma 2, and its proof follows, where we are in the stationary binary setting (Sect. 2.1.3), where the target PR to learn, $\mathcal{P}(1)$, is denoted p^* , and the estimates of EMA for item 1, denoted $\hat{p}^{(t)}$, form a random walk ($\hat{p}^{(t)}$ is the estimate immediately after the update at time t). Fig. 25 shows the main ideas of the proofs, e.g. the expected step size is β^2 towards p^* when \hat{p} is not too close.

Lemma. *EMA's movements, i.e. changes in the estimate $\hat{p}^{(t)}$, enjoy the following properties, where $\beta \in [0, 1]$:*

1. *Maximum movement, or step size, no more than β : $\forall t, |\hat{p}^{(t+1)} - \hat{p}^{(t)}| \leq \beta$.*
2. *Expected movement is toward p^* : Let $\Delta^{(t)} := p^* - \hat{p}^{(t)}$. Then, $\mathbb{E}(\Delta^{(t+1)} | \hat{p}^{(t)} = p) = (1 - \beta)(p^* - p) = (1 - \beta)\Delta^{(t)}$.*
3. *Minimum expected progress size: With $\delta^{(t)} := |\Delta^{(t)}| - |\Delta^{(t+1)}|$, $\mathbb{E}(\delta^{(t)}) \geq \beta^2$ whenever $|\Delta^{(t)}| \geq \beta$ (i.e. whenever \hat{p} is sufficiently far from p^*).*



(a) Convergence to within the band (from below in this picture). (b) Expected steps and expected positions

Figure 25: A picture of the properties in Lemma 2, upper bounding the expected number of time steps to enter the band $p^* \pm \beta$ by β^{-2} , whether from below or above the band (Theorem 1), where $\Delta^{(t)} := p^* - \hat{p}^{(t)}$ and $\delta^{(t)} := |\Delta^{(t)}| - |\Delta^{(t+1)}|$. (a) At any point, there are two possible outcomes after an update (weaken or boost), and the movement, δ , could be toward or away from p^* (e.g. $\delta < 0$), but always $|\delta| \leq \beta$. (b) As long as \hat{p} is not in the band, there is an expected movement, $E(\delta)$, of at least β^2 , toward p^* . $E(\delta)$ is smallest when \hat{p} is near p^* and largest, up to β , when \hat{p} is farthest ($\hat{p} = 0$ or $\hat{p} = 1$).

Proof. (proof of part 1) On a negative update, $\hat{p}^{(t)} - \hat{p}^{(t+1)} = \hat{p}^{(t)} - (1 - \beta)\hat{p}^{(t)} = \beta\hat{p}^{(t)} \leq \beta$, and on a positive update, $\hat{p}^{(t+1)} - \hat{p}^{(t)} = (1 - \beta)\hat{p}^{(t)} + \beta - \hat{p}^{(t)} = \beta - \hat{p}^{(t)}\beta \leq \beta$ (as $\hat{p}^{(t)} \in [0, 1]$).

(part 2) We write the expression for the expectation and simplify: p^* of the time, we have a positive update, i.e. both weaken and boost $((1 - \beta)p + \beta)$, and the rest, $1 - p^*$ of the time, we have weaken only $((1 - \beta)p)$. In both cases, the term $(1 - \beta)p$, is common and is factored:

$$\begin{aligned} \mathbb{E}(\Delta^{(t+1)} | \hat{p}^{(t)} = p) &= p^* (p^* - ((1 - \beta)p + \beta)) + (1 - p^*) (p^* - (1 - \beta)p) \\ &\quad \text{(next, the term, } p^* - (1 - \beta)p, \text{ is common and is factored)} \\ &= (p^* + (1 - p^*)) (p^* - (1 - \beta)p) - p^* \beta \\ &= p^* - (1 - \beta)p - p^* \beta = p^* (1 - \beta) - (1 - \beta)p \\ &= (1 - \beta)(p^* - p) \end{aligned}$$

(part 3) Note from our definition of $\delta^{(t)}$, $\delta^{(t)} > 0$ when distance to p^* is reduced (when $|\Delta^{(t+1)}| < |\Delta^{(t)}|$). When \hat{p} is close to p^* , e.g. $\hat{p} = p^*$, the expected distance may not shrink, but when outside the band, we can show a minimum positive progress: Assume $\hat{p}^{(t)} \leq p^* - \beta$, then $\delta^{(t)} = p^* - \hat{p}^{(t)} - (p^* - \hat{p}^{(t+1)})$ ($\hat{p}^{(t+1)}$ is also below p^*) or $\delta^{(t)} = \hat{p}^{(t+1)} - \hat{p}^{(t)}$, and:

$$\begin{aligned} \mathbb{E}(\hat{p}^{(t+1)} - \hat{p}^{(t)}) &= \mathbb{E}(\delta^{(t)}) = \mathbb{E}(p^* - \hat{p}^{(t)} - (p^* - \hat{p}^{(t+1)})) = \mathbb{E}(p^* - \hat{p}^{(t)}) - \mathbb{E}(p^* - \hat{p}^{(t+1)}) \\ &\quad \text{(the above transformation used the linearity of expectation)} \\ &= \mathbb{E}(p^* - \hat{p}^{(t)}) - (1 - \beta)\mathbb{E}(p^* - \hat{p}^{(t)}) = \beta\mathbb{E}(p^* - \hat{p}^{(t)}) \quad \text{(from part 2)} \\ &\geq \beta^2 \quad \text{(from the assumption } |p^* - \hat{p}^{(t)}| \geq \beta) \end{aligned}$$

And similarly for when $\hat{p}^{(t)} \geq p^* + \beta$, then $\delta^{(t)} = \hat{p}^{(t)} - \hat{p}^{(t+1)}$. \square

Note that from property 2 above, there is always progress towards p^* in expectation, meaning that if $\hat{p}^{(t)} < p^*$, then $E(\hat{p}^{(t+1)}) > \hat{p}^{(t)}$, and if $\hat{p}^{(t)} > p^*$, then $E(\hat{p}^{(t+1)}) < \hat{p}^{(t)}$. This is the case even if the probability of moving away is higher than 0.5 ($\hat{p} \leq p^* < 0.5$). We note however, that the result being in expectation, both the actual outcomes for $\hat{p}^{(t+1)}$ can be farther from p^* than $\hat{p}^{(t)}$ (consider when $\hat{p}^{(t)} = p^*$). Property 3 puts a floor (a minimum) on amount of the progress towards p^* in expectation, when $\hat{p} \notin [p^* - \beta, p^* + \beta]$. For instance, when $\hat{p}^{(t)} \leq p^* - \beta$, it puts a minimum on the expected positions $\mathbb{E}(\hat{p}^{(t+1)}), \mathbb{E}(\hat{p}^{(t+2)}), \mathbb{E}(\hat{p}^{(t+3)}), \dots$, until one such point crosses the band, Fig. 25(b), and Theorem 1 follows.

Theorem. *EMA, with a fixed rate of $\beta \in (0, 1]$, has an expected first-visit time bounded by $O(\beta^{-2})$ to within the band $p^* \pm \beta$. The required number of updates, for first-visit time, is lower bounded below by $\Omega(\beta^{-1})$.*

Proof. We are interested in maximum of first-time k when the expected $\mathbb{E}(\hat{p}^{(k)}) \in [p^* - \beta, p^* + \beta]$. Using the maximum movement constraint, as long as $|p^* - \hat{p}^{(t)}| > \beta$, an EMA update does not change the sign of $p^* - \hat{p}^{(t)}$ (\hat{p} does not switch sides wrt p^* , e.g. if greater than p^* , it remains greater after the update). Thus, before an estimate $\hat{p}^{(t)} < p^*$ changes sides, and exceed p^* , it has to be within or come within the band $p^* \pm \beta$. Therefore, start with an arbitrary location $\hat{p}^{(1)}$ outside the band, say $\hat{p}^{(1)} < p^* - \beta$ (similar arguments apply when $\hat{p}^{(1)} > p^* + \beta$), and consider the sequence, $\hat{p}^{(1)}, \hat{p}^{(2)}, \hat{p}^{(3)}, \dots, \hat{p}^{(k)}$, where $\forall t, 1 \leq t \leq k, \hat{p}^{(t)} < p^* - \beta$. We can now lower bound the expected position of $\hat{p}^{(k)}, k \geq 2$ wrt $\hat{p}^{(1)}$, to be at least $(k-1)\beta^2$ above $\hat{p}^{(1)}$:

$$\begin{aligned} \mathbb{E}(\hat{p}^{(k)} - \hat{p}^{(1)} | \hat{p}^{(1)} = p) &= \mathbb{E}(\hat{p}^{(k)} - \hat{p}^{(k-1)} + \hat{p}^{(k-1)} - \hat{p}^{(1)} | \hat{p}^{(1)} = p) \\ &\quad \text{(insert all intermediate sequence members)} \\ &= \mathbb{E}\left(\sum_{2 \leq t \leq k} \hat{p}^{(t)} - \hat{p}^{(t-1)} | \hat{p}^{(1)} = p\right) \\ &= \sum_{2 \leq t \leq k} \mathbb{E}(\hat{p}^{(t)} - \hat{p}^{(t-1)} | \hat{p}^{(1)} = p) \geq (k-1)\beta^2, \end{aligned}$$

where we used the linearity of expectation, and the β^2 lower bound for the last line. With $p^* \leq 1$, an upper bound of $\frac{1}{\beta^2}$ on maximum first-visit time follows: k cannot be larger than $\frac{1}{\beta^2}$ if we want to satisfy $\forall 1 \leq t \leq k, \mathbb{E}(\hat{p}^{(t)}) < p^* - \beta$, or one of $t \in \{1, \dots, \frac{1}{\beta^2} + 1\}$ has to be within the band $p^* \pm \beta$.

The lower bound $\Omega(\beta^{-1})$ on k follows from the upperbound of β on any advancement towards p^* . \square

The dynamics of the estimates $\hat{p}^{(t)}$ can be likened, in some respects, to oscillatory physical motions such as the motion of a pendulum and a vertically hung spring: the expected movement is 0 at target p^* , corresponding to the resting length of the spring, or its equilibrium length, where spring acceleration is 0, and the expected movement is highest at the extremes (farthest from p^*), akin to the acceleration (vector) of the spring being highest when it's most stretched or compressed.

C Further Material on the Qs (Queues) Method

We begin by reviewing a few properties of a single completed cell of a queue in the Qs method, which is equivalent to the experiment of tossing a biased two-sided coin, with unknown heads PR $p^* > 0$ (the target of estimation), counting the tosses until and including the first heads outcome. We can repeat this experiment until we get $k \geq 1$ heads outcomes. The count in each completed cell follows the geometric distribution, and the total number of trials, or the total count over all completed cells, minus the number of heads, has the more general negative binomial distribution (with parameters k and p^*). In the next section we look at estimators for p^* using counts from several completed cells, and describe how the general method of Rao-Blackwellization can be applied there to get a superior estimator, in a sense described next. In Sect. C.3, we proceed to multiple queues, and explore the spread of the PR estimates in a *qMap*.

Ideally, we desire estimators that have no or little bias, that is, if we took the average over many repetitions of the same experiment (e.g. by different people using the same data collection technique, and assuming p^* is not changing), the average over all the estimates would converge to p^* . We also prefer low variance, implying that any particular estimate in time has low chance of being far from target. The two estimation goals are often distinct, for instance an estimator can have zero variance (fully stable) but nonzero bias, and different ways of collecting data and estimation techniques can exhibit these tradeoffs. We observe, for instance, that the bias of a (MLE) technique below gets worse, in the ratio sense, as the target $p^* \rightarrow 0$.

C.1 A Single Completed Queue Cell

With C denoting random variable (r.v.) for the count in a completed cell of a queue, in the binary iid setting (Sect. 2.1.3 and 5.3), the expectation of the estimator $X = \frac{1}{C}$ for $p^* \in (0, 1]$, which is known to be the maximum likelihood estimator (MLE) for the geometric and the more general negative binomial distributions [32, 16, 11], can be expressed

as the infinite series below: p^* of the time, we get a heads outcome on the first toss, and the estimate $\frac{1}{C}$ for p^* is 1, and $(1 - p^*)p^*$ of the time, we get a single tails and then a heads, and the estimate is $1/2$, and so on. The series is called a geometric-harmonic series, and has a closed form in terms of the natural logarithm:

$$\mathbb{E}(X) = \mathbb{E}\left(\frac{1}{C}\right) = p^* \frac{1}{1} + (1 - p^*)p^* \frac{1}{2} + (1 - p^*)^2 p^* \frac{1}{3} + \dots = p^* \sum_{i \geq 1} (1 - p^*)^{i-1} \frac{1}{i} = \frac{-p^* \ln(p^*)}{1 - p^*}$$

From the series, $p^* + (1 - p^*)p^* \frac{1}{2} + \dots$, it is seen for $p^* \in (0, 1)$, as all series elements are positive, that $\mathbb{E}(\frac{1}{C}) > p^*$, or the MLE $X = \frac{1}{C}$ is a biased, upper bound, estimator of p^* in expectation. The ratio $\frac{\mathbb{E}(\frac{1}{C})}{p^*} = \frac{-\ln(p^*)}{1 - p^*}$, and we can verify that this ratio grows unbounded as $p^* \rightarrow 0$ ($\lim_{p^* \rightarrow 0} \frac{-\ln(p^*)}{1 - p^*} = +\infty$). At $p^* = 1$, $\mathbb{E}(\frac{1}{C}) = 1$ and there is no bias, thus the bias, in a relative or ratio to p^* sense, gets worse as p^* gets smaller.⁴¹

We now look at the variance, $\mathbb{V}(X)$ of r.v. $X = \frac{1}{C}$, and how its ratio to p^* changes as p^* is reduced. For any r.v. X , $\mathbb{V}(X) := \mathbb{E}((X - \mathbb{E}(X))^2)$, or $\mathbb{V}(X) = \mathbb{E}(X^2) - (\mathbb{E}(X))^2$ (linearity of expectation).

$$\frac{\mathbb{V}(X)}{p^*} = \frac{\mathbb{E}(X^2)}{p^*} - \frac{(-p^* \ln(p^*)/(1 - p^*))^2}{p^*}$$

The limit of the 2nd term, $\frac{p^* (\ln(p^*))^2}{(1 - p^*)^2}$, as $p^* \rightarrow 0$, is 0, and for the first term:

$$\begin{aligned} \mathbb{E}(X^2) &= p^* \frac{1}{1^2} + (1 - p^*)p^* \frac{1}{2^2} + (1 - p^*)^2 p^* \frac{1}{3^2} + \dots = p^* \sum_{i \geq 1} (1 - p^*)^{i-1} \frac{1}{i^2} \\ \Rightarrow \lim_{p^* \rightarrow 0} \frac{\mathbb{E}(X^2)}{p^*} &= \lim_{p^* \rightarrow 0} \sum_{i \geq 1} (1 - p^*)^{i-1} \frac{1}{i^2} = \sum_{i \geq 1} \frac{1}{i^2} = \frac{\pi^2}{6} \end{aligned}$$

The last step is from the solution to the Basel problem.⁴² Therefore, $\lim_{p^* \rightarrow 0} \frac{\mathbb{V}(X)}{p^*} = \frac{\pi^2}{6}$. We note that at $p^* = 1$, the variance is 0 (as $\mathbb{E}(X) = 1$, and also $\mathbb{E}(X^2) = 1$ from the series above). So the ratio of variance to p^* , the relative variance, grows but is bounded as $p^* \rightarrow 0$. That the variance goes up is consistent with the observation that rates of violation also go up, as p^* is reduced, in Table 3 (using a similar estimator), and Table 4 on performance of Qs (using 5 and 10 queue cells).

C.2 Multiple Completed Cells: Rao-Blackwellization

We have $k \geq 2$ completed queue cells, with C_i denoting the count of cell i , $1 \leq i \leq k$, or repeating the experiment toss-until-heads k times. We first sketch the Rao-Blackwellization (RB) derivation for an unbiased minimum variance estimator, then briefly look at a few related properties and special cases.

Let the (good) estimator $G_k = \frac{k-1}{(\sum_{1 \leq i \leq k} C_i) - 1}$. The RB technique establishes that this is an unbiased estimator, i.e. $\mathbb{E}(G_k) = p^*$, and moreover it is the minimum variance unbiased estimator (MVUE) [49]. We begin with the simple and unbiased but crude estimator $\Theta_1 = [C_1 = 1]$, where we are using the Iverson bracket: p^* of the time Θ_1 is 1 (the first toss is heads), and otherwise $\Theta_1 = 0$, thus indeed $\mathbb{E}(\Theta_1) = p^*$. This estimator is crude (highly variant) as it ignores much information such as the other counts C_i , $i \geq 2$, and we can use RB to derive an improved estimator from Θ_1 . Let $Y = \sum_{i=1}^k C_i$ (Y is the total number of tosses), $Y \sim \text{NB}(k, p^*)$, i.e. Y has the negative binomial distributions with parameters k and p^* . Y is a sufficient statistic for Θ_1 [49, 11]. Then the RB estimator is the conditional expectation $\mathbb{E}(\Theta_1|Y)$, and because Θ_1 is unbiased, this estimator is also unbiased as conditioning does not change bias status and can only improve the variance, and as Y is a sufficient statistic, this estimator is in fact the MVUE [59, 8, 37], and can be simplified to:

⁴¹One can also verify that the derivative of the ratio, $\frac{-1}{p^*(1-p^*)} - \frac{\ln(p^*)}{(1-p^*)^2}$, is negative with $p^* \in (0, 1)$, therefore the ratio is indeed a decreasing function as $p^* \rightarrow 1$.

⁴²The Basel problem, solved by Euler, and named after Euler's hometown, is finding a closed form for sum of the reciprocals of the squares of the natural numbers: $\sum_{i \geq 1} \frac{1}{i^2}$ [11].

$$\mathbb{E}(\Theta_1|Y = y) = P(C_1 = 1|Y = y) = \frac{k-1}{y-1} \quad (\text{Rao-Blackwellization of } \Theta_1 := [[C_1 = 1]])$$

where we know that the last coin toss is always a heads (from our data collection set up) and this leaves $k-1$ heads and $y-1$ unaccounted-for tosses. Take the case of $k=2$ cells or heads. The last heads is fixed, and the first one has $y-1$ positions to pick from, all equally likely, thus $P(C_1 = 1|Y = y) = \frac{1}{y-1}$ when $k=2$. More generally for $k \geq 2$, as the tosses are exchangeable with this conditioning, *i.e.* throwing $k-1$ balls into $y-1$ bins (each bin can contain 1 ball only), the probability that one falls in bin 1 is $\frac{k-1}{y-1}$.⁴³

With $k=2$ completed cells (thus $Y \geq 2$), one can show that the estimator $\frac{1}{Y-1}$ is unbiased more directly (but the property of minimum variance is stronger in above):

$$\mathbb{E}\left(\frac{1}{Y-1}\right) = \sum_{i \geq 2} \frac{P(Y=i)}{i-1} = \sum_{i \geq 2} \frac{(i-1)p^{*2}(1-p^*)^{i-2}}{i-1} = p^{*2} \sum_{i \geq 2} (1-p^*)^{i-2} = p^*$$

where, $P(Y=i) = (i-1)p^{*2}(1-p^*)^{i-2}$, as there are $i-1$ possibilities for the first heads outcome, each having equal probability $p^{*2}(1-p^*)^{i-2}$, and the last equality follows from simplifying the sum of the geometric series ($\sum_{i \geq 0} r^i = \frac{1}{1-r}$, for $r \in (0,1)$).

From the RB estimator, it follows that $\mathcal{U}_k = \frac{k}{Y}$ and $\mathcal{L}_k = \frac{k-1}{Y}$ (where $Y := \sum_{i=1}^k C_i$ as in above) with increasing k form a sequence respectively of upper bounds and lower bounds, in expectation, for p^* : $\mathbb{E}(\mathcal{L}_k) < p^* < \mathbb{E}(\mathcal{U}_k)$. That the estimator \mathcal{U}_k is biased positive can also be seen from an application of Jensen's inequality [12], using linearity of expectation on the sum of r.v.'s, and the fact that $\mathbb{E}(C_i) = \frac{1}{p^*}$ (the mean of the geometric distribution, which can be verified by writing the expectation expression), as follows: Jensen's inequality for expectation is $f(\mathbb{E}(X)) < \mathbb{E}(f(X))$, where the strict inequality holds when these two conditions are met, 1) r.v. X has finite expectation and positive variance (true, in our case, when $p^* < 1$), and 2) $f(x)$ is strictly convex. In our case, $f(x) = \frac{1}{x}$ (a strictly convex function). For one completed cell, we have $f(\mathbb{E}(X)) = f(\mathbb{E}(C_1)) = f(\frac{1}{p^*}) = p^*$, therefore, using Jensen's inequality, $p^* < \mathbb{E}(f(X)) = \mathbb{E}(\frac{1}{C_1})$. Similarly, for $k \geq 2$, $f(\mathbb{E}(Y)) = f(\mathbb{E}(\sum C_i)) = f(\frac{k}{p^*}) = \frac{p^*}{k}$. And $\mathbb{E}(f(Y)) = \mathbb{E}(\frac{1}{Y})$, therefore (via Jensen's), $p^* < k\mathbb{E}(\frac{1}{Y}) = \mathbb{E}(\mathcal{U}_k)$.

C.3 Multiple Queues: PR Sums and the Spread of the PRs

Unlike EMA, with its particular weakening step, even though the Qs method also has in effect a weakening step (a negative update), the PR estimates from all the queues of a Qs predictor do not form a DI or even an SD, as the sum can exceed 1.0. Sect. 5.5 gave an example, and here we delve deeper. Let \mathcal{W} denote the item to (raw) PR from the Qs method, *i.e.* before any normalizing (and at any time point $t \geq 1$). When we feed \mathcal{W} to FC(), scaling is performed to ensure a SD is extracted. In effect, FC() normalizes by the sum, but how large does $a(\mathcal{W})$ (sum of the raw PRs) get, violating the SD property, in the worst case?

C.3.1 MLEs via Single-Cell Queues

Assume each queue had one cell only, and we used the simple MLE, $\frac{1}{C_0}$, and the stream is composed of n unique items (and with no pruning): then the PR estimates are 1 (for the latest observed item), $1/2$ (next to latest), $1/3$, and so on, and $a(\mathcal{W})$ has the growth rate of a harmonic series, which for n (unique) items, is approximately $\ln(n) + 0.577$ (0.577 is called the Euler-Mascheroni constant).

While $a(\mathcal{W})$ can be above 1.0, a related question is about the form and spread of the PRs in \mathcal{W} . For instance, can \mathcal{W} contain 3 or more PRs equal to $\frac{1}{2}$, or 4 or more $\frac{1}{3}$ PRs, violating the SD property by having too many equal PRs? Given a threshold p , *e.g.* $p = p_{min}$, let

$$N(\mathcal{W}, p) := |\{i | \mathcal{W}(i) > p\}|. \quad (12)$$

$N(\mathcal{W}, p)$ is more constrained than $a(\mathcal{W})$, as we will see below. $N(\mathcal{W}, p)$ is of interest when we want to use the raw PR values in \mathcal{W} from a Qs technique, and do not want to necessarily normalize \mathcal{W} at every time t , for instance for the

⁴³One can also look at the process sequentially, and the probability that the first ball misses ($\frac{y-2}{y-1}$), but the second ball falls in position 1 is $\frac{y-2}{y-1} \frac{1}{y-2}$, and so on, or $P(C_1 = 1|Y = y) = \sum_{j=1}^{k-1} (\frac{y-j}{y-1} \frac{1}{y-j}) = \frac{k-1}{y-1}$.

efficient sparse-update time-stamp Qs method when keeping many PRs for millions of items (Sect. D.1). If the PRs formed a SD, then $\frac{1}{p}$ would be the bound. In the simpler case of Qs with $qcap = 1$ and using the MLE $\frac{1}{C_0}$, we can show the same constraint $\frac{1}{p}$ holds, in the next lemma below. Note that when pruning the $qMap$ we are in effect using the MLE with $qcap = 1$, thus understanding its properties is motivated from the pruning consideration as well.

Let the denominator of PR $\mathcal{W}(i)$ be denoted by Y_i . In the case of MLE with $qcap = 1$, Y_i is C_0 , and more generally it is the sum of cell counts. $Y_i^{(t)}$ denotes the value at time t .

Lemma 12. *For the Qs technique with $qcap = 1$, using the MLE $\frac{1}{C_0}$, we have the following properties at any time point $t \geq 2$ (on any input sequence):*

1. $Y_i^{(t)} = 1$ if i was observed at time $t - 1$, and otherwise $Y_i^{(t)} = Y_i^{(t-1)} + 1$.
2. There is exactly one item i with $Y_i^{(t)} = 1$ and thus $PR \mathcal{W}^{(t)}(i) = 1$, the item observed at $t - 1$. For any integer $k \geq 2$, there is at most one item with $Y_i^{(t)} = k$ or $PR \mathcal{W}^{(t)}(i) = \frac{1}{k}$.
3. For any threshold $p > 0$, $N(\mathcal{W}, p) < \frac{1}{p}$.

Proof. Property 1 follows from how the Qs technique allocates new queue cells and increments counts: at each time t exactly one item is observed, its C_0 initialized to one upon update, it thus gets a PR of 1 at $t + 1$. Any other item i in the map \mathcal{W} gets its C_0 incremented, to 2 or higher, or $Y_i^{(t)} = Y_i^{(t-1)} + 1$. Thus exactly one item, the observed item at $t - 1$, has $Y_i^{(t)} = 1$. Property 2 completes using induction on $k \geq 1$, the base case is 1st half of property 2, and for the induction step, we use part 1: Assuming it holds for all integer up to $k \geq 1$, the property for $k + 1$ can be established by contradiction: if there are two or more items with $Y^{(t)} = k + 1$, these items must have had $Y^{(t-1)} = k$ (neither could have been observed at $t - 1$) contradicting the at-most-one property for k .

From part 2, it follows that the maximum number of PRs $N(\mathcal{W}, p)$ is k for probability threshold $p = \frac{1}{k} > 0$, where k is an integer, $k \geq 1$ (with at most one PR $\frac{1}{j}$, for each $j \in \{1, 2, \dots, k\}$). As all PRs in \mathcal{W} are limited to integer $\frac{1}{k}$ fractions (the harmonic numbers), the constraint remains $\frac{1}{p}$ for any threshold $p > 0$ (not just integer fractions). \square

C.3.2 Some Properties when Estimating via GetPR() (MVUEs, Several Cells per Queue)

We next explore the same question of the number of PR values, and related properties, when using more cells per queue, and where we use the **GetPR()** function in the Qs technique (Fig. 8). Let $q(i)$ be short for $qMap(i)$, i.e. the queue for i (when the queue exists). Thus for item i , the PR $\mathcal{W}(i)$ is $\text{GetPR}(q(i))$. Here, with several cells, we need to use the count for cell0, C_0 , e.g. we use the estimate $\mathcal{W}(i) = \frac{1}{C_0 + C_1 - 1}$ for two cells. Otherwise, if counts from only completed cells, say C_1 and C_2 are used (skipping cell0), we can have a worst-case sequence (with non-stationarity) such as $AAABBBCCC \dots$ (an item never occurs after appearing a few times) where the PR estimates (using only completed cells) for many items are all 1. Using the partial cell0 breaks this possibility, and we can establish properties similar to the previous section. Let $|q(i)|$ denote the number of cells in the queue, and define Y_i to be the denominator used in **GetPR()**, $Y_i := \sum_{0 \leq j < |q(i)|} C_j - 1$, thus $\mathcal{W}(i)$ is either 0, when there is no queue for i , or otherwise $\mathcal{W}^{(t)}(i) = \frac{|q^{(t)}(i)| - 1}{Y_i^{(t)}}$ ($\mathcal{W}(i)$ can still be 0 when $|q(i)| = 1$), where $Y_i^{(t)}$ is the denominator and $q^{(t)}(i)$ is the queue of i at t .

Lemma 13. *For the Qs technique with $qcap \geq 2$, for any item i with a queue $q(i)$, $|q(i)| \leq qcap$, using the PR estimate $\mathcal{W}(i) = \frac{|q(i)| - 1}{Y_i}$, where $Y_i := \sum_{0 \leq j < |q(i)|} C_j - 1$, for any time point $t \geq 1$:*

1. $\mathcal{W}^{(t)}(i)$, when nonzero, has the form $\frac{a}{b}$, where a and b are integers, with $b \geq a \geq 1$.
2. If i is not observed at t , then $Y_i^{(t+1)} = Y_i^{(t)} + 1$ or i is removed from the map $qMap$. When i is observed at t (exactly one such), then $Y_i^{(t+1)} \leq Y_i^{(t)}$ when $|q^{(t)}(i)| = qcap$, and $Y_i^{(t+1)} = Y_i^{(t)} + 1$ when $|q^{(t)}(i)| < qcap$.
3. If i is observed at t , then $\mathcal{W}^{(t+1)}(i) \geq \mathcal{W}^{(t)}(i)$. If i is not observed at t , then $\mathcal{W}^{(t+1)}(i) < \mathcal{W}^{(t)}(i)$ or $\mathcal{W}^{(t+1)}(i) = \mathcal{W}^{(t)}(i) = 0$.

Proof. Part 1 follows from Y_i being an integer, and the Qs technique outputs a non-zero PR only when $|q(i)| > 1$, in which case $Y_i > 0$ (with two or more queue cells), and we also have $|q(i)| - 1 \leq Y_i$ (each queue cell has count of at least 1, therefore, $Y_i + 1 = \sum_{0 \leq j < |q(i)|} C_j \geq |q(i)|$).

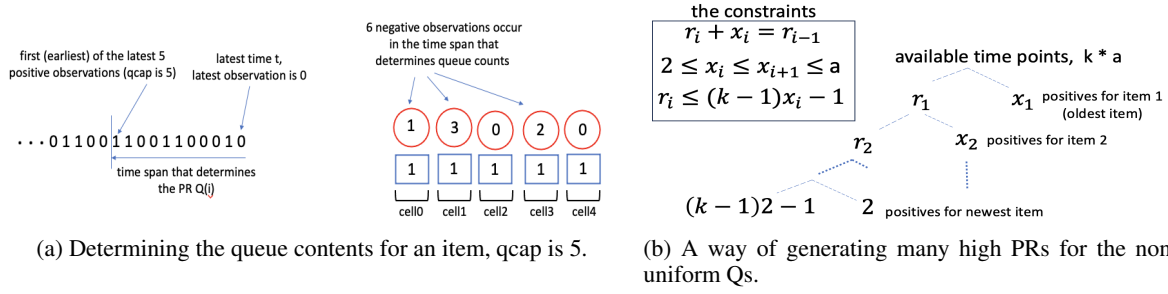


Figure 26: (a) For the uniform Qs technique, at any time t , for any item i , what determines the queue counts of i , in particular the negative counts, and therefore the sum $Y_i^{(t)}$ and $\mathcal{W}^{(t)}(i)$, is the time span t' to t , where between t' to t (inclusive, or in $[t', t]$) exactly a (qcap) positive observations occur (the latest a positives). Left: In this example qcap = $a = 5$, and an example binary sequence for item i is shown. Here, $t' = t - (5 + 6) + 1$, and exactly $a = 5$ positives and 6 negatives occur from t' to t . Right: The contents of the 5 queue cells at time t . In the span $[t', t]$, 6 negative observations occur, the count in cell0 is 2 (one positive, one negative), in cell1 is 3, and so on. (b) For non-uniform Qs, a process that generates a sequence leading to many items with PR above $\frac{1}{k}$: for the first or oldest (top) item, item 1, allocate $x_1 = a$ (or near a) positives, and remainder r_1 negatives, $r_1 \leq (k-1)x_1 - 1$, so that $\frac{x_1-1}{x_1+r_1-1} > \frac{1}{k}$. Then, split the remainder r_1 (the negatives for item 1), into x_2 and remainder $r_2 \leq (k-1)x_2 - 1$, x_2 positives for item 2, and repeat. The constraints are that $x_i \geq 2$ and the remainders r_i be as large as possible subject to $r_i < (k-1)x_i$, and $x_i + r_i = r_{i-1}$. This process is possible in part because, for emitting a positive PR, we do not require exactly a positives (x_i can be less than a). With high k and a , this can lead to many items, roughly $\log_{\frac{k}{k-1}}(ak)$, with PR above $\frac{1}{k}$.

Proof of part 2: if an item i in $qMap$ is not observed at t and removed from $qMap$, its count in cell0 is always incremented for $t+1$, i.e. $Y_i^{(t+1)} = Y_i^{(t)} + 1$. Upon observing item i at t , when $|q^{(t)}(i)| = \text{qcap}$, one cell is dropped with count ≥ 1 , and one cell is added, thus $Y_i^{(t+1)} \leq Y_i^{(t)}$, and when $|q^{(t)}(i)| < \text{qcap}$, one cell with count 1 is added, thus $Y_i^{(t+1)} = Y_i^{(t)} + 1$.

Proof of part 3: On a negative update, the denominator of $\mathcal{W}(i)$, Y_i , always goes up from part 2, while the numerator (or number of queue cells) doesn't change. On a positive update, when the queue is at capacity, the numerator does not change, while denominator may go down (part 2). When the queue hasn't reached capacity ($|q^{(t)}(i)| < \text{qcap}$), both the numerator and denominator go up by 1 each, but as the denominator is never smaller than numerator (part 1), the result is $\mathcal{W}^{(t+1)}(i) \geq \mathcal{W}^{(t)}(i)$. \square

As property 3 above states, an item's PR may not change after a positive update: This happens when the item's queue is at capacity and the last cell of the queue, to be discarded, has a 1 (one cell with count of 1 is dropped, but another such is added at the back, and Y_i is not changed). The other case for no change is when $\mathcal{W}(i) = 1$ already initially and without discarding any cell (which can occur after several consecutive initial observations of the item).

With $\text{qcap} > 2$, we can have $N(\mathcal{W}, p) \geq \frac{1}{p}$. For instance, with qcap of 4, on the sequence of $AAAABB$, item A reaches $\mathcal{W}(A) = 1$ at $t = 3$ (after the update at $t = 2$) through 5, and goes down to $3/5$ at $t = 7$, while B reaches 1 at the $t = 7$, thus with threshold $p = 3/5$, $N(\mathcal{W}^{(7)}, p) = 2 > \frac{1}{p} = 5/3$.

Let us call the variant of Qs as the *uniform* Qs technique where for any item i , while $|q(i)| < \text{qcap}$, $\mathcal{W}(i) := 0$, i.e. wait until queue of i has reached its capacity before outputting a positive PR. This variant simplifies the analysis of the worst-case number of high PRs as we explore below. Note that plain Qs with qcap of 2 is already uniform.

For any item i , for any time t , consider the most recent, or the last, $a = \text{qcap}$ positive observations of item i and let t' be the time of the first (earliest) of the last a positives. From the way the uniform Qs method works, it follows that this time span determines the queue counts for item i , in particular the number of negatives in t' to t in effect determines the PR $\mathcal{W}^{(t)}(i)$, as the number of positives is always a . Fig. 26(a) gives an example for qcap of 5. We use reasoning about such time spans to bound the number of items with high PR :

Lemma 14. *For the uniform Qs technique with $a := \text{qcap}$, thus integer $a \geq 2$, consider items i with $\mathcal{W}(i) > 0$ (i.e. queue $q(i)$ exists and $|q(i)| = a$), where the PR estimate $\mathcal{W}(i) = \frac{a-1}{Y_i}$, $Y_i := \sum_{0 \leq j < |q(i)|} C_j - 1$, is used. Then at any time point $t \geq 1$, for any integer $k > 1$, $N(\mathcal{W}, \frac{1}{k}) \leq k - 1$.*

Proof. At any time $t \geq a$, for an item i (where $\mathcal{W}(i) = \frac{a-1}{Y_i} > 0$), go back in time until first time $t' = t - \Delta$ where a positives are observed (as it is uniform Qs, and $\mathcal{W}(i) > 0$, we must have observed at least a positives from 1 to t , i.e. t' is well defined). Fig. 26(a) shows an example for $a = 5$. Let c be the count of the negatives (i.e. when item i is not observed) in this time span, i.e. $[t - \Delta, t]$ (from $t - \Delta$ to t inclusive). We have Y_i is $c + a - 1$ (a positives and c negatives), and $\mathcal{W}^{(t)}(i) = \frac{a-1}{c+a-1}$.

We will show that we have to upper bound c , call it \bar{c} , if we want $\mathcal{W}(i)$ to be sufficiently high, and the bound \bar{c} in turn upper bounds the length of the time span Δ , i.e. t' to current time t (how much into the past we can go). As each such item requires a positives (positive observations) in the same span, the maximum span is $\bar{c} + a$ for any such item, or $[t - (\bar{c} + a), t]$, and at any time point we get only one positive observation, we deduce we cannot “fit”, or have too many such high PR items in the same time span.

For example, for threshold $p = \frac{1}{2}$ (showing $N(\mathcal{W}, \frac{1}{2}) \leq 1$), we must have $\bar{c} \leq a - 1$, as if $c \geq a$, then $\mathcal{W}^{(t)}(i) \leq \frac{a-1}{a+a-1} = \frac{a-1}{2a-1} < \frac{a}{2a}$ (for the last, we used $1 < a < 2a$). Therefore, any such item has a positives in the last $\Delta \leq 2a - 1$ time points. We can have at most one item with a positives in that span (leaving $a - 1$ positives for all other items implying for any other item, its negative count c is at least a or its PR at t is $\leq 1/2$).

More generally, for any item i with $\mathcal{W}(i) > \frac{1}{k}$, $k \geq 2$, then we must have $c \leq \bar{c} = (k - 1)a - 1$ (if $c \geq (k - 1)a$, $\mathcal{W}(i) \leq \frac{a-1}{(k-1)a+a-1} \leq \frac{1}{k}$), or the maximum span $\Delta = ka - 1$ for all such items. Any such item, within the same span of at most $[t - ka + 1, t]$ requires a positives. There can be at most $k - 1$ such items. \square

When $\text{qcap} = 2$, like the case of Lemma 12 (i.e. using one cell and the MLE), the (positive) PRs in $\mathcal{W}(i)$ are the harmonic fractions, but there is more variation here compared to the case of MLE with qcap of 1. For instance, it is possible that no item gets PR of 1 at certain time points $t \geq 2$, while we can have two items with PR $\frac{1}{2}$, and in general, up to k items with PR $\frac{1}{k}$, at which case we get a perfect DI (the sum adds to 1). In other cases, such as the sequence $AABBCDD \dots$, the sum can exceed 1 substantially. The underlying cause for violating the DI property is that different items have different starting time points (to keep a bounded memory while reacting to new items, and non-stationarities), thus one recent item, using its own frame of reference (starting time point), can have PR of 1 (item D in the example $[AABBCDD]$), while simultaneously, another item, seen earlier in time, has a positive PR such as $\frac{1}{2}$ for C .

As expected, with larger $\text{qcap} > 2$, the fractions can be more granular: There can be at most 1 PR greater than $\frac{1}{2}$ at any time point (from above Lemma), and with $\text{qcap} = 2$, the only possibility is 1.0, but with $\text{qcap} = 3$, both 1.0 and $\frac{2}{3}$ are possible.

With the non-uniform Qs, there can still be at most one item with PR of 1, but the non-uniform Qs allows for additional degrees of freedom for integer $k > 1$: Fig. 26(b) shows a way of building a sequence that results in a large set S of items with PR above $\frac{1}{k}$. For simplicity we can assume the occurrence of items in S , to be described, forms the whole sequence (though the actual sequence could be longer going further into the past with items not in S). First take the item with the highest number of positives in S , call it item 1: item 1 will have $x_1 = a$ positives in the sequence and the largest possible negatives r_1 , such that $\frac{x_1-1}{x_1+r_1-1} > \frac{1}{k}$ (so roughly $r_1 < (k-1)x_1$). We can think of the positives of item 1 appearing together and before the r_1 negatives, the occurrence of other items of S .⁴⁴ The negatives for item 1, r_1 is then split into x_2 ($2 \leq x_2 \leq x_1$), x_2 being the count of positives for item 2, and remainder r_2 (count of negatives for item 2), and again we could assume positives of item 2 appear before its negatives (and after item 1’s positives). In general, the x_i (count of positives for item i) should be no less than 2, and $x_i + r_i = r_{i-1}$, $i \geq 2$. We want each r_i to be as large as possible, or r_{i+1} be not much smaller than r_i , so we can fit many items in S . Thus x_i , $i \geq 2$ should be as small as possible, subject to $\frac{x_i-1}{r_i+x_i-1} > 1/k$ and $x_i \geq 2$. Thus each $r_{i+1} \approx \min(\frac{k-1}{k}r_i, r_i - 2)$.

For instance with $k = 2$ and $a = 8$, we can get $x_1 = 8$ and $r_1 = 6$ ($\frac{7}{13} > 1/2$), and r_1 is split into $x_2 = 4$, $r_2 = 2$, and finally $x_3 = 2$, $r_3 = 0$ ($|S| = 3$). The corresponding sequence would be: $[1111111222233]$ (item 1 appears 8 times,

⁴⁴Though only the oldest occurrence of item 1 needs to occur before any other item in S , so that presence of other items are counted as negatives for item 1. A similar consecutive property can be assumed for other items of S .

then item 2 and item 3). More generally, we can get roughly $\log_2 a$ items with PR exceeding $\frac{1}{2}$ when $k = 2$. Higher k (and capacity a) leads to more items, up to $\log_b(k-1)a$, where base $b = \frac{k}{k-1}$.⁴⁵

D An Efficient Time-Stamp Variant of Qs and Queue-Less DYAL

We describe the slightly different time-stamp method, which allows for a more efficient $O(1)$ updating for Qs. We then discuss alternative (queue-less) possibilities for DYAL (Sect. D.2).

D.1 A Time-Stamp Method for Sparse Updates

A small change to the values kept in the queues of the Qs method makes the updating more efficient. In this *time-stamp* variant, Fig. 27, each predictor also keeps a single counter, or its own private *clock*. Upon an update, the predictor increments its clock. Nothing is done to the queues of items not observed (thus, yielding a sparse efficient update). For the observed item, a new cell is allocated, similar to the case of plain Qs, and the current clock value is copied into it (instead of being initialized to 1, which was the case for plain Qs). Existing cells of this queue, if any, are shifted right, as before. Thus each queue cell simply carries the value of the clock at the time the cell was allocated, and the difference between consecutive cells is in effect the count of negative outcomes (the gaps), from which proportions can be derived. When predicting, any item with no queue or a single-cell queue in $qMap$, gets 0 PR, as before. An item with more than one cell gets a positive PR, using a close variant of the $GetPR()$ function of Fig. 8 (Fig. 27). The count corresponding to a queue is the current clock value minus the clock value of $cell_k$ (the oldest queue cell). The count is guaranteed to be positive, and is equivalent to the denominator used in $GetCount()$. Then the PR is the ratio of number of cells in the item's queue, k , to its count.

This variation has the advantage that updating is $O(1)$ only with the mild assumption that Qs operations and counting take constant time (*i.e.* incrementing clock and the operations on a single item's queue), while for the plain Qs technique, recall that it is $O(|qMap|)$. In this sense, this extension is strictly superior.⁴⁶ However, during prediction, if that involves predicting all items' PRs in the map, complexity remains $O(|qMap|)$, so within the online cycle of predict-observe-update, time costs would not change asymptotically. However, the time-stamp variant is useful in scenarios where, instead of asking for all PRs, one queries for the probability of one or a few items only, *e.g.* when one seeks the (approximate non-stationary) prior of a few items. In particular, when the number of items for which one seeks to keep a prior for is large, *e.g.* millions (thus, we are interested in estimating small probabilities, such as $p \leq 10^{-6}$), a sparse update is attractive.

D.1.1 Overflow (of Counts)

Incrementing the clock with each update can lead to large clock values (log of stream length) and require significant memory for a predictor that frequently updates. One can manage such, and in effect limit the window size and the prediction capacity, *i.e.* the number of items for which an approximate PR is kept at any point, by periodically pruning and shifting the update count value to a lower value.

D.2 Discussion: Why not multiple EMAs with different rates?

Why can't we use two (or more) tiers of EMA, one with high fixed rate, so agile and adaptive, another with a low and fixed rate, so stable for fine tuning, rather than the current hybrid two-tier approach in DYAL that also uses queues and predictand-specific β s? Queues are an effective way to differentiate between noise items (below p_{min}) from salient items (with good likelihood of success). On the other hand, EMA with a high fixed rate β is too coarse (non-differentiating) for learning PRs below the β .

It may be possible to use multiple *non-fixed* rate, "scanning" EMAs, where the learning rate for each scanner is repeatedly reset to high but decreased over time (such as via harmonic decay), and using more than one rate per predictand, to achieve similar goals (change detection and convergence). We leave exploring this to future work.

⁴⁵The size $|S|$ will be less than $\log_{k/(k-1)}(k-1)a$, as $r_{i+1} := \min(\frac{k-1}{k}r_i, r_i - 2)$ (we need to allocate at least $k = 2$ to x_{i+1})

⁴⁶The time-stamps can get large, taking log of stream length. One can shift and reset periodically (Sect. D.1.1).

```

UpdateTimeStampQs( $qMap, o$ )
  // Each predictor has its own clock (initially 0).
  // Update the clock.
   $clock \leftarrow clock + 1$ 
  If item  $o \notin qMap$ : // when  $o \notin qMap$ , insert.
    // Allocate & insert  $q$  for  $o$ .
     $qMap[o] \leftarrow Queue()$ 
    // Exactly one positive update.
    // (No explicit negative update)
    PositiveUpdate( $qMap[o]$ )

PositiveUpdate( $q$ ) // Adds a new (back) cell.
  // Existing cells shift one position. Oldest cell
  // is discarded, in when  $q$  is at capacity.
  If  $q.nc < q.qcap$ :
     $q.nc \leftarrow q.nc + 1$  // Grow the queue  $q$ .
  For  $i$  in  $[1, \dots, q.nc - 1]$ : // Inclusive.
     $q.cells[i] \leftarrow q.cells[i - 1]$  // shift contents.
   $q.cells[0] \leftarrow clock$  // set newest,  $cell_0$ , to clock.

GetPR( $q$ ) // Extract a PR, using  $q.nc$ 
  // (number of cells) and the time-stamps.
  If  $q.nc \leq 1$ : Return 0 // Too few? (grace period).
  Return  $\frac{q.nc - 1}{clock - q.cells[q.nc - 1]}$ 

```

Figure 27: Time-stamp queuing, with $O(1)$ updates, showing those function that are different from plain Qs technique of Fig. 8: queue fields, *e.g.* $q.nc$, and the **Queue()** functions remain the same. There is no **NegativeUpdate()** here. Others such as **GetCount()** could be adapted too.

deviation thresh. \rightarrow	1.1	1.5	2	1.1	1.5	2	1.1	1.5	2
	Qs, 3			DYAL, 0.1			DYAL, 0.0001		
[0.025, 0.25], 10	0.906	0.542	0.277	0.904	0.637	0.496	0.864	0.591	0.408
[0.025, 0.25], 50	0.907	0.539	0.265	0.900	0.625	0.476	0.529	0.167	0.088
$\mathcal{U}(0.01, 1.0)$, 10	0.877	0.522	0.282	0.894	0.615	0.463	0.890	0.562	0.351
$\mathcal{U}(0.01, 1.0)$, 50	0.873	0.507	0.263	0.849	0.563	0.424	0.750	0.303	0.156
	Static EMA, 0.1			Static EMA, 0.01			DYAL, 0.01		
[0.025, 0.25], 10	0.898	0.619	0.469	0.827	0.510	0.357	0.813	0.481	0.329
[0.025, 0.25], 50	0.896	0.604	0.451	0.680	0.257	0.128	0.673	0.247	0.126
$\mathcal{U}(0.01, 1.0)$, 10	0.892	0.608	0.446	0.926	0.684	0.478	0.896	0.583	0.360
$\mathcal{U}(0.01, 1.0)$, 50	0.847	0.543	0.404	0.830	0.400	0.206	0.786	0.315	0.143

Table 15: As in Sect. 7.2, for an additional evaluation setting ($d = 1.1$) and algorithm parameters.

E Additional Synthetic Experiments

E.1 Tracking One Item

Table 15 reports under the same synthetic setting of Table 5, *i.e.* tracking the single item 1 in binary sequences, with a few different parameter values: deviation-rates with $d = 1.1$ (convergence to within 10%), Qs with $qcap$ of 3 (as DYAL uses this as its default), and DYAL with lower rates. As expected, $d = 1.1$ yields high deviation rates, and O_{min} of 50 helps lower the rate for any d and method. Low minimum rates for DYAL (0.0001) help it achieve lowest deviation rates for $d = 1.1$.

Table 16 repeats the uniform-setting experiments of Table 5, but with the extra constraint that each stable period be at least 1000 time points.

E.2 Multiple Items, $P_{max} = 0.1$

Table 17 presents multi-item synthetic experiments with $P_{max} = 0.1$ when generating the underlying true \mathcal{P} (GenSD()). Average number of different SDs, generating a sequence, in these experiments is around 3 with $O_{min} = 50$, and around 13 with $O_{min} = 10$. We observe similar patterns to Table 6 in that DYAL is less sensitive to the choice of β_{min} , and is competitive with the best of other EMA variants. Compared to Table 6, with overall lower PRs for the salient items and in a narrower range (0.01 to 0.1), the log-loss performances are worse, and static EMA with $\beta = 0.01$ is more competitive with DYAL. Paired experiments and counting the number of wins show that DYAL with $\beta_{min} = 0.01$ beats the best of others convincingly, in Table 18, while DYAL with $\beta_{min} = 0.001$ struggles compared to other EMA variants with $\beta = 0.01$.

F Further Material on Real-World Experiments

Descriptions of the methods used for concept composition and interpretation within the simplified Expedition system.

deviation threshold \rightarrow	1.5	2	1.5	2
	Qs, 5		Qs, 10	
$\mathcal{U}(0.01, 1.0), 10$	0.226 ± 0.036	0.064 ± 0.023	0.103 ± 0.035	0.021 ± 0.020
$\mathcal{U}(0.01, 1.0), 50$	0.233 ± 0.049	0.052 ± 0.022	0.102 ± 0.029	0.023 ± 0.022
	static EMA, 0.01		static EMA, 0.001	
$\mathcal{U}(0.01, 1.0), 10$	0.093 ± 0.045	0.041 ± 0.023	0.487 ± 0.114	0.271 ± 0.117
$\mathcal{U}(0.01, 1.0), 50$	0.099 ± 0.051	0.043 ± 0.028	0.462 ± 0.149	0.311 ± 0.164
	Harmonic EMA, 0.01		Harmonic EMA, 0.001	
$\mathcal{U}(0.01, 1.0), 10$	0.094 ± 0.052	0.038 ± 0.018	0.413 ± 0.125	0.237 ± 0.105
$\mathcal{U}(0.01, 1.0), 50$	0.125 ± 0.084	0.050 ± 0.028	0.364 ± 0.161	0.241 ± 0.144
	DYAL, 0.01		DYAL, 0.001	
$\mathcal{U}(0.01, 1.0), 10$	0.048 ± 0.023	0.025 ± 0.024	0.100 ± 0.039	0.039 ± 0.034
$\mathcal{U}(0.01, 1.0), 50$	0.074 ± 0.060	0.022 ± 0.031	0.084 ± 0.044	0.036 ± 0.019

Table 16: Repeating the uniform setting of Table 5 but with the extra constraint that each stable period be at least 1000 time points. The deviation rates are averages over 20 sequences. Deviation rates substantially improve (compared to Table 5), because the stable periods are uniformly longer.

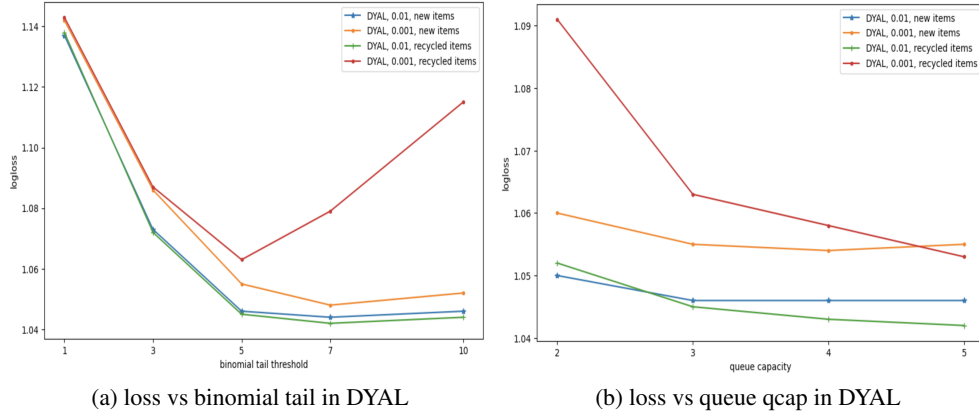


Figure 28: Sensitivity of DYAL to parameters, in synthetic multi-item setting: (a) binomial tail threshold (controlling when to switch to queues) (b) the queue capacity qcqp. These are same 50 sequences as described in Table 6, under both new-item and recycle generation settings, and with $O_{min} = 50$.

F.1 Simplified Interpretation

Each interpretation episode begins at the character level. We do a “bottom-up” randomized search, where we repeatedly pick a primitive concept and invoke and match its holonyms (bigrams that contain it) to the input line, near where the invoking concept has matched, with the constraint that the invoking concept should be matched (covered) too, and repeat until there are no available holonyms or no holonyms match. We only do exact match here, *i.e.* no approximate matching (“ab” matches if both “a” and “b” are present, with “b” immediately following “a”). We keep the top two concepts along a bottom-up path, the top-matching concepts. We repeat such bottom to top searches and matches until all characters (positions) in the input line have been covered, *i.e.* have one or more matching concepts. From the set of matching concepts, the process generates candidate interpretations and selects a final interpretation: a candidate interpretation is a sequence of top-matching concepts (one of the two that are end of each path), covering all the positions (characters) in the input line, and without any overlap, and where two new non-primitive concepts, *i.e.* below a frequency (observation-count) threshold, cannot be adjacent. Often there are several candidate interpretations, and we pick one with minimum number of concepts in it, breaking ties randomly.

F.2 Simplified Composition

The simplified concept generation process is as follows: in every episode, once the interpretation process is done, one obtains a final interpretation, that is a sequences of concepts (a mix of unigrams, bigrams, etc) covering all the

	1.5any	1.5obs	logloss	1.5any	1.5obs	logloss	opt. loss
new items ↓	Qs, 5			Qs, 10			
10, [0.01, 0.1]	1.00	0.46	3.02	1.00	0.40	3.05	2.84 ±0.02
50, [0.01, 0.1]	1.00	0.41	2.94	0.99	0.24	2.91	2.83 ±0.04
	static EMA, 0.01			static EMA, 0.001			
10, [0.01, 0.1]	1.00	0.28	3.02	1.00	0.75	3.68	2.84
50, [0.01, 0.1]	0.99	0.19	2.89	0.73	0.22	3.07	2.83
	harmonic EMA, 0.01			harmonic EMA, 0.001			
10, [0.01, 0.1]	1.00	0.28	3.02	1.00	0.75	3.70	2.84
50, [0.01, 0.1]	0.99	0.19	2.89	0.71	0.22	3.07	2.83
	DYAL, 0.01			DYAL, 0.001			
10, [0.01, 0.1]	1.00	0.28	3.01	0.98	0.27	3.11	2.84
50, [0.01, 0.1]	1.00	0.20	2.88	0.73	0.07	2.88	2.83
recycle items ↓	Qs, 5			Qs, 10			
10, [0.01, 0.1]	1.00	0.41	2.95	0.99	0.26	2.93	2.84 ±0.02
50, [0.01, 0.1]	1.00	0.40	2.94	0.99	0.21	2.89	2.84 ±0.04
	static EMA, 0.01			static EMA, 0.001			
10, [0.01, 0.1]	1.00	0.21	2.90	1.00	0.33	2.98	2.84
50, [0.01, 0.1]	1.00	0.18	2.88	0.70	0.11	2.88	2.84
	harmonic EMA, 0.01			harmonic EMA, 0.001			
10, [0.01, 0.1]	1.00	0.21	2.90	1.00	0.32	2.98	2.84
50, [0.01, 0.1]	1.00	0.18	2.88	0.67	0.10	2.89	2.84
	DYAL, 0.01			DYAL, 0.001			
10, [0.01, 0.1]	1.00	0.22	2.90	1.00	0.30	2.95	2.84
50, [0.01, 0.1]	1.00	0.18	2.88	0.65	0.08	2.87	2.84

Table 17: Here, $P_{max} = 0.1$ for GenSD() (instead of 1.0), and otherwise, as in Table 6: averages over 50 sequences, about $\sim 10k$ length each, O_{min} of 10 and 50 (1st column of the table), uniform sampling of p^* in $[0.01, 0.1]$, and changing the SD whenever *all items* are observed O_{min} times.

DYAL vs. →	Qs, 10	static, 0.01	harmonic, 0.01	Qs, 10	static, 0.01	harmonic, 0.01
DYAL, 0.01 ↓	new items			recycle items		
10, 0.01, [0.01, 0.10]	0, 50	0, 50	0, 50	0, 50	0, 50	0, 50
50, 0.01, [0.01, 0.10]	0, 50	0, 50	0, 50	0, 50	0, 50	0, 50
DYAL, 0.001 ↓	new items			recycle items		
10, 0.01, [0.01, 0.10]	50, 0	50, 0	50, 0	50, 0	50, 0	50, 0
50, 0.01, [0.01, 0.10]	0, 50	43, 7	43, 7	0, 50	10, 40	7, 43

Table 18: Number of losses and wins in 'paired' experiments for the setting of Table 17: the 2nd number in each pair is the number of wins of DYAL (when log-loss lower), on the same set of 50 sequences (each $\sim 10k$). For instance, in top left cell, Qs with $qcap=10$ loses to DYAL when $O_{min} = 10$, on all 50 sequences. DYAL with $\beta_{min} = 0.01$ beats all others, but the results are mixed with $\beta_{min} = 0.001$.

characters in the line input to the episode. Note that in the beginning of the entire learning process, when no new concepts are generated, the final interpretation is simply the sequences of primitive concepts corresponding to the characters. Interpretation is easy at the character level (does not involve search and matching).

Adjacent concepts pairs in an interpretation are processed in the following manner to possibly generate new concepts (compositions or holonyms): Skip the pair with some probability p_g (0.9 in our experiments). Otherwise, again skip the pair if either does not meet the minimum observed-count requirement, where we experimented with 100, 500, and 2000. When a pair meets the count threshold, generate the composition if it does not already exist (a hashmap look up). Therefore, if "a" and "b" are two concepts, with "b" often occurring after "a" in the input (lines or interpretations), with high probability at some point the composition concept "ab" is generated. Note that the generation probability p_g as well as the threshold on frequency affect how fast new concepts (items) are generated, or the degree of internal non-stationarity: the higher the count threshold the lower the generation rate of new concepts, and the more time the system has for, in effect, evaluating and integrating a new concept.

F.3 Discussion: Separation of Prediction from Concept Use

Although we could use the prediction weights to influence the generation and selection of candidate interpretations, we use the above simple interpretation and concept generation methods to completely divorce prediction weight learning from the trajectory of concept generation and use, and to simulate internal non-stationarity. We note that the bigrams and the higher n -grams that are generated and used have good quality. For instance, when we define a split location, the boundary between two adjacent concepts as *good* (good split) if it coincides with a blank space (or other punctuation), and bad otherwise (splits within a word), we observe that the ratio of bad to good splits substantially improves over time (e.g. from around 75% to below 30%), as larger concepts are generated and used via the above simple processes, suggesting that the larger n -grams learned increasingly correspond to words, phrases, etc. And manual examination of the learned n -grams supports this finding.

Learning and using the predictions should improve the interpretation process, for instance approximate matching and use of predictions are important when there is substantial noise, such as typos in the input text, requiring inference based on larger context to fix. However, in the experiments of this paper, we have separated the processes to more easily compare different prediction (weight learning) techniques.

F.4 Further Evidence of Stationarity vs. Non-Stationarity

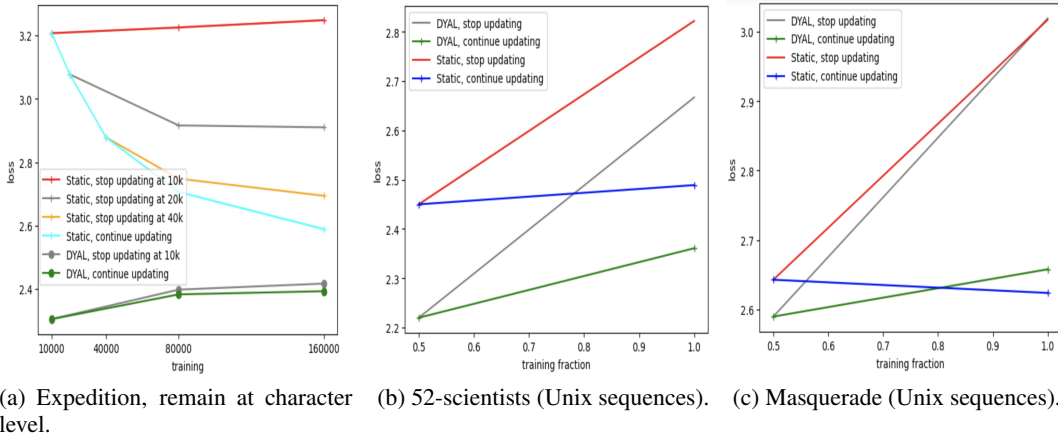


Figure 29: Performances (log-loss) when we stop the learning at certain time t vs. continued updating (continuing learning). (a) On the stationary character-level prediction. (b) and (c) on Unix sequences: Continuing the updates vs. stopping the updates at half the sequence length, and measuring performance at that point and once the sequence finishes (averaged log-loss over all the sequences in each data source). When we stop the updates, the performance takes a substantial hit compared to continued updating, whether using DYAL or static EMA, on Unix sources (indicating non-stationarity), but not on the character-level Expedition (indicating stationarity).

Fig. 29 shows log-loss performances at two or more time points t , comparing performance of continuing to update (continued learning), vs. stopping of the updates (freezing the current weights for prediction on the rest of the sequence).

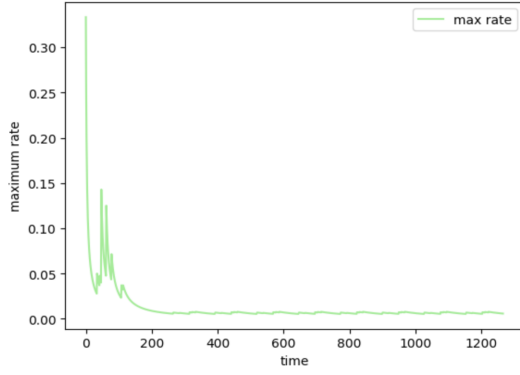
Fig. 29(a) is on Expedition at character level, the same set up of Sect. 8.2, except that here we may stop the learning at an early point. For static (EMA) and DYAL, using $\beta = 0.001$, we stop the updates at time 10k and we compare this to the regime of continuing the updates. We report the loss at 10k and at 80k and 160k. For static, we also included plots when stopping the updates at 20k and 40k. We observe the performance when stopping the updates at say 10k, at 80k or 160k is close (often better) than what it was at 10k, indicating the input distribution has not changed. The plots should be contrasted against Fig. 29(b-c) described next. We suspect the reason the performance of static at times improves, even though we have stopped the updates, is that due to its low fixed learning rate, and that we report the average over all of the times till that point, the effect of latest learning is not fully reflected, and as we allow more time (report log-loss at higher t), the result is more reflective of more recent and better performance. For DYAL, its performance converges quickly (by $t=10k$) on this stationary data and the performance only slightly degrades with higher t as some new items are observed (similar to Fig. 22).

For Fig. 29(b) and 29(c), we are comparing continued learning vs. stopping at half the sequence length, on 52-scientists and Masquerade, using static EMA and DYAL with β of 0.05 (similar setting and results to Sect. 8.3.2). For Masquerade, all sequences are 5k long, thus we report (average) performance at $t = 2.5k$ (the average log-loss performance up to time $t = 2.5k$), and then either stop or continue the learning till the end, *i.e.* $t = 5k$, and report performance at 5k as well for both situations. As in previous results, the reported losses (at different time snapshots) are the result of averaging over all the 50 sequences (users) of Masquerade. For 52-scientists, sequences have different lengths, so the times at which we report performances (use for averaging) are sequence dependent. For instance, for a sequence of total length 200, we use the performance at $t = 100$, then also use the performances at $t = 200$ for the two cases of continued updates and stopping the updates at $t = 100$ (and average each over the 52 sequences). We observe that in all cases, whether for DYAL or static EMA, stopping the learning leads to substantial increase in loss compared to continuing the updates (learning), and worse than the average performance at half the length, the latter observation implying presence of (external) non-stationarity. We have tried several learning rates (not just the best performing rate of 0.05), and obtained similar results.

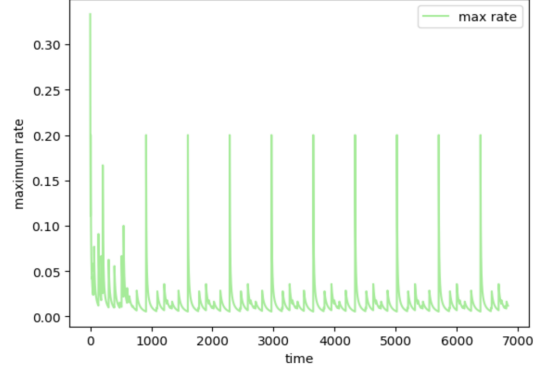
Another way to see evidence of non-stationarity is to look at the max-rate, the maximum of the learning-rate, in the *rateMap* of DYAL, as a function of time. Whenever the max-rate goes up, it is evidence that an item is changing PR, for instance a new item is being added. Furthermore, here for each sequence, we concatenate it with itself k times, $k = 10$ or $k = 3$ in Fig. 30. For example, if the original sequence has the three items [A, C] (*i.e.* $o^{(2)} = C$), then the 3x replication (self-concatenation) is [A,C,A,C,A,C]. If the start of a sequence has a distribution substantially different from the ending then, when concatenated, we should repeatedly see max-rate jump up. We looked at 10s of such plots. The max-rate repeatedly go up in plots of all sequences from the 52-scientists (whether with default parameters or with β_{min} of 0.05), and all except 1 of the 50 Masquerade sequences, and similar pattern on all except the shortest handful of sequences from 104-Expedition. These short ones are around a 100 time points long, and in the first pass, the predictor learns the distribution and does not need to change it substantially. Fig. 30 shows max-rate on 6 self-concatenated sequences, one example where the max-rate does not change much after the first pass, the other 5 where we see max-rate jumping up repeatedly. These sequences do not necessarily have many (near 100) unique salient items (occurring a few times), implying that in some, there exist salient items with high proportion that are replaced with other such over time. For instance, there are 13 sequences in the 52-scientists with number of items seen 3 or more times below 30. Replicating the longer sequences leads to too many ups in the plots (spikes) to be discernable, such as the right example plot from 52-scientists.⁴⁷

As one concrete example, in one sequence from the 52-scientists, with length 1490, the number of increases in max-rate was 10 on the original sequence, and then 7 increases in all subsequent replications. The times of increase, the command (item) observed, and its rate (changing the maximum rate, and the EMA PR in the first pass were: [(15, 'quit', '0.11', '0.12'), (28, 'more', '0.20', '0.25'), (43, '/bin/pdplk', '0.14', '0.17'), (59, '/bin/pdp60', '0.07', '0.08'), (105, 'pdp60', '0.12', '0.14'), (170, 'mv', '0.20', '0.25'), (230, 'rm', '0.07', '0.07'), (607, 'users', '0.33', '0.40'), (1408, 'rlogin', '0.06', '0.12'), (1409, 'quit', '0.08', '0.17')], thus at time $t=50$, the item 'quit' gets the learning rate of 0.11 (increasing the max-rate) and obtains PR of 0.12. The maximum rate before the increase is often 0.05 (the minimum rate in these experiments). In the 2nd pass, and all subsequent passes, the 7 increase points are: [(1492, 'mail', '0.33', '0.33'), (1519, 'more', '0.17', '0.37'), (1601, 'pdp60', '0.07', '0.15'), (1663, 'mv', '0.12', '0.29'), (2097, 'users', '0.33', '0.40'), (2898, 'rlogin', '0.06', '0.12'), (2899, 'quit', '0.08', '0.17')].

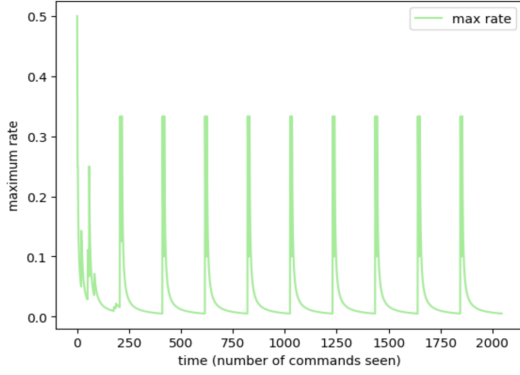
⁴⁷Note also that the number of times max-rate goes up is a subset of the times that an item changes substantially (when its PR and β are set according to the queue), *i.e.* an item's β may go up but that event may not change the maximum.



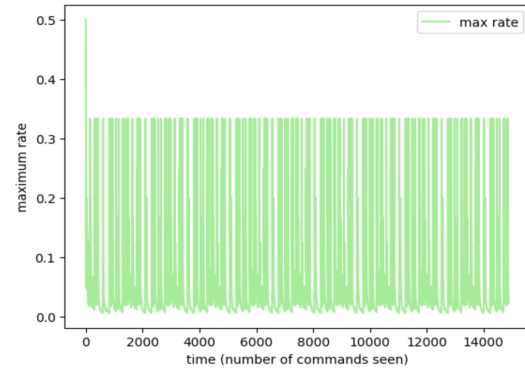
(a) Expedition, sequence 5, original length of 127.



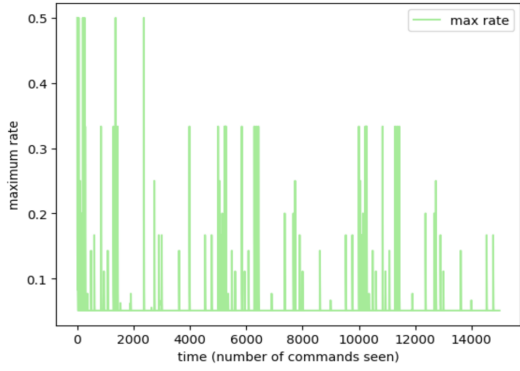
(b) Expedition, sequence 36, original length 684.



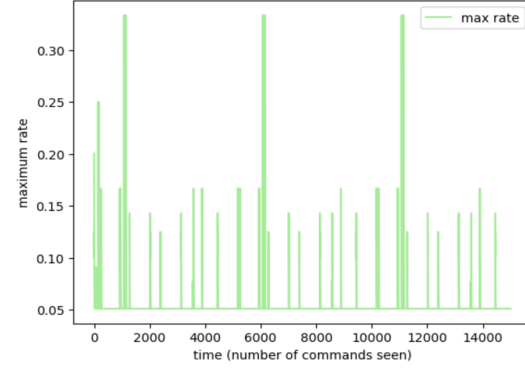
(c) 52-scientists, shortest sequence.



(d) 52-scientists, sequence 20.



(e) Masquerade, 3x.



(f) Masquerade, 3x.

Figure 30: The maximum learning rate within DYAL (max over the entries in *rateMap*) as a function of time, on two sequences each from 104-Expedition, 52-scientists, and Masquerade, where each sequence is concatenated with itself 10 times, 3x for Masquerade, thus the length of the original sequence is 127 in top left, but after 10x concatenation, it is 1270 ('sequence 5' means the 5th shortest sequence). We observe that the max-rate repeatedly jumps up, exhibiting pulsing or spiking patterns, indicating change, except for a handful of very short sequences of the 104-Expedition sequences, and one sequence with only a few unique items from Masquerade.